Alma Mater Studiorum – Università di Bologna

DOTTORATO DI RICERCA IN

CHIMICA

Ciclo XXXII

Settore Concorsuale: 03/A1

Settore Scientifico Disciplinare: CHIM 01

Development and validation of new separative methods coupled to mass spectrometry for bioactive signaling molecules

Presentata da: Emanuele Porru

Coordinatore Dottorato **Supervisore**

Prof.ssa Domenica Tonelli Prof. Aldo Roda

Esame finale anno 2020

Abstract

The present thesis deals with the development and validation of analytical methods based on chromatography coupled with mass spectrometry, which are aimed to the analysis of target molecules in complex matrices. The target compounds have different applications, ranging from the clinical chemistry to the nutraceutical field. Since the requested proper standards of selectivity, sensitivity and accuracy used to depend strongly on the selected application, several efforts have been dedicated to the phase of development and validation of highly customized analytical methods, suitable for the specific system under investigation.

The first part of my thesis, which has been sub-divided into Paper I, Paper II and Paper III, is focused on the analysis of the end products of cholesterol catabolism: bile acids. Paper I involved the evaluation of a class of intestinal bile acid metabolites: Oxo-bile acids. They make up for a significant fraction of the bile acid metabolites produced by gut microbiota. Their formation might thus have physiological relevance in the cross-talk signaling between gut and liver. With the aim to further investigate the physiological role of oxo-bile acids, for the first time a fully validated RP-HPLC-ESI-MS/MS analytical method for the quantitative determination of 21 oxo-bile acids, along with seven primary and secondary bile acids, in human faeces has been developed, with the purpose to provide a useful analytical tool exploitable for precision medicine applications. Paper II reports the study of serum bile acid profile in a cohort of inflammatory bowel disease patients, namely Ulcerative colitis and Crohn's disease. Such pathologies represent chronic inflammatory conditions with a deficient intestinal absorption. This study represents the first attempt to screenshot serum bile acid profiles in a cohort of IBD patients to evaluate the effect and efficacy of anti-TNF alpha treatment in the enterohepatic circulation and metabolism of bile acids. Multivariate statistical analysis was used for this purpose. Paper 3 of this chapter deals with a study concerning trapping of conjugated and free bile acids in subdural hematoma. Bile acids have a high affinity to albumin, and subdural hematomas contain almost as high albumin levels as the peripheral circulation. We speculated that bile acids originating from the circulation may be "trapped" in the albumin in subdural hematomas. The analysis was carried out using an isotope-dilution mass spectrometry method for serum and subdural hematoma samples.

The last part of my thesis mainly focused on the analysis of berberine and its metabolic products. Berberine has been recognized for multiple pharmacological properties including antimicrobial activity, lipid-lowering capacity, inhibition of ventricular tachyarrhythmia, and reduction of endothelial inflammation. Among its phase I metabolites, berberrubine, more than berberine itself, shows the highest bioavailability, suggesting that this molecule may be potentially more effective than its precursor. In this context, the main purpose of the reported study, described in the paper IV, was to evaluate the potential use of M1 as nutraceutical, with the goal to open new perspectives in its use instead of BBR.

Index

• General overview

Analytical chemistry studies and utilizes instruments and methods able to separate, identify, and quantify matter. One of the main purposes of the modern analytical chemistry consists on developing new suitable methods to identify and quantify compounds of interest within several disciplines. Therefore, it represents a fundamental tool for all fields of science, from the oldest to the more recent applications.
Analytical chemists typically operate at the extreme edges of analysis, extending and improving the ability of all chemists to make meaningful measurements on smaller, more complex samples, on shorter time scales, and on species present at lower concentrations. Throughout its history, analytical chemistry has provided many of the tools and methods necessary for research in the other traditional areas of chemistry, as well as fostering multidisciplinary research in, to name a few, medicinal chemistry, clinical chemistry, toxicology, forensic chemistry, materials science, geochemistry, and environmental chemistry.

A founding founder of Analytical Chemistry said:

In 1912 I went to a book sale and bought ten books for fifty cents. One of the books was by Ostwald The Scientific Foundations of Analytical Chemistry. Ostwald wrote at the beginning of that book that analytical chemists are the maidservants of other chemists. This made quite an impression on me, because I didn't want to be a maidservant.

— Izaak Kolthoff

It is true that most chemists routinely make qualitative and quantitative measurements. For this reason, some scientists suggest that analytical chemistry is not a separate branch of chemistry, but simply the application of chemical knowledge. But the craft of analytical chemistry is not in performing a routine analysis on a routine sample, which is more appropriately called chemical analysis.
Analytical chemistry means improving established analytical methods, extending existing analytical methods to new types of samples, and developing new analytical methods for measuring chemical phenomena. It’s not a maidservant but rather an indispensable co-worker of all the scientists.

Mass spectrometry is a powerful analytical technique. The process involves the conversion of the sample into gaseous ions, with or without fragmentation, which are then characterized by their mass to charge ratio (m/z). There are several different designs of mass spectrometers which differ in detail, but the sequence of the phenomena is the same for each: ionization, acceleration, deflection and detection of the studied analyte.

Modern techniques of mass spectrometry were devised by Arthur Jeffrey Dempster and F.W. Aston in 1918 and 1919 respectively, even if a lot of scientist have contributed to the development of the mass

spectrometry techniques. How not mention the Nobel Prize in Chemistry John Bennett Fenn for the development of electrospray ionization and its application to study biological macromolecules.

Mass spectrometry has gradually become one of the most popular techniques. Some scientist suggests mass spectrometry as the best and powerful analytical technique nowadays. Why?
Mass spectrometry is sensible and precise, it multiplexes molecule analysis and it can handle a lot of samples. The robustness, power and reproducibility of MS rapidly lead to tangible results, explaining why this technique greatly outperforms conventional approaches.

The current work presents the development of new analytical methods and the improvement of established ones in mass spectrometry, coupled with liquid and gas chromatography systems. The main configuration used in this thesis is high pressure liquid chromatography (HPLC) with a triple quadrupole mass spectrometry and electrospray interface (ESI). Electrospray is one of the most common technique coupled with triple quadrupole. It is a soft ionization technique, since it leads to very little fragmentation. This can be advantageous in the sense that the molecular ion (or more accurately a pseudo molecular ion) is always observed. On the other hand, little structural information can be gained from the simple mass spectrum obtained, but this disadvantage can be overcome by coupling ESI with tandem mass spectrometry.

In triple quadrupole (QQQ) configuration, tandem mass spectrometry (MS/MS) is obtained by using the combination of two mass analyzers and a collision cell. The first MS filters for the precursor ion followed by an eventual fragmentation in the collision cell by means of a collision gas (e.g. nitrogen). A second mass analyzer then filters for the product ions, generated by fragmentation. This is usually done in a triple quadrupole MS configuration, although it does not represent the only applicable one for such purpose. Therefore, the advantages of MS/MS reside in an (often) increased sensitivity, in terms of signal to noise ratio, and in the possibility to gain structural information on your analytes based on the fragmentation pattern.

Chapter 1. Bile acids

Bile acids (BAs) have been recognized for multiple physiological activities in the enterohepatic circulation of vertebrates. This class of molecules contributes to the intestinal nutrient absorption and the biliary transport of lipids, toxic metabolites, and xenobiotics [Lefebvre P. 2009]. They are normally concentrated and stored in the gallbladder (in vertebrates possessing a gallbladder). When the gallbladder contracts following movement of lipid-rich chyme into the duodenum, BAs and other constituents of bile are delivered to the small bowel.

Bile acids are the final products of cholesterol metabolism which take place in the liver (biosynthesis and chemical structures in figure 1). In human and in several vertebrate species, the main molecules synthesized through this catabolic pathway are cholic (CA) and chenodeoxycholic acid (CDCA). Nevertheless, the BA pool differs significantly for its quality and quantity composition among vertebrates, which make BAs one of the most complex and heterogeneous family of biomolecules [Hofmann A.F. 2010].

The first and limiting step in BA synthesis is the hydroxylation of cholesterol in position 7α, catalyzed by 7α cytochrome P450 (CYP7A1) to form 7α-hydrocholesterol [Russell D.W. 1992]. Subsequently, it undergoes hydroxylation, sterol ring saturation, epimerization of the hydroxyl group in 3-β position, until the last conjugation step with the aminoacids glycine and taurine (figure 1). The conjugation step is catalysed by two enzymes, the BA-CoA synthetase (BACS; also known as BA CoA ligase) and the BA-CoA amino acid N-acetyltransferase, for the formation of amphipathic molecules used to emulsify and absorb lipids in the intestine. The conjugation process is also required to allow an efficient BA secretion into bile, since the conjugates are more polar than the free forms [Vessey D.A 1978]. In bile BAs are up to 90% conjugated with glycine and taurine and in limited extent as free acids. The conjugation renders the BA more hydrophilic with low O/W LogP and therefore not absorbed by the intestine by passive diffusion allowing to perform theit physilogical role in the duodenum and upper intestine.

FIGURE 1. BILE ACID SYNTHESIS FROM CHOLESTEROL

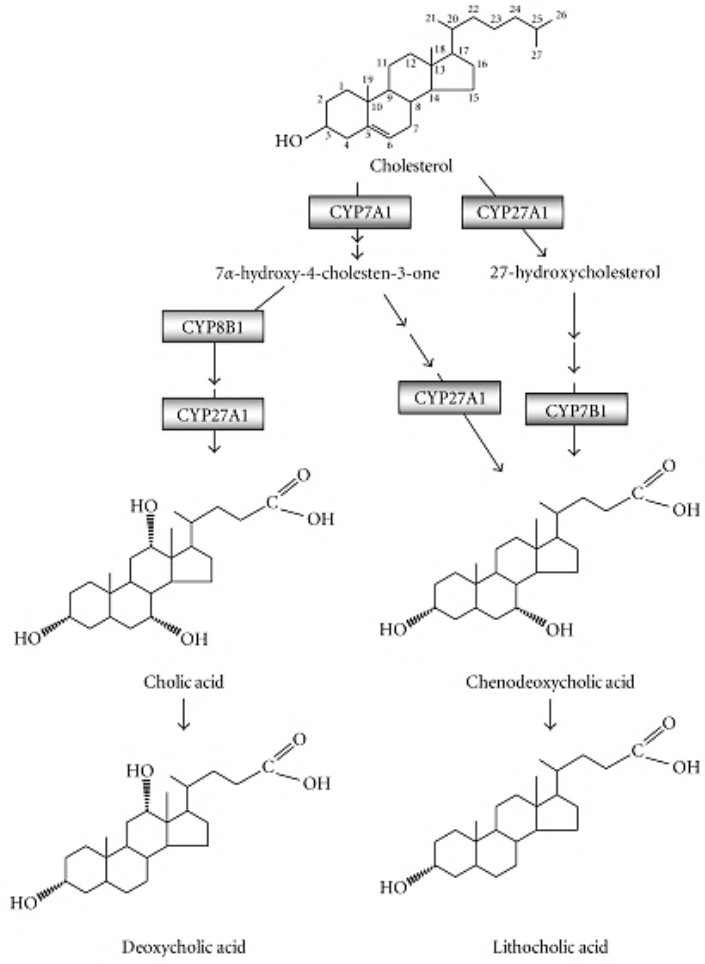

During the intestinal transit in human, about 95% of BAs are reabsorbed to maintain the 3-5 g of the physiological pool. This recycling is necessary because of the limited capability of hepatocytes to produce BAs. Specifically, their de novo synthesis compensates for their daily faecal loss, which is around 10-15% (0.5 g/day) of the total pool. Conjugated BAs are absorbed only by apical sodium-dependent BA transporter (ASBT) or ileal BA transporter in the enterocytes of the terminal ileum. Inside the enterocytes, BAs bind to the intestinal BA binding protein (IBABP) and they are discharged into the portal circulation via the organic solute transporter (OST α/β), localized in the basolateral membrane, and brought back to liver where they are efficiently (70-90%) removed from blood [Dawson P.A. 2009]. Unabsorbed primary BAs undergo several metabolic reactions by gut microbiota enzymes, largely present in colon. Specifically, the deconjugation and dehydroxylation step of CA and CDCA, lead to the formation of free deoxycholic (DCA) and free lithocholic (LCA) acids respectively, while C7 epimerization of the CDCA hydroxyl group produces ursodeoxycholic acid (UDCA). Secondary unconjugated BAs can be reabsorbed passively in the large intestine and released into the portal circulation, that transports them to the liver. As well as their metabolic precursors, secondary BAs

are conjugated with glycine and taurine (and to a lesser extent with glucuronic or sulfuric acid) and secreted into the bile [Gérard P. 2014].

BAs are endogenous ligands for the Farnesoid X receptor (FXR), also known as NR1H4 (nuclear receptor subfamily 1, group H, member 4) [Makishima M. 1999]. This nuclear receptor is largely expressed in liver and intestine, but also in adipose tissue, kidney, pancreas, and vessel walls. As a ligand-activated transcription factor, FXR binds to DNA as a monomer or as a heterodimer with a common partner for nuclear receptors, retinoid X receptor (RXR; NR2B1), in order to regulate the expression of diverse genes involved in the metabolism of BAs, lipids, and carbohydrates [Monte M.J. 2009]. FXR can be activated by either free or conjugated BAs, but the stronger binding affinity is towards CDCA (EC50 = approximately 10 mmol/L), with lower affinities for LCA, DCA, and CA in this order. UDCA and hydrophilic BAs are not able to activate the receptor [Fujino T. 2004]. The interaction of BAs with the hepatic FXR causes an inhibition of BA synthesis; this occurs via the upregulation of the transcription of the orphan receptor small heterodimeric partner (SHP1; NR0B2). The latter inhibits the activity of CYP7A1 by inhibition of another orphan receptor, the liver receptor homolog 1 (Lrh1; NR5A2), which in turn positively regulates the CYP7A1. Finally, the FXR localized in enterocytes stimulates also the production and secretion of fibroblast growth factor (FGF-19) into the portal circulation and, in the liver, binds the surface FGF receptor 4 associated with the β-Klotho protein; this ligand-receptor complex activates a mitogen-activated protein kinase cascade that inhibits the activity of CYP7A1 [Inagaki T. 2005].

BAs also act as signalling molecules through the BA-dedicated G protein-coupled receptor (GPCR) TGR5 (GPR131) (Kawamata 2003, Maruyama 2002). Stimulation of the TGR5 signalling pathway confers to BAs the ability to modulate energy expenditure by controlling the activity of type 2 deiodinase and the subsequent activation of thyroid hormone in brown adipose tissue (BAT) and muscle. Additionally, TGR5 plays a critical role in the control of intestinal GLP-1 release and in the maintenance of glucose homeostasis [Thomas C. 2009]. TGR5 also seems to be involved with several inflammatory diseases including fatty liver infiltration, atherosclerosis, diabetes mellitus (DM) and the inflammatory bowel diseases (IBDs) [Yoneno K. 2013]. Indeed, BA-activated FXR and TGR5 signalling has been reported to suppress inflammation in macrophages, in intestine and hepatocytes, and to increase energy expenditure in brown adipose tissue.

The interest in BA area has never ended in the last century, and for this reason several analytical methods have been developed and improved [Griffiths W.J. 2010]. Over the last decade, liquid chromatography-tandem mass spectrometry has become the method of election for the quantification BAs and their conjugates quantification in different matrices, such as plasma, blood, urine, and faeces. However, also GC is a robust, simple and inexpensive lab tool for volatile or semi-volatile compound analysis. The only drawback of GC versus HPLC for bile acid analysis is that polar functional groups (carboxyl and hydroxyl) need to be derivatized into GC-detectable forms. However, being gas chromatography historically the first tool to

analyse BAs, it still represents a viable, very mature technique for this purpose, which also provides a different selectivity in respect to more modern LC-MS approaches.

This section focused on different aspect of bile acid physiology and analytical technique. The first paper highlights the importance of a metabolic products of bile acids by gut microbiota. The second paper is dedicated to the correlation between inflammatory bowel disease and bile acid malabsorption. Both analytical approaches are developed and validated using liquid chromatography. The last paper in this section concerns the bioaccumulation of bile acids in subdural hematoma and their quantification by gas chromatography. This latter study has been carried out at the Division of Clinical Chemistry at Karolinska Institute as part of a visiting research program under the supervision of Prof. Ingemar Björkhem and Prof. Paolo Parini.

Reference

Dawson, P. A., Lan, T., & Rao, A. (2009). Bile acid transporters. Journal of lipid research, 50(12), 2340-2357.

Fujino, T., Une, M., Imanaka, T., Inoue, K., & Nishimaki-Mogami, T. (2004). Structure-activity relationship of bile acids and bile acid analogs in regard to FXR activation. Journal of lipid research, 45(1), 132-138.

Gérard, P. (2014). Metabolism of cholesterol and bile acids by the gut microbiota. Pathogens, 3(1), 14-24.

Griffiths, W. J., & Sjövall, J. (2010). Bile acids: analysis in biological fluids and tissues. Journal of lipid research, 51(1), 23-41.

Hofmann, A. F., Hagey, L. R., & Krasowski, M. D. (2010). Bile salts of vertebrates: structural variation and possible evolutionary significance. Journal of lipid research, 51(2), 226-246.

Inagaki, T., Choi, M., Moschetta, A., Peng, L., Cummins, C. L., McDonald, J. G., ... & Gerard, R. D. (2005). Fibroblast growth factor 15 functions as an enterohepatic signal to regulate bile acid homeostasis. Cell metabolism, 2(4), 217-225.

Lefebvre, P., Cariou, B., Lien, F., Kuipers, F., & Staels, B. (2009). Role of bile acids and bile acid receptors in metabolic regulation. Physiological reviews, 89(1), 147-191.

Makishima, M., Okamoto, A. Y., Repa, J. J., Tu, H., Learned, R. M., Luk, A., ... & Shan, B. (1999). Identification of a nuclear receptor for bile acids. Science, 284(5418), 1362-1365.

Monte, M. J., Marin, J. J., Antelo, A., & Vazquez-Tato, J. (2009). Bile acids: chemistry, physiology, and pathophysiology. World journal of gastroenterology: WJG, 15(7), 804.

Russell, D. W., & Setchell, K. D. (1992). Bile acid biosynthesis. Biochemistry, 31(20), 4737-4749.

Thomas, C., Gioiello, A., Noriega, L., Strehle, A., Oury, J., Rizzo, G., ... & Pellicciari, R. (2009). TGR5-mediated bile acid sensing controls glucose homeostasis. Cell metabolism, 10(3), 167-177.

Vessey, D. A. (1978). The biochemical basis for the conjugation of bile acids with either glycine or taurine. Biochemical Journal, 174(2), 621-626.

Yoneno, K., Hisamatsu, T., Shimamura, K., Kamada, N., Ichikawa, R., Kitazume, M. T., ... & Sato, T. (2013). TGR 5 signalling inhibits the production of pro-inflammatory cytokines by in vitro differentiated inflammatory and intestinal macrophages in Crohn's disease. Immunology, 139(1), 19-29.

Paper 1

Identification and quantification of oxo-bile acids in human faeces with liquid chromatography-mass spectrometry: A potent tool for human gut acidic sterolbiome studies.

Reproduced from:

Identification and quantification of oxo-bile acids in human faeces with liquid chromatography–mass spectrometry: A potent tool for human gut acidic sterolbiome studies.

Franco P.*, Porru E.*, Fiori J., Gioiello A., Cerra B., Roda G., Caliceti C., Simoni P., Roda A. (2019).
*co-first author

Journal of Chromatography A, 1585, 70-81. https://doi.org/10.1016/j.chroma.2018.11.038

Abstract

Bile acids (BAs) are endogenous steroids involved in the transport of lipids in bile, acting also as molecular signalling hormones. Primary BAs synthesized in the liver undergo several metabolic pathways in the intestine by gut microbiota to produce secondary BAs. Together with secondary BAs, other metabolites have been recovered from human faeces, including many oxo-BA analogues produced in the colon through oxidation of BA hydroxy groups. However, the complete oxo-BA characterization in biospecimens (particularly intestinal content and faeces) has not been reported yet, hampering the assessment of their potential physiological role.

Herein, we have developed and validated a new RP-HPLC-ESI-MS/MS method in negative ionization mode for the simultaneous analysis of 21 oxo-BAs and their 7 metabolic BA precursors in human faeces. The elution was performed in gradient mode and 28 compounds, including primary, secondary BAs, and their oxo-derivatives, were separated within 50 min at 40 °C column temperature. The method is accurate (bias% <13%), precise (CV% <10%), with limits of quantification (LOQ <30 ng/$mL_{extract\ samples}$), similar for all the studied compounds. The matrix effect does not significantly affect the analysis accuracy, allowing the use of standard solutions for the quantifications, without matrix-matched protocols. Thanks to the high detectability and the relatively high concentration of oxo-BAs (about µg/$g_{wet\ faeces}$), the method does not require a pre-analytical clean-up step.

This method was used to identify and quantify oxo-BAs in human faecal samples from healthy subjects, serving as a proof of concept for application in patients with hepatobiliary disease and bacteria overgrowth.

1. Introduction

Bile acids (BAs) are the end-products of cholesterol catabolism. Thanks to their amphipathic nature, they aggregate to form mixed micelles with phospholipids. Thus, they act as vehicle to promote the intestinal absorption of dietary lipids, including their precursor cholesterol [Hofmann A.F. 1964].

BAs do not merely act as excretory molecules; they play an active role in several physiological pathways acting as hormone-like molecules. They were found to be endogenous ligands of the Farnesoid X receptor (FXR) and the G-protein-coupled receptor TGR5 [Parks D.J. 1999, Jones S.A. 2012]. Recently, the semisynthetic 6α-ethylchenodeoxycholic acid, OCA (Ocaliva™), was approved by the Food and Drug Administration (FDA) to treat patients with primary biliary cholangitis (PBC). The FXR agonistic activity of OCA is 100-fold higher than its endogenous analogue chenodeoxycholic acid (CDCA) [Roda A. 2017].

In humans, primary BAs, cholic acid (CA) and CDCA, are synthesized in the liver from cholesterol, and then amidated with glycine and taurine [Chiang J.Y. 2009]. Once fulfilled their role in lipid absorption, conjugated

BAs are actively absorbed into the terminal ileum. The unabsorbed fraction undergoes several bacterial metabolic reactions in the colon to produce 7-dehydroxylated secondary metabolites: deoxycholic acid (DCA), lithocholic acid (LCA), and the 7β epimer of CDCA: ursodeoxycholic acid (UDCA). These reactions include the deconjugation, 7α-dehydroxylation, oxidation, and epimerization of one or more hydroxyl groups [Hylemon P.B. 1985] (Fig. 1).

FIG. 1. POTENTIAL MICROBIAL METABOLIC PATHWAY OF PRIMARY AND SECONDARY BAS TO FORM OXO-DERIVATIVES.

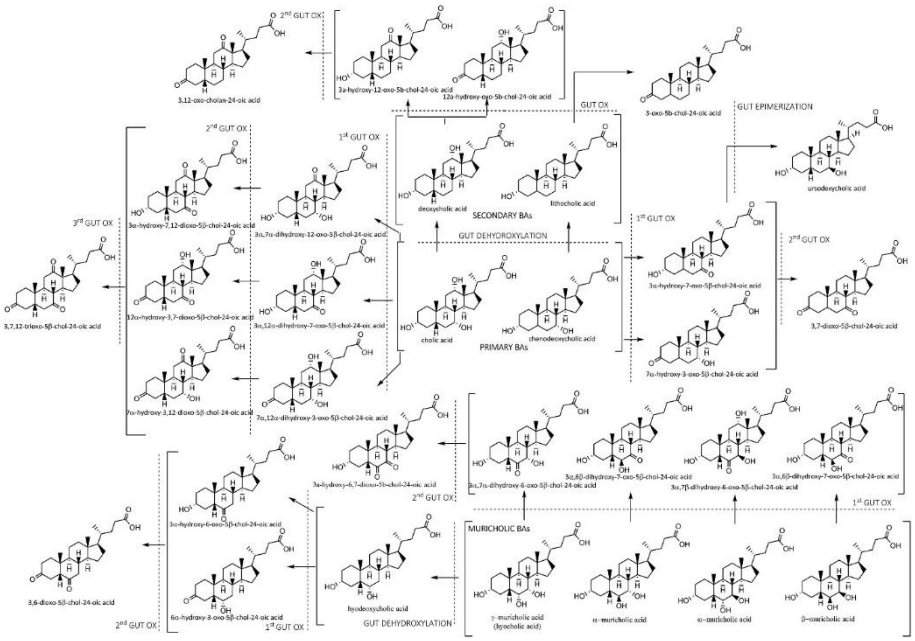

In addition to secondary BAs, oxo-BA analogues make up for a significant fraction (about 20–30%) of the BAs metabolites produced by gut microbiota in the colon and then excreted through faeces. Oxo-analogues are BAs with one or more oxo groups in positions C3, C6, C7, or C12. Their qualitative and quantitative composition is highly variable and is mainly related to the composition of intestinal bacteria and to the intestinal transit time. The intestinal transit time modulates the length of exposure to the enzymes (oxidases, dehydrogenases) present in a given bacterium [Sánchez B. 2018, Subbiah M.T. 1976].

The bacterial 7-dehydroxylase removes the OH group to form secondary BAs. This enzyme competes with and depends on the 7α -hydroxysteroid dehydrogenase (7α-HSDH), which reduces oxo-BAs or catalyses the oxidation of the hydroxyl group. Similarly, the 3α/β-HSDH and 12α/β-HSDH are responsible for the redox reactions at the hydroxyl groups at the C3 and C12 positions, respectively. These dehydrogenases are produced by different strains of bacteria in human microbiota, such as C. absonum and C. perfringens [Doden H. 2018]. The full ensemble of HSDH enzymes in gut microbiota is potentially able to produce mono, di, and tri oxo-derivatives in positions C3, C7, and C12 and, to a lesser extent in humans, in position C6 as well.

Some oxo-BAs are ligands for FXR, with 7oxo-LCA being even more potent than other BAs [Wang H. 1999]. Their formation should thus have physiological relevance for the cross-talk signalling between gut and liver. They may also be inhibitors of carbonic anhydrase I and II, androgen receptor antagonists, and CYP3A4 substrates [Trifunović J. 2017].

Recently, Ridlon and Bajaj [Ridlon J.M. 2015] proposed the term "sterolbiome" to describe the genetic potential of the gut microbiome to produce endocrine molecules from endogenous and exogenous steroids. In this context, the same authors focused on the unclear and still undefined role of the formation of oxo-BAs by gut microbiota. Indeed, this reaction is not energetically favoured, and the formation of more hydrophobic compounds is quite uncommon in terms of excretion purposes. As reported by Roda et al. [Roda A. 1983], oxo-BAs have higher CMC values (e.g. 7oxo-CDCA (25 mM)) than their precursors (e.g. CDCA (9 mM)), indicating lower detergency and lower cytotoxicity.

These considerations suggest that oxo-BAs could still maintain a biological role and do not merely act as "inert" excretion molecules. Unfortunately, the lack of proper analytical methods for the complete analysis of oxo-BAs hampers a full elucidation of their potential biological role. Indeed, even if the analysis of BAs has been largely performed, only few papers reported a partial identification of oxo-BAs in faeces [Danielsson H. 1963, Kakiyama G. 2014, Eneroth P. 1966]. Nevertheless, HPLC coupled with mass spectrometry is an analytical technique widely used for BAs determination [Scherer M. 2009, García-Cañaveras J.C. 2012]. Several extraction protocols for their analysis in faeces have been proposed using different solvents, such as alcohols, particularly isopropanol [Hamilton J.P. 2007, Humbert L. 2012]. These protocols, especially if combined to the selectivity of mass spectrometry detectors, proved to afford good recoveries and accurate quantifications, and their long-term stability in biological matrices accounts for highly reproducible analytical results.

With the aim to further investigate the physiological role of oxo-BAs, herein we report the development of a RP-HPLC-ESI-MS/MS analytical method for the simultaneous determination of 21 oxo-BAs, along with seven primary and secondary BAs, in human faeces. The number of oxo-BAs object of this study, as reported in Table 1, was determined by selecting the most probable metabolites to occur in vivo as consequence of different oxidation reactions at the BAs hydroxyl groups, as schematized in Fig. 1.

TABLE 1. RETENTION TIMES AND MS TRANSITIONS OF ALL 21 OXO-BAS INVESTIGATED AND THEIR BA PRECURSORS.

Oxo-BA	Retention time (min)	Transition
3,7,12-trioxo-cholan-24-oic acid	6.1	[401.2] > [401.2]
7α,12β-dihydroxy-3-oxo-cholan-24-oic acid*	10.2	[405.2] > [405.2]
7β,12α-dihydroxy-3-oxo-cholan-24-oic acid *	10.6	[405.2] > [405.2]

Oxo-BA	Retention time (min)	Transition
3α,6α-dihydroxy-7-oxo-cholan-24-oic acid	14.9	[405.2] > [405.2]
3α,12α-dihydroxy-7-oxo-cholan-24-oic acid	16.4	[405.2] > [405.2]
3α,7α-dihydroxy-12-oxo-cholan-24-oic acid	17.6	[405.2] > [405.2]
3,7-dioxo-cholan-24-oic acid*	18.4	[387.2] > [387.2]
6α,7α-dihydroxy-3-oxo-cholan-24-oic acid	18.9	[405.2] > [405.2]
3,12-dioxo-cholan-24-oic acid*	19.3	[387.2] > [387.2]
7β-hydroxy-3-oxo-cholan-24-oic acid	20.3	[389.2] > [389.2]
3,6-dioxo-cholan-24-oic acid*	20.5	[387.2] > [387.2]
7α,12α-dihydroxy-3-oxo-5β-cholan-24-oic acid	20.8	[405.2] > [405.2]
6α-hydroxy-3-oxo-cholan-24-oic acid	21.2	[389.2] > [389.2]
3α-hydroxy-6-oxo-cholan-24-oic acid	22.3	[389.2] > [389.2]
3α-hydroxy-7-oxo-cholan-24-oic acid	23.6	[389.2] > [389.2]
12β-hydroxy-3-oxo-cholan-24-oic acid	24.8	[389.2] > [389.2]
3α-hydroxy-12-oxo-cholan-24-oic acid	25.8	[389.2] > [389.2]
3α-hydroxy-6,7-dioxo-cholan-24-oic acid	25.9	[403.2] > [403.2]
7α-hydroxy-3-oxo-cholan-24-oic acid	29.1	[389.2] > [389.2]
12α-hydroxy-3-oxo-cholan-24-oic acid	29.9	[389.2] > [389.2]
3-oxo-cholan-24-oic acid	36.4	[373.2] > [373.2]

BA	Retention time (min)	Transition
3α,6α,7α-trihydroxy-5b-cholan-24-oic acid (HCA)	20.7	[407.2] > [407.2]
3α,7β-dihydroxy-5b-cholan-24-oic acid (UDCA)	23.1	[391.2] > [391.2]
3α,6α-dihydroxy-5b-cholan-24-oic acid (HDCA)	24.5	[391.2] > [391.2]
3α,7α,12α-trihydroxy-5b-cholan-24-oic acid (CA)	27.8	[407.2] > [407.2]
3α,7α-dihydroxy-5b-cholan-24-oic acid (CDCA)	32.9	[391.2] > [391.2]
3α,12α-dihydroxy-5b-cholan-24-oic acid (DCA)	33.7	[391.2] > [391.2]
3α-hydroxy-5b-cholan-24-oic acid (LCA)	37.6	[375.2] > [375.2]

***non-baseline resolved peaks**

In colon, due to the presence of bacteria enzymes, the epimerization reaction is very common, therefore several structures of BAs differing both in position and orientation of hydroxyl groups occur, potentially leading to several oxo-BAs structures. The method was applied to analyse faecal samples from healthy human volunteers in order to define the most representative oxo-BAs as the result of their production related to gut

microbiota composition, with the final goal to open new perspectives towards acidic sterolbiome studies in health and disease.

2. Materials and methods

2.1. Chemicals and solutions

Authentic chemical standards of CA, HCA, CDCA, DCA, 2,2,4,4-d4 DCA, HDCA, UDCA, LCA, 2,2,4,4-d4 LCA (all provided as sodium salts) were purchased from Sigma-Aldrich (Saint Louis, USA). Standards of 3,7,12-trioxo-5β-cholan-24-oic acid, 7α,12α-dihydroxy-3-oxo-5β-cholan-24-oic acid, 3α,12α-dihydroxy-7-oxo-5β-cholan-24-oic acid, 3α,7α-dihydroxy-12-oxo-5β-cholan-24-oic acid, 7α-hydroxy-3-oxo-5β-cholan-24-oic acid, 3α-hydroxy-7-oxo-5β-cholan-24-oic acid, 3,7-dioxo-5β-cholan-24-oic acid, 12α-hydroxy-3-oxo-5β-cholan-24-oic acid, 3α-hydroxy-12-oxo-5β-cholan-24-oic acid, 3,12-dioxo-5β-cholan-24-oic acid, 3-oxo-5β-cholan-24-oic acid, 3α,6α-dihydroxy-7-oxo-5β-cholan-24-oic acid, 3α-hydroxy-6,7-dioxo-5β-cholan-24-oic acid, 3α-hydroxy-6-oxo-5β-cholan-24-oic acid, and 3,6-dioxo-5β-cholan-24-oic acid were purchased from Steraloids (Newport, USA).

Standards of 7α,12β-dihydroxy-3-oxo-5β-cholan-24-oic acid, 12β-hydroxy-3-oxo-5β-cholan-24-oic acid, 7β-hydroxy-3-oxo-5β-cholan-24-oic acid, 7β,12α-dihydroxy-3-oxo-5β-cholan-24-oic acid, 6α-hydroxy-3-oxo-5β-cholan-24-oic acid, and 6α,7α-dihydroxy-3-oxo-5β-cholan-24-oic acid were synthesized following a procedure reported below, as they were not commercially available. The purity of the synthetized compounds was determined by NMR and HPLC coupled with mass spectrometry. All the standards used in this study were >95% pure. Solid choloylglycine hydrolase (CGH) 12 U/mg and 3α hydroxysteroid NAD(P) oxidoreductase enzyme were purchased from Sigma Aldrich (Saint Louis, USA).

Isopropanol, methanol (CH3OH), and acetonitrile (ACN), all of HPLC-grade (Lichrosolv®), were purchased from Merck (Darmstadt, Germany). Acetic acid (98% pure), formic acid (98% pure), and ammonium hydroxide (98% pure) were purchased from Fluka (Buchs, Switzerland). Water of HPLC-MS grade (Millipore) was produced using the depurative system Milli-Q Synthesis A 10 (Molsheim, France). LiChrosolv Oasis HLB (hydrophilic − lipophilic balance 200 mg, 6 mL) and C18 (200 mg, 6 mL) SPE columns were purchased from Waters (Milford, MA, USA). Other solvents were all of analytical grade.

Stock solutions of each analyte and IS were prepared in isopropanol at a concentration of 1 mg/mL and stored at −20 °C. These stock solutions were further diluted in isopropanol to obtain working solutions containing all the analytes used for method optimization and calibration curves. These working solutions were stored at 4 °C and used for 4 weeks at the most.

2.2. Synthesis of commercially unavailable oxo-BA standards

Oxo-BAs were synthesized by regioselective C3-oxidation from their precursor using Fetizon's reagent [Tserng K.Y. 1978]. For all the synthesized compounds, analytical and spectroscopic data are consistent with literature [Nahar L. 2003, Bortolini O. 2002, Riva S. 1988, Fantin G. 1993]. Purity for tested compound was > 95%.

2.3. Synthesis of isotopically-labeled internal standards (IL-ISs)

2,2,4,4-d4-12α-hydroxy-3-oxo-5β-cholan-24-oic acid and 2,2,4,4-d4-3-oxo-5β-cholan-24-oic acid were enzymatically synthesized respectively from the commercially available 2,2,4,4-d4-deoxycholic acid and 2,2,4,4-d4-lithocholic acid (Sigma Aldrich, 98 atom % D, 98% CP) using 3α hydroxysteroid NAD(P) oxidoreductase enzyme (3αHSDH), following the experimental protocols reported [Bovara R. 1996, Nakagaki M. 1983]. The efficiency in the reactions (>95%) was evaluated for the studied compounds by LC-ESI-MS-MS.

2.4. Faecal sample preparation

Faecal samples were collected from 10 healthy volunteers, 5 males and 5 females, 25–40 years old. The subjects were under regular diet and none of them had history of alimentary disorders or hepatobiliary diseases (protocol No. 7-2209-USPER). Sample preparation was performed as described in our previous studies [Roda A. 2014], with some minor changes. Briefly, aliquots of wet faecal sample homogenate (1 g) were extracted with 3 mL of isopropanol. The mixture was stirred for 30 min at 37 °C, then centrifuged at 2100 rpm for 5 min. The supernatant was then diluted 1:10 (v/v) with 40% isopropanol in 15 mM ammonium acetate at pH 8.00, filtered, transferred to an autosampler vial, and 5 µL injected into the HPLC-ESI-MS system. The results obtained from the analysis, expressed as µg/mL of extract, were converted to µg/g of wet faeces by applying the following formula:

$C = C0*(V/m)$

where:

C represents the concentration expressed as µg/g

C0 represents the concentration expressed as µg/mL

V represents the volume of isopropanol (in mL) used for the extraction

m represents the weight of wet faeces (in grams) subjected to extraction

2.5. HPLC-ESI-MS/MS conditions

Liquid chromatography was performed using a 2690 Alliance system (Waters, Milford, MA, USA). Analytical separation was achieved using a XSelect CSH C18 (5 µm, 150 mm × 2.0 mm i.d, Waters) column kept at a constant temperature of 40 °C throughout the analyses. The mobile phase was constituted by HPLC grade water with 15 mM ammonium acetate at pH 8.00 (A component) and CH3OH (B component). Final separation was achieved at 0.15 mL/min flow rate under gradient elution conditions: 40% B for 2 min, 40–55% B from 2 to 5 min, 55% from 5 to 10 min, 55–65% B from 10 to 20 min, 65–80% B from 20 to 30 min, and 90% B from 30 to 45 min. Re-equilibration at 40% B between analyses was achieved in 5 min, for a total run time of 50 min. The injected sample volume was 5 µL. The autosampler temperature was kept at a temperature of 10 °C, in order to avoid any potential degradation occurring at higher temperature and to preserve sample from precipitation.

The column effluent was introduced into the ESI source (negative ionization mode), connected to a triple quadruple mass spectrometer (Quattro-LC, Micromass) operating in the multiple reaction monitoring (MRM) acquisition mode. Nitrogen was used as nebulizer gas at 75 L/h flow rate and as desolvation gas at 850 L/h. Ion source block and desolvation temperatures were set at 130 °C and 250 °C, respectively. Capillary and cone voltages were -2.7 kV and 60 V, respectively. The MS/MS experimental conditions were tuned by direct infusion of the single analytes. The MS/MS transitions specific for each compound were monitored for the quantification. Table 1 summarizes the retention times and the MS/MS transitions of each single compound.

It is worth to mention that, although no fragmentation reaction occurs to BAs and the $[M-H]^-$ ion is the only one used for each unconjugated BA, the terminology MS/MS transition will be still used throughout the text for convenience and for uniformity purposes.

2.6. Method validation

The method for the determination of oxo-BAs in faecal samples was validated according to International Conference of Harmonization (ICH) guidelines [Guidance for industry 2016].

Selectivity was evaluated by comparing the chromatograms obtained from standards, samples, and spiked sample solutions.

A seven-point calibration curve (0.05, 0.1, 0.5, 1, 5, 10, and 20 µg/mL), obtained by dilution of the working solution with 40% isopropanol in 15 mM ammonium acetate buffer at pH = 8, was used for the linearity study and quantification of the different compounds in faeces.

Calibration curves (0.05, 0.1, 0.5, 1, 5, 10, and 20 µg/mL) using isotopically-labeled internal standards (IL-ISs) were prepared from serial dilutions of the working solution of BAs and ISs with 40% isopropanol in 15 mM ammonium acetate buffer at pH 8. IS concentrations were kept at a constant concentration of 1 µg/ml. Linear calibration curve parameters were obtained from the plot of the analyte peak area against analyte concentration using a least-squares regression analysis. The calibration curves with IL-ISs were obtained plotting the ratio of the analyte to the internal standard signals as a function of the analyte concentration of the standards.

Accuracy and precision, expressed as bias% and coefficient of variation (CV%) respectively, were determined intra and inter-daily, through triplicate analysis over three different days (n = 9), by analyzing quality controls (QCs) at low (0.2 µg/mL), medium (2 µg/mL), and high (15 µg/mL) concentration levels in mobile phase. Bias was calculated as the ratio percentage between the difference of experimental standard concentration ($[std]_{exp}$) and theoretical standard concentration ($[std]_{theor}$) over theoretical standard concentration. General equation used for the calculation of bias% is reported below (equation 1):

Equation 1. $$bias\% = \frac{[std]_{exp} - [std]_{theor}}{[std]_{theor}} \times 100$$

The precision was determined by coefficient of variation percentage (CV%) as the ratio between the standard deviation (SD) and the experimental standard concentration ($[std]_{exp}$). General equation used for the calculation of CV% is reported below (equation 2):

Equation 2. $$CV\% = \frac{SD}{[std]_{exp}} \times 100$$

Limit of detection (LOD) and limit of quantification (LOQ) of the method for each single analyte were experimentally determined by injecting step-wise dilution of the standard solutions. The use of MRM acquisition mode to obtain S/N ratios was possible because matrix effect was considered negligible and the base line was not significantly different between standard and sample solutions. LOD and LOQ were expressed as the concentrations affording a signal-to-noise (S/N) ratio of 3 and 10, respectively.

The matrix effect was evaluated at three concentration levels, comparing the calibration curve slopes and standard areas obtained from standard solutions and spiked samples. The matrix effect (ME%) for all analytes was evaluated as ratio between the absolute matrix effect and the peak area of standard solutions in mobile phase (A_{mp}). The absolute matrix effect was calculated as difference between the peak area of the spiked standard sample (A_{matrix}) and the peak area of the standard solution. For naturally occurring analytes in faeces, during the evaluation of matrix effects, the endogenous contribute was subtracted from the analysis of spiked samples. General equation used for the calculation of M.E.% is reported below:

Equation 3. $$ME\% = \frac{A_{matrix} - A_{mf}}{A_{mf}} \times 100$$

T-test was used to compare the calibration curve slopes ($p < 0.05$).

When isotopically-labeled internal standards (IL-ISs) were available, matrix effect was evaluated by comparing the bile acid contents in real faecal samples in the presence and in the absence of internal standard.

The faecal sample recovery (Rec%) was assessed at three concentration levels (low, medium and high) by comparing analyte peak areas of sample fortified before and after extraction. General equation used for the calculation of recovery percentage is reported below:

$$Rec\% = \frac{[Std]_{before}}{[Std]_{after}} \times 100$$

In these conditions, both samples are subjected to the same matrix effect contribute (if present), making eventual differences dependent only to the efficiency of the extraction. For naturally occurring analytes in faeces, during the evaluation of recovery, the endogenous contribute was subtracted from the analysis of spiked samples.

Stability was evaluated by analysing the QC solutions, stored at 4 °C over a period of 3 months using freshly prepared calibration curves.

2.7. Plasma sample analysis

Oxo-BAs and their precursors were analyzed in plasma samples from healthy volunteers using the same HPLC-ESI-MS/MS method developed for faeces, following an enzymatic deconjugation step and the pre-treatment reported by Roda et al. [Roda A. 2017].

Briefly, plasma samples (300 µL) were mixed with 1.6 mL of 10 mM ammonium acetate buffer (pH 5.6) and 100 µL of a 96 U/mL CGH solution, and the obtained solution was incubated overnight at 37 °C. After incubation, the resulting solution was heated to 64 °C for 30 min, then subjected to the following SPE procedure on C18 cartridges. The SPE cartridge was conditioned with 5 mL of CH_3OH and 5 mL of water prior to sample loading. Plasma samples were loaded into the conditioned cartridge, washed with 10 mL of water, and then eluted with 5 mL of isopropanol. The eluate was dried under vacuum, then reconstituted with 100 µL of 40% isopropanol in 15 mM ammonium acetate buffer at pH 8, filtered, transferred to an autosampler vial, and 5 µL injected into the HPLC-ESI-MS system.

The recovery relative to the SPE procedure on BA-free serum samples was calculated for each analyte at three concentration levels as the percentage ratio between the peak area of solution spiked before the extraction and solution spiked after the SPE procedure. BA-free serum samples were obtained by subjecting

healthy human plasma to a catalytic-carbon-based procedure, as reported by Carrot et al. [Carrott P.J.M. 2007].

3. Results and discussion

3.1. Synthesis of the oxo BAs

3-Oxo BAs (H-N) were synthesized by regioselective C3 oxidation of bile acids precursors A-G using Fetizon's reagent (Fig. 2). In particular, BAs A-G were firstly esterified with catalytic amounts of p-toluensulfonic acid (p-TSA) in CH3OH under ultrasound irradiation. Methyl esters thus formed were then refluxed in freshly distilled toluene with 2 equiv. of Fetizon's reagent (silver carbonate-Celite) [Tserng K.Y. 1978]. Crude mixtures were finally submitted to alkaline hydrolysis (NaOH in CH3OH) affording the desired 3-keto bile acids H-N, in 62–78% yield after chromatographic purification on silica gel.

FIG. 2. SYNTHESIS OF 3-OXO BILE ACIDS H–N. REAGENT AND CONDITIONS: (I) P-TSA, MEOH, ULTRASOUNDS, 2 H; (II) FETIZON REAGENT, DRY TOLUENE, REFLUX, 16 H; (III) MEOH, NAOH, REFLUX, 5 H, 45-77% YIELD OVER THREE STEPS.

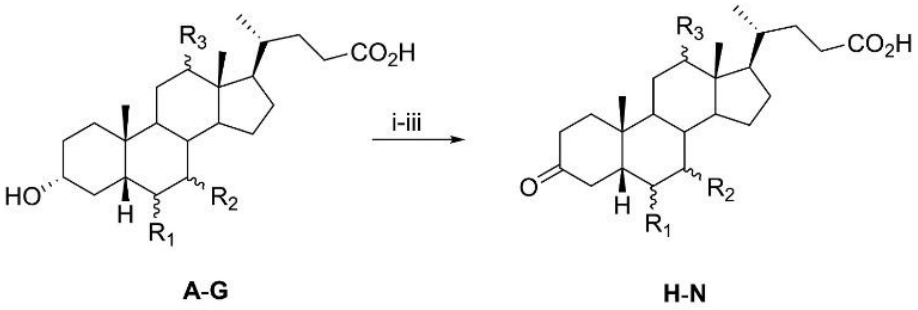

R_1= H; R_2= H; R_3= H (**A,H**)
R_1= H; R_2= βOH; R_3= H (**B,I**)
R_1= H; R_2= βOH; R_3= αOH (**C,J**)
R_1= αOH; R_2= H; R_3= H (**D,K**)
R_1= αOH; R_2= αOH; R_3= H (**E,L**)
R_1= H; R_2= H; R_3= βOH (**F,M**)
R_1= H; R_2= αOH; R_3= βOH (**G,N**)

While BAs A-E were commercially available, 12β-hydroxy derivatives F and G, namely lagodeoxycholic (lagoDCA) and lagocholic (lagoCA), were prepared from deoxycholic acid (DCA, O) and cholic acid (CA, P), respectively (Fig. 3). Initially, DCA (O) and CA (P) were esterified with CH3OH in presence of catalytic amounts of pTSA under ultrasound conditions and then protected at the C3 position by using acetic anhydride (Ac2O) in pyridine/toluene to give intermediates Q and R in 76% and 78% yield, respectively. Compounds Q and R were oxidized at C12 position by means of pyridinium chlorochromate (PCC) in CH2Cl2, reduced with t-BuNH2BH3 reduction and hydrolyzed with NaOH in CH3OH, furnishing the desired products F and G in 46% and 44% yield, respectively (Fig. 3, steps iii-v).

FIG. 3. SYNTHESIS OF 3A,12B-DIHYDROXY-5B-CHOLAN-24-OIC ACID (LAGODCA, F) AND 3A,7A,12B-TRIHYDROXY-5B-CHOLAN-24-OIC ACID (LAGOCA, G). REAGENT AND CONDITIONS: (I) P-TSA, MEOH, ULTRASOUNDS, 2 H; (II) AC2O, DRY PYRIDINE, DRY TOLUENE, R.T., 16 H, 76% FROM O; 78% FROM P; (III) PCC, CH2CL2, R.T., 4 H; (IV) T-BUNH2BH3, DRY CH2CL2, 0 °C, THEN R.T., 6 H; (IV) NAOH, MEOH, REFLUX, 4 H, 46% FROM Q, 44% FROM R.

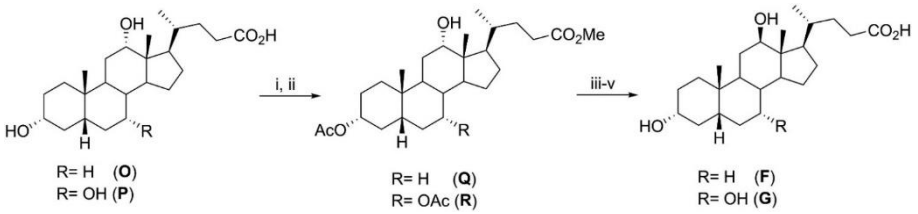

3.2. Synthesis of the Deuterium isotopically-labeled internal standards

3αHSDH enzyme catalyses the oxidation of the 3α hydroxy groups of all bile acids to 3-oxo analogues in presence of NADP as a cofactor with a high regio- and stereo-selectivity and without differences among the different BAs. The regeneration of NADP from NADPH was carried out by glutamate dehydrogenase (GlutDH) at the expenses of α-ketoglutarate [Bovara R. 1996]. Briefly the oxidation reaction was carried out in a 50 mL reactor equipped with a Diaflo PM 10 membrane, containing 40 mL of 50 mM potassium phosphate buffer, pH 8.5, 1 mM 2,2,4,4-d4-lithocholic acid or deoxycholic 2,2,4,4-d4-acid, 5 mM α-ketoglutarate, 0.1 M ammonium acetate, 0.01 mM NADP, 0.1 mM DTT, 2U of 3αHSDH and 4U of GlutDH at 28 °C for 24 hours. Reaction progress was monitored by TLC on precoated silica gel 60 F254 plates (Merck) using chloroform-methanol-acetic acid (10:1:0.5) mixture as eluting system. Plates were sprayed with the Komarowsky's reagent to reveal the compounds.

At the end of the reaction, the solution was filtered, acidified to pH 4 and extracted using ethyl acetate. The 3oxo derivatives were efficiently separated from the unreacted 2,2,4,4-d4-Lithocholic acid or 2,2,4,4-d4-Deoxycholic acid by preparative TLC on silica-coated plates using the same mixture employed for monitoring the reaction progress. The isolated 3-oxo products where then eluted with methanol and dried under gentle nitrogen stream. The purity of the isolated products was assessed by LC-ES-MS, resulting in pure compounds (>95%) thus suitable to be used as internal standards

3.3. Chromatographic condition set up

Ethylene Bridged Hybrid (BEH) and High Strength Silica (HSS) technology are the two most frequently used for the BA analysis [Yin S. 2017]. CSH coloumns are BEH variants specific for basic buffer, used in several studies [Roda A. 2014] for the chromatographic separation of BAs.

Phenyl-hexyl and C18 columns (Xselect CSH 5 u M 2,1 × 150 mm 5 µm) were tested in this study. To select the optimal separation conditions, single solutions and a mixture of oxo-BAs underwent a series of iterated

analyses, using a conventional experimental design approach. The best results were achieved with the C18 column, which provided good chromatographic separation and peak symmetry in a relatively short time.

As a second step, different mobile phase compositions were evaluated at different solvent gradients, according with common solvents and buffer used for BAs analysis and for the few oxo-BAs investigated so far [Goto J. 1991, Muto A. 2012, Perwaiz S. 2002]. As organic component (solvent B), CH3OH, CH3CN, and a 50:50 v/v mixture were screened, while formic acid 1% (pH 3), acetic acid 0.1% (pH 5), and ammonium acetate 15 mM (pH 8) were tested as aqueous solvent (solvent A). In terms of chromatographic resolution, peak shapes, and analysis times, the best compromise was obtained by using a mobile phase made of ammonium acetate 15 mM (pH = 8) and CH3OH. The use of an acidic mobile phase is generally preferred when working in negative ionization mode [Zhou S. 2000]. However, our results show that sensitivity increases by increasing the pH. This result might be explained by the fact that the basic characteristics of the mobile phase contribute to the deprotonation of the analytes.

Finally, we investigated the influence of flow rate, in the range 0.10–0.50 mL/min, and column temperature, in the range 20–60 °C. The flow rate was set at 0.15 mL/min because higher flow rates corresponded to increased backpressure, leading to poorer peak shape and loss of resolution. Indeed, the optimized flow rate was the best choice to obtain a suitable chromatographic separation, limiting the overlap of structural isomers. The best temperature compromise was 40 °C because temperature increase slightly reduced the retention times, peak symmetry, and backpressure (data not shown).

FIG. 4. TOTAL ION CURRENT CHROMATOGRAM REPORTING THE SEPARATION OF ALL 21 OXO-BAS INVESTIGATED. 7A,12B-DIHYDROXY-3-OXO-CHOLAN-24-OIC ACID (1), 7B,12A-DIHYDROXY-3-OXO-CHOLAN-24-OIC ACID (2), 3A,6A-DIHYDROXY-7-OXO-CHOLAN-24-OIC ACID (3), 3A,12A-DIHYDROXY-7-OXO-CHOLAN-24-OIC ACID (4), 3A,7A-DIHYDROXY-12-OXO-CHOLAN-24-OIC ACID (5), 6A,7A-DIHYDROXY-3-OXO-CHOLAN-24-OIC ACID (6), 7A,12A-DIHYDROXY-3-OXO-CHOLAN-24-OIC ACID (7), 7B-HYDROXY-3-OXO-CHOLAN-24-OIC ACID (8), 6A-HYDROXY-3-OXO-CHOLAN-24-OIC ACID (9), 3A-HYDROXY-6-OXO-CHOLAN-24-OIC ACID (10), 3A-HYDROXY-7-OXO-CHOLAN-24-OIC ACID (11), 12B-HYDROXY-3-OXO-CHOLAN-24-OIC ACID (12), 3A-HYDROXY-12-OXO-CHOLAN-24-OIC ACID (13), 7A-HYDROXY-3-OXO-CHOLAN-24-OIC ACID (14), 12A-HYDROXY-3-OXO-CHOLAN-24-OIC ACID (15), 3,7-DIOXO-CHOLAN-24-OIC ACID (16), 3,12-DIOXO-CHOLAN-24-OIC ACID (17), 3,6-DIOXO-CHOLAN-24-OIC ACID (18), 3,7,12-TRIOXO-CHOLAN-24-OIC ACID (19), 3A-HYDROXY-6,7-DIOXO-CHOLAN-24-OIC ACID (20), 3-OXO-CHOLAN-24-OIC ACID (21).

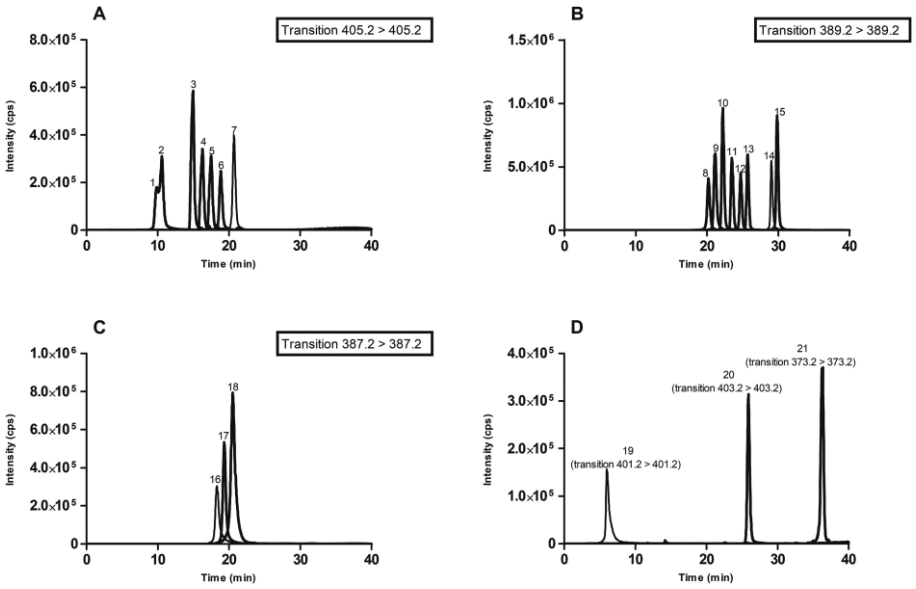

Fig. 4 shows the chromatograms relative to the different investigated transitions. Fig. 4A refers to the transition 405.2 > 405.2, comprising seven oxo-BAs bearing one keto and two hydroxyl groups. All the compounds in this window are completely separated, with the exception of peaks 1 and 2, which can still be discriminated for a qualitative identification, despite the partial coelution. In case of their simultaneous presence in samples, only the quantification of their sum can be performed, also considering their similar response factors.

Fig. 4B refers to the transition 389.2 > 389.2, comprising the oxo-BAs bearing one keto and one hydroxyl group. A complete chromatographic separation was achieved for all 8 compounds, with satisfying peak shape and limited retention times.

Fig. 4C refers to the transition 387.2 > 387.2, comprising the oxo-BAs bearing two keto groups. The hydroxyl groups oriented toward one side of the molecule are absent. Their replacement with planar keto groups does not allow the stationary phase to properly discriminate between these compounds. As a consequence, a poor chromatographic separation was obtained, even though the peaks are resolved at about 20% height and the different retention times can still be used for the correct identification. The integration mode of these non-baseline resolved peaks has been chosen depending on peak high and width (drop method, valley method), to obtain better accuracy.

In the linearity experiments, for analytes at similar concertation levels, the drop method integration lead to higher correlation coefficient values.

Fig. 4D refers to the transitions 403.2 > 403.2, 401.2 > 401.2, and 373.2 > 373.2, corresponding to the oxo-BAs bearing, respectively, two keto and one hydroxyl groups, three keto groups, and only one keto group. In this case, by virtue of their unique m/z, these compounds are singularly revealed with high selectivity.

Secondary BAs are present at high concentrations in faecal matrix. We used the described protocol to analyze them and primary BAs to exclude their potential interference, obtaining a more comprehensive LC–MS method. DCA and LCA are the most abundant BAs in faeces. As depicted in Fig. 5, their retention times (Table 1) differ from those of their oxidized metabolites, excluding a potential signal suppression due to their coelution.

FIG. 5. TOTAL ION CURRENT CHROMATOGRAM OF ENDOGENOUS PRIMARY AND SECONDARY BAS OBTAINED USING THE DEVELOPED HPLC-ESI-MS/MS METHOD.

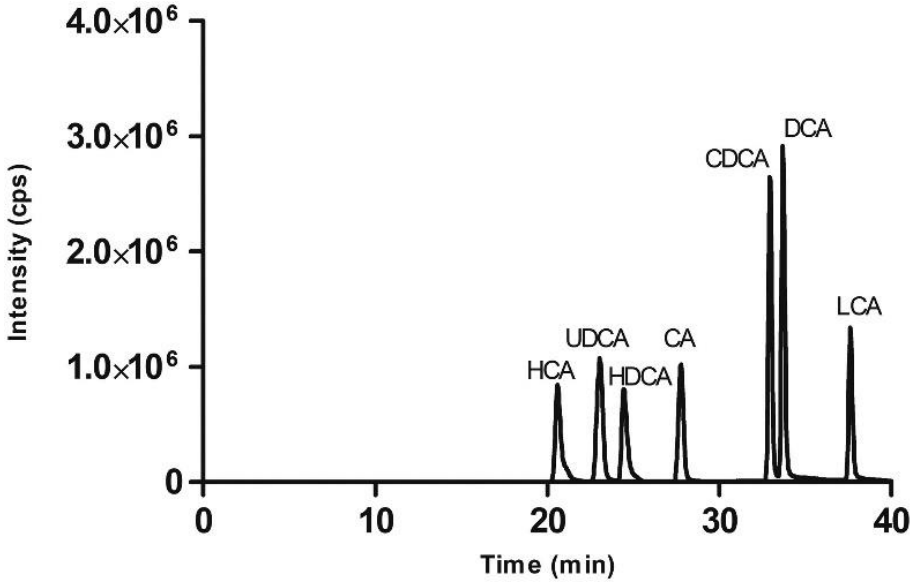

Considering this result, the described method might be useful for the simultaneous qualitative and quantitative determination of both oxo-BAs and their metabolic precursors.

3.4. Mass spectrometry set-up

Bile acids and their oxo-derivatives are acidic steroids with a carboxylic group in C-24 position and with a pKa = 5, not related to the number, position of substituents in the sterol moiety. Therefore, they are easily detectable in ES negative ion mode operating at a pH higher than 6.5.

The method was intended for application to a complex matrix (i.e. faeces), so the full scan acquisition mode was excluded, while both MRM and SIM were tested to verify which mode ensured the best performances.

Unfortunately, BAs and their oxo-derivatives do not extensively fragment and the only actual fragmentation reaction, corresponding to the transition $[M-H]^- > [M-H-CO2]^-$, was observable only at very high collision energies and was of very limited use because of the low sensitivity. However, despite this limitation, better sensitivity (higher signal-to-noise ratio) and linearity were experienced working in MRM mode at very low collision energies, monitoring the transition $[M-H]^- > [M-H]^-$, rather than SIM.

We conducted experiments involving the direct infusion of single compounds onto the ESI interface. These experiments highlighted the need to avoid CH3OH in the extraction and sample preparation. Indeed, its use led to the formation of acetals or hemiacetals, especially for compounds bearing the oxo group in 3-position (Figure 6A).

FIG 6. MASS SPECTRA OBTAINED IN FULL SCAN MODE FROM THE DIRECT INFUSION OF 7A,12A-DIHYDROXY-3-OXO-CHOLAN-24-OIC ACID SOLUTION (1 □G/ML) IN MEOH (A) AND IPROH (B). THE SIGNALS AT M/Z 405.2 AND 451.2 CORRESPOND TO THE DEPROTONATED MOLECULE AND THE RESPECTIVE ACETAL, RESPECTIVELY.

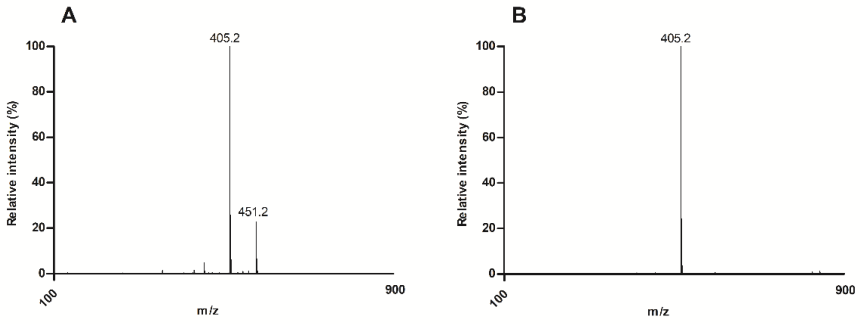

This inconvenience was overcome by using a secondary alcohol, like isopropanol, which does not react with the oxo group since it is less nucleophilic than a primary alcohol (Figure 6B).

3.5. Method validation

Calibration curve parameters for all the considered compounds, in the range 0.05–20 μg/mL, were obtained by plotting the peak area of the analyte standards against their theoretical concentration through a linear least-square regression analysis. The resulting calibration curve equations were in the form of $Y = a (\pm \delta a)X + b (\pm \delta b)$. The selected calibration interval, identical for all the investigated oxo-BAs, ranged from the minimum amount quantifiable with a bias% lower than 10% to concentrations typical of secondary BAs in healthy subject, the most abundant in faecal extracts. In cases where the concentration in samples falls outside the calibration range, it is still possible to perform different proper dilution. Calibration curve determination coefficients (r2) were ≥ 0.995 for all molecules, showing excellent linearity over two orders of concentrations.

Experimental LOD values ranged from 5 ng/mL to 10 ng/mL, while LOQ values ranged from 15 ng/mL to 30 ng/mL for all compounds. Results are shown in Table 2.

TABLE 2. LOD AND LOQ VALUES OF THE DEVELOPED METHOD FOR ALL THE INVESTIGATED COMPOUNDS.

Compound	LOD (ng/mL)	LOQ (ng/mL)
7α,12α-dihydroxy-3-oxo-5-cholan-24-oic acid	10	30
7α,12β-dihydroxy-3-oxo-cholan-24-oic acid	10	30
3α,12α-dihydroxy-7-oxo-cholan-24-oic acid	10	30
3α,7α-dihydroxy-12-oxo-cholan-24-oic acid	10	30
7α-hydroxy-3-oxo-cholan-24-oic acid	5	15
3α-hydroxy-7-oxo-cholan-24-oic acid	5	15
3,7-dioxo-cholan-24-oic acid	5	15
12α-hydroxy-3-oxo-cholan-24-oic acid	5	15
12β-hydroxy-3-oxo-cholan-24-oic acid	5	15
3α-hydroxy-12-oxo-cholan-24-oic acid	10	30
3,12-dioxo-cholan-24-oic acid	10	30
3-oxo-cholan-24-oic acid	5	15
7β-hydroxy-3-oxo-cholan-24-oic acid	10	30
7β,12α-dihydroxy-3-oxo-cholan-24-oic acid	5	15
3α,6α-dihydroxy-7-oxo-cholan-24-oic acid	5	15
3α-hydroxy-6,7-dioxo-cholan-24-oic acid	10	30
3,7,12-trioxo-cholan-24-oic acid	10	30
3α-hydroxy-6-oxo-cholan-24-oic acid	10	30
3,6-dioxo-cholan-24-oic acid	10	30
6α-hydroxy-3-oxo-cholan-24-oic acid	10	30
6α,7α-dihydroxy-3-oxo-cholan-24-oic acid	5	15
3α,7α,12α-trihydroxy-cholan-24-oic acid (CA)	10	30
3α,6α,7α-trihydroxy-cholan-24-oic acid (HCA)	10	30
3α,7α-dihydroxy-cholan-24-oic acid (CDCA)	5	15
3α,12α-dihydroxy-cholan-24-oic acid (DCA)	5	15
3α,6α-dihydroxy-cholan-24-oic acid (HDCA)	10	30
3α,7β-dihydroxy-cholan-24-oic acid (UDCA)	10	30
3α-hydroxy-cholan-24-oic acid (LCA)	5	15

Precision and accuracy, expressed as variation coefficients% and bias%, were less than 13% for all compounds at the different concentration levels of the QCs: low (0.2 µg/mL), medium (2 µg/mL), and high (15 µg/mL) (Tables 3).

TABLE 3. ACCURACY AND PRECISION VALUES OF THE DEVELOPED METHOD FOR ALL THE INVESTIGATED COMPOUNDS

Compound	Intraday values (n=3)						Inter day values (n=9)					
	QClow		QCmed		QChigh		QClow		QCmed		QChigh	
	Bias %	C V %	Bias %	C V %	Bias %	C V %	Bias %	C V %	Bias %	C V %	Bias %	C V %
7α,12α-dihydroxy-3-oxo-cholan-24-oic acid	8	5	7	4	10	5	9	5	7	4	10	5
7α,12β-dihydroxy-3-oxo-cholan-24-oic acid	12	4	10	3	9	7	10	5	10	5	8	7
3α,12α-dihydroxy-7-oxo-cholan-24-oic acid	9	4	8	3	7	4	8	5	9	5	6	6
3α,7α-dihydroxy-12-oxo-cholan-24-oic acid	8	3	11	3	6	6	7	4	10	4	8	6
7α-hydroxy-3-oxo-cholan-24-oic acid	10	6	9	4	8	3	10	6	8	6	8	4
3α-hydroxy-7-oxo-cholan-24-oic acid	13	5	10	5	7	4	10	6	10	7	8	4
3,7-dioxo-cholan-24-oic acid	7	7	12	5	9	3	8	7	11	6	8	4
12α-hydroxy-3-oxo-cholan-24-oic acid	8	6	10	4	11	6	9	5	10	5	11	6
12β-hydroxy-3-oxo-cholan-24-oic acid	12	3	8	3	8	6	11	5	8	3	7	6
3α-hydroxy-12-oxo-cholan-24-oic acid	11	7	7	5	10	6	9	5	6	5	9	6
3,12-dioxo-cholan-24-oic acid	12	5	11	7	12	5	11	6	11	7	11	5
3-oxo-cholan-24-oic acid	8	4	7	7	7	7	8	5	7	7	8	7
7β-hydroxy-3-oxo-cholan-24-oic acid	9	3	10	6	9	3	9	3	9	7	8	3
7β,12α-dihydroxy-3-oxo-cholan-24-oic acid	11	3	8	3	6	6	9	5	8	4	8	6
3α,6α-dihydroxy-7-oxo-cholan-24-oic acid	10	6	12	5	8	4	10	6	9	6	8	5
3α-hydroxy-6,7-dioxo-cholan-24-oic acid	12	4	12	3	9	3	9	5	11	5	8	3
3,7,12-trioxo-cholan-24-oic acid	8	5	10	7	10	5	8	4	11	8	9	5
3α-hydroxy-6-oxo-cholan-24-oic acid	13	5	7	6	11	4	11	6	7	6	9	4
3,6-dioxo-cholan-24-oic acid	11	5	11	7	6	4	10	6	10	7	6	6
6α-hydroxy-3-oxo-cholan-24-oic acid	10	3	8	4	9	3	9	3	8	4	9	3
6α,7α-dihydroxy-3-oxo-cholan-24-oic acid	12	3	10	6	10	6	10	4	11	6	9	7
3α,7α,12α-trihydroxy-cholan-24-oic acid (CA)	10	4	9	8	11	6	9	5	8	9	11	6
3α,6α,7α-trihydroxy-cholan-24-oic acid (HCA)	9	6	8	5	10	5	8	6	10	5	9	7
3α,7α-dihydroxy-cholan-24-oic acid (CDCA)	7	7	5	4	6	6	8	8	6	5	8	4

3α,12α-dihydroxy-cholan-24-oic acid (DCA)	9	8	5	8	8	4	7	8	5	4	8	4
3α,6α-dihydroxy-cholan-24-oic acid (HDCA)	8	5	9	8	7	6	9	5	9	7	7	5
3α,7β-dihydroxy-cholan-24-oic acid (UDCA)	7	6	8	5	5	6	8	5	8	4	8	7
3α-hydroxy-cholan-24-oic acid (LCA)	5	6	5	7	8	5	7	7	7	7	8	5

Selectivity was established by injection of single standards and mixtures thereof in order to determine the retention times. Standard solutions were compared to fortified samples with known amounts of analyte. These comparisons showed that there were no interferences due to the matrix components. During the quantification in faecal samples, standard additions in real matrix was used to exclude erroneous quantifications due to small chromatographic shifts. Despite the use of no specific MRM ionic transition for the quantification of isomeric compounds, total co-elution was never obtained also for the most similar dioxo derivatives (MRM [387.2] > [387.2]).Therefore, the possibility of a wrong interpretation of the chromatographic peaks in the real samples is unlikely, even when other oxo-BAs than the ones here studied are potentially present.

The matrix effect percentage was evaluated at three concentration levels by comparing the calibration curve slopes and areas, obtained from standard solutions and samples spiked with standards; when available, isotopically-labeled internal standards (IL-ISs) were also used as described in section 2.6. Values greater and lower than 0% indicated ionic increase (positive matrix effect) and ionic suppression (negative matrix effect), respectively. Matrix effect values were considered negligible being always in a range −13.5 to −4.5% for all studied analytes (Table 4).

TABLE 4. RECOVERY (REC%) AND MATRIX EFFECT (ME%) VALUES OF THE DEVELOPED METHOD FOR ALL THE INVESTIGATED COMPOUNDS IN FACES.

	ME%			Rec % (mean ± SD)		
	QClow	QCmed	QChigh	QClow	QCmed	QChigh
7α,12α-dihydroxy-3-oxo-cholan-24-oic acid	-5.2	-10.2	-9.8	95±5	94±8	94±7
7α,12β-dihydroxy-3-oxo-cholan-24-oic acid	-1.2	-7.2	-8.6	98± 6	94±10	98±4
3α,12α-dihydroxy-7-oxo-cholan-24-oic acid	-6.7	-7.8	-8.4	98±6	93±8	96±8
3α,7α-dihydroxy-12-oxo-cholan-24-oic acid	-7.8	-12.3	-7.5	99±10	95±6	97±6
7α-hydroxy-3-oxo-cholan-24-oic acid	-8.2	-6.5	-8.5	97± 6	93±8	97±2
3α-hydroxy-7-oxo-cholan-24-oic acid	-8.6	-8.1	-11.5	94±6	92±6	98±5

3,7-dioxo-cholan-24-oic acid	-6.8	-13.5	-10.3	96± 5	95±8	97±3
12α-hydroxy-3-oxo-cholan-24-oic acid	-8.4	-6.6	-12.4	97±5	95±6	97±3
12β-hydroxy-3-oxo-cholan-24-oic acid	-9.2	-8.4	-7.2	97±8	92±8	97±8
3α-hydroxy-12-oxo-cholan-24-oic acid	-9.2	-10.5	-10.2	94±7	96±8	96±3
3,12-dioxo-cholan-24-oic acid	-2.3	-4.4	-7.4	95±8	95±7	98±5
3-oxo-cholan-24-oic acid	-6.4	-7.4	-5.3	97±6	92±6	98±3
7β-hydroxy-3-oxo-cholan-24-oic acid	-5.3	-12.4	-6.2	101±6	93±8	98±4
7β,12α-dihydroxy-3-oxo-cholan-24-oic acid	-3.2	-5.5	-7.1	95±8	95±7	92±6
3α,6α-dihydroxy-7-oxo-cholan-24-oic acid	-6.2	-8.4	-10.1	98±4	92±6	94±7
3α-hydroxy-6,7-dioxo-cholan-24-oic acid	-8.6	-8.2	-5.8	94±7	93±8	99±4
3,7,12-trioxo-cholan-24-oic acid	-7.3	-10.2	-4.5	96±8	96±9	98±6
3α-hydroxy-6-oxo-cholan-24-oic acid	-4.2	-11.2	-6.6	97±6	93±9	97±4
3,6-dioxo-cholan-24-oic acid	-7.2	-6.7	-7.1	94±6	93±8	95±5
6α-hydroxy-3-oxo-cholan-24-oic acid	-4.9	-8.4	-8.3	94±5	92±7	96±8
6α,7α-dihydroxy-3-oxo-cholan-24-oic acid	-5.6	-7.1	-7.5	101±5	94±5	94±8
3α,7α,12α-trihydroxy-5b-cholan-24-oic acid (CA)	-9.2	-10.4	-8.1	98±6	95±6	95±6
3α,6α,7α-trihydroxy-5b-cholan-24-oic acid (HCA)	-0.8	-6.8	-7.1	97±7	93±8	98±3
3α,7α-dihydroxy-5b-cholan-24-oic acid (CDCA)	-9.2	-7.7	-8.4	93±4	95±7	97±4
3α,12α-dihydroxy-5b-cholan-24-oic acid (DCA)	-8.2	-7.4	-5.8	98±3	95±4	95±9
3α,6α-dihydroxy-5b-cholan-24-oic acid (HDCA)	-10.5	-11.3	-8.2	93±5	92±4	95±7
3α,7β-dihydroxy-5b-cholan-24-oic acid (UDCA)	-6.2	-10.9	-6.8	92±5	92±5	97±6
3α-hydroxy-5b-cholan-24-oic acid (LCA)	-7.7	-11.4	-10.2	97±6	95±8	96±5

Moreover, the curve slopes obtained with standard additions did not differ significantly from those in neat solution (p n.s.) in the same concentration range.

The quantifications in real samples using IL-ISs afforded results not significantly different (p n.s.) to those obtained without internal standard (Table 5).

TABLE 5. COMPARISON BETWEEN THE RESULTS OBTAINED FROM CALIBRATION CURVES OF STANDARD SOLUTIONS IN ABSENCE OF INTERNAL STANDARD (A) AND IL-IS METHOD (B).

Sample 1					
Analyte	**IL-IS**	**A**	**B**	**P-value**	**Difference %***
3-oxo-cholan-24-oic acid	3-oxo-cholan-24-oic acid -2,2,4,4-d4	87 ± 9	92 ± 6	***0,6560***	***-5.43***
12α-hydroxy-3-oxo-cholan-24-oic acid	12α-hydroxy-3-oxo-cholan-24-oic acid-2,2,4,4-d4	51 ± 4	54 ± 7	***0.5543***	***-5.56***
3α,12α-dihydroxy-cholan-24-oic acid (DCA)	3α,12α-dihydroxy-cholan-24-oic acid-2,2,4,4-d4	614 ± 27	625 ±18	***0.5887***	***-1.76***
3α-hydroxy-cholan-24-oic acid (LCA)	3α-hydroxy-cholan-24-oic acid-2,2,4,4-d4	182 ± 12	180 ±15	***0.8657***	***1.11***
Sample 2					
Analyte	**IL-IS**	**A**	**B**	**P-value**	**Difference %***
3-oxo-cholan-24-oic acid	3-oxo-cholan-24-oic acid – 2,2,4,4-d4	41 ± 6	43 ± 8	***0.7465***	***-4.65***
12α-hydroxy-3-oxo-cholan-24-oic acid	12α-hydroxy-3-oxo-cholan-24-oic acid-2,2,4,4-d4	36 ± 6	36 ± 3	***1.0000***	***0.00***
3α,12α-dihydroxy-cholan-24-oic acid (DCA)	3α,12α-dihydroxy-cholan-24-oic acid-2,2,4,4-d4	739 ± 38	746 ± 28	***0.8101***	***-0.94***
3α-hydroxy-cholan-24-oic acid (LCA)	3α-hydroxy-cholan-24-oic acid -2,2,4,4-d4	158 ± 9	172 ± 12	***0.2729***	***-8.14***
Sample 3					
Analyte	**IL-IS**	**A**	**B**	**P-value**	**Difference %***
3-oxo-cholan-24-oic acid	3-oxo-cholan-24-oic acid-2,2,4,4-d4	62 ± 4	63 ± 6	***0.5110***	***-1.61***
12α-hydroxy-3-oxo-cholan-24-oic acid	12α-hydroxy-3-oxo-cholan-24-oic acid-2,2,4,4-d4	61 ± 6	65 ± 7	***0.8220***	***-6.15***
3α,12α-dihydroxy-cholan-24-oic acid (DCA)	3α,12α-dihydroxy-cholan-24-oic acid-2,2,4,4-d4	214 ± 15	219 ± 22	***0.7613***	***-2.28***
3α-hydroxy-cholan-24-oic acid (LCA)	3α-hydroxy-cholan-24-oic acid-2,2,4,4-d4	84 ± 11	81 ± 13	***0.7755***	***3.70***
Sample 4					
Analyte	**IL-IS**	**A**	**B**	**P-value**	**Difference %***
3-oxo-cholan-24-oic acid	3-oxo-cholan-24-oic acid -2,2,4,4-d4	87 ± 8	89 ± 6	***0.7465***	***-2.29***
12α-hydroxy-3-oxo-cholan-24-oic acid	12α-hydroxy-3-oxo-cholan-24-oic acid -2,2,4,4-d4	22 ± 2	24 ± 3	***0.3911***	***-8.33***
3α,12α-dihydroxy-cholan-24-oic acid (DCA)	3α,12α-dihydroxy-cholan-24-oic acid-2,2,4,4-d4	432 ± 19	443 ± 17	***0.4964***	***-2.48***
3α-hydroxy-cholan-24-oic acid (LCA)	3α-hydroxy-cholan-24-oic acid-2,2,4,4-d4	100 ± 7	106 ± 5	***0.2936***	***-5.66***
Sample 5					
Analyte	**IL-IS**	**A**	**B**	**P-value**	**Difference %***
3-oxo-cholan-24-oic acid	3-oxo-cholan-24-oic acid -2,2,4,4-d4	90 ± 9	87 ± 12	***0.7465***	***3.45***
12α-hydroxy-3-oxo-cholan-24-oic acid	12α-hydroxy-3-oxo-cholan-24-oic acid-2,2,4,4-d4	86 ± 5	92 ± 28	***0.3325***	***-6.52***
3α,12α-dihydroxy-cholan-24-oic acid (DCA)	3α,12α-dihydroxy-cholan-24-oic acid-2,2,4,4-d4	774 ± 32	785 ± 27	***0.6727***	***-1.40***
3α-hydroxy-cholan -24-oic acid (LCA)	3α-hydroxy-cholan-24-oic acid-2,2,4,4-d4	68 ± 4	67 ± 6	***0.8220***	***1.49***
Sample 6					
Analyte	**IL-IS**	**A**	**B**	**P-value**	**Difference %***

3-oxo-cholan-24-oic acid	3-oxo-cholan-24-oic acid -2,2,4,4-d4	47 ± 4	50 ± 5	***0.4232***	***-6.00***
12α-hydroxy-3-oxo-cholan-24-oic acid	12α-hydroxy-3-oxo-cholan-24-oic acid-2,2,4,4-d4	44 ± 5	49 ± 3	***0.2117***	***-10.20***
3α,12α-dihydroxy-cholan-24-oic acid (DCA)	3α,12α-dihydroxy-cholan-24-oic acid-2,2,4,4-d4	254 ± 18	272 ± 15	***0.2541***	***-6.62***
3α-hydroxy-cholan-24-oic acid (LCA)	3α-hydroxy-cholan-24-oic acid-2,2,4,4-d4	95 ± 9	96 ± 9	***0.8983***	***-1.05***
Sample 7					
Analyte	**IL-IS**	**A**	**B**	**P-value**	**Difference %***
3-oxo-cholan-24-oic acid	3-oxo-cholan-24-oic acid -2,2,4,4-d4	33 ± 3	36 ± 5	***0.4232***	***-8.33***
12α-hydroxy-3-oxo-cholan-24-oic acid	12α-hydroxy-3-oxo-cholan-24-oic acid-2,2,4,4-d4	79 ± 8	83 ± 6	***0.5265***	***-5.06***
3α,12α-dihydroxy-cholan-24-oic acid (DCA)	3α,12α-dihydroxy-cholan-24-oic acid-2,2,4,4-d4	587 ± 32	599 ± 52	***0.7507***	***-2.00***
3α-hydroxy-5β-cholan-24-oic acid (LCA)	3α-hydroxy-cholan-24-oic acid-2,2,4,4-d4	82 ± 6	90 ± 5	***0.1507***	***-8.89***
Sample 8					
Analyte	**IL-IS**	**A**	**B**	**P-value**	**Difference %***
3-oxo-cholan-24-oic acid	3-oxo-cholan-24-oic acid -2,2,4,4-d4	65 ± 3	68 ± 2	***0.2230***	***-4.41***
12α-hydroxy-3-oxo-cholan-24-oic acid	12α-hydroxy-3-oxo-cholan-24-oic acid-2,2,4,4-d4	59 ± 4	63 ± 4	***0.2879***	***-6.35***
3α,12α-dihydroxy-5β-cholan-24-oic acid (DCA)	3α,12α-dihydroxy-cholan-24-oic acid-2,2,4,4-d4	291 ± 12	284 ± 16	***0.5771***	***2.46***
3α-hydroxy-5β-cholan-24-oic acid (LCA)	3α-hydroxy-5β-cholan-24-oic acid-2,2,4,4-d4	103 ± 6	111 ± 5	***0.1507***	***-7.21***
Sample 9					
Analyte	**IL-IS**	**A**	**B**	**P-value**	**Difference %***
3-oxo-cholan-24-oic acid	3-oxo-cholan-24-oic acid -2,2,4,4-d4	51 ± 3	56 ± 6	***0.2663***	***-9.80***
12α-hydroxy-3-oxo-cholan-24-oic acid	12α-hydroxy-3-oxo-cholan-24-oic acid-2,2,4,4-d4	33 ± 3	36 ± 5	***0.4232***	***-8.33***
3α,12α-dihydroxy-cholan-24-oic acid (DCA)	3α,12α-dihydroxy-cholan-24-oic acid-2,2,4,4-d4	215 ± 10	222 ± 14	***0.5199***	***-3.15***
3α-hydroxy-5β-cholan-24-oic acid (LCA)	3α-hydroxy-cholan-24-oic acid-2,2,4,4-d4	100 ± 10	100 ± 8	***1.0000***	***0.00***
Sample 10					
Analyte	**IL-IS**	**A**	**B**	**P-value**	**Difference %***
3-oxo-cholan-24-oic acid	3-quinoid-cholan-24-oic acid -2,2,4,4-d4	30 ± 3	32 ± 2	***0.3911***	***-6.66***
12α-hydroxy-3-oxo-cholan-24-oic acid	12α-hydroxy-3-oxo-cholan-24-oic acid-2,2,4,4-d4	64 ± 4	65 ± 5	***0.8202***	***-1.56***
3α,12α-dihydroxy-cholan-24-oic acid (DCA)	3α,12α-dihydroxy-5β-cholan-24-oic acid-2,2,4,4-d4	545 ± 34	559 ± 29	***0.3906***	***-2.50***
3α-hydroxy-cholan-24-oic acid (LCA)	3α-hydroxy-cholan-24-oic acid-2,2,4,4-d4	62 ± 3	67 ± 4	***0.1583***	***-7.46***
					****(A-B)/B·100***

Based on these results, we excluded the use of further purification steps, such as SPE protocols. Indeed, as SPE preconcentrates the analyte along with interferents that have similar polarities, this clean-up process

could sometimes magnify the ion suppression/enhancement effects, thus its use is recommended only if necessary [Gosetti F. 2010].

According to the good performances of the method in terms of precision and accuracy and considering the few steps required for pre-analytical sample preparation, the use of internal standard, although generally recommended, provided no evident benefits. Indeed, the similar results achieved when quantification was performed with deuterated IS, as reported above in the text, further demonstrate the validity of the method. For these reasons the use of an internal standards was not applied for the results reported in Table 8. This choice was also supported by previous studies showing that, in some cases, the external calibration is convenient compared to the internal standard technique [Haefelfinger P. 1981].

The recovery percentage from faecal matrix was evaluated at three concentration levels. The calculated values were higher than 92% for all the investigated analytes at the three concentration levels (Table 4).

Stability evaluated over a period of 3 months showed that standard solutions obtained in isopropanol and stored at 4 °C had concentration variations below 10%, therefore in line with the accuracy of the method.

A full method validation was not carried out for plasma analysis. Indeed, plasma samples were analyzed in order to determine the potential intestinal absorption in the colon of oxo-BAs. A complete profiling of these compounds and their accurate quantification in this fluid was not in the scope of this work, therefore only a semiquantitative determination has been provided (see below paragraph “plasma sample analysis”). The recovery percentage from plasma samples was evaluated at three concentration levels. The calculated values were higher than 92% for all the investigated analytes at the three concentration levels (Table 6).

TABLE 6. BA RECOVERIES AFTER SPE EXTRACTION IN PLASMA SAMPLES

Compound	QC low (%±SD)	QC med (%±SD)	QC high. (%±SD)
7α,12α-dihydroxy-3-oxo-cholan-24-oic acid	91±8	93±5	94±6
7α,12β-dihydroxy-3-oxo-cholan-24-oic acid	94±9	94±6	96±4
3α,12α-dihydroxy-7-oxo-cholan-24-oic acid	92±7	93±4	93±8
3α,7α-dihydroxy-12-oxo-cholan-24-oic acid	90±5	98±6	94±6
7α-hydroxy-3-oxo-cholan-24-oic acid	93±4	95±5	96±6
3α-hydroxy-7-oxo-cholan-24-oic acid	94±4	93±6	94±3
3,7-dioxo-cholan-24-oic acid	91±7	95±2	96±4
12α-hydroxy-3-oxo-cholan-24-oic acid	90±8	97±6	95±9
12β-hydroxy-3-oxo-cholan-24-oic acid	92±6	94±4	96±8
3α-hydroxy-12-oxo-cholan-24-oic acid	97±2	95±6	94±6
3,12-dioxo-cholan-24-oic acid	94±8	93±7	97±5
3-oxo-cholan-24-oic acid	91±8	92±8	94±8
7β-hydroxy-3-oxo-cholan-24-oic acid	93±7	94±5	94±5
7β,12α-dihydroxy-3-oxo-cholan-24-oic acid	93±4	95±7	95±4

3α,6α-dihydroxy-7-oxo-cholan-24-oic acid	96±5	92±6	93±6
3α-hydroxy-6,7-dioxo-cholan-24-oic acid	92±4	96±7	92±6
3,7,12-trioxo-cholan-24-oic acid	93±5	97±6	96±8
3α-hydroxy-6-oxo-cholan-24-oic acid	96±4	94±3	97±4
3,6-dioxo-cholan-24-oic acid	96±6	93±8	96±5
6α-hydroxy-3-oxo-cholan-24-oic acid	92±3	92±8	96±5
6α,7α-dihydroxy-3-oxo-cholan-24-oic acid	93±4	95±4	93±6
3α,7α,12α-trihydroxy-cholan-24-oic acid (CA)	94±7	94±7	94±6
3α,6α,7α-trihydroxy-cholan-24-oic acid (HCA)	91±3	92±4	94±5
3α,7α-dihydroxy-cholan-24-oic acid (CDCA)	93±6	96±6	93±7
3α,12α-dihydroxy-cholan-24-oic acid (DCA)	96±6	96±5	92±8
3α,6α-dihydroxy-cholan-24-oic acid (HDCA)	97±5	93±6	91±4
3α,7β-dihydroxy-cholan-24-oic acid (UDCA)	96±6	92±5	96±3
3α-hydroxy-cholan-24-oic acid (LCA)	98±4	93±4	96±6

3.6. Profile of oxo-BAs in faecal samples

The described method was used for a targeted metabolomic study of endogenous BAs in order to define which oxo-derivatives occur in healthy conditions. As conjugated-BAs must be first deconjugated by bacterial Bile Salts Hydrolase (BSH) to be metabolized into secondary BAs or oxo-analogues, no conjugated secondary BA or oxo-BAs are present in the intestinal content, therefore only compounds in their free form have been analyzed in faecal extracts. We analyzed 10 samples of human faeces from healthy subjects under similar dietetic regimen for at least two weeks. As expected, several oxo-BAs were recovered, although with high inter-sample variability. Fig. 7 shows a typical chromatogram obtained, while Table 8 reports the quantification of the identified analytes.

FIG. 7. TOTAL ION CURRENT CHROMATOGRAM OBTAINED IN MRM ACQUISITION MODE FROM THE ANALYSIS OF OXO-BAS (A) AND ENDOGENOUS FREE BAS (B) IN FAECAL SAMPLES. PEAKS RELATIVE TO OXO-BAS WERE IDENTIFIED AS FOLLOWS: 3A,12A-DIHYDROXY-7-OXO-CHOLAN-24-OIC ACID (1), 3,12-DIOXO-CHOLAN-24-OIC ACID (2), 7B-HYDROXY-3-OXO-CHOLAN-24-OIC ACID (3), 12B-HYDROXY-3-OXO-CHOLAN-24-OIC ACID (4), 3A-HYDROXY-12-OXO-CHOLAN-24-OIC ACID (5), 12A-HYDROXY-3-OXO-CHOLAN-24-OIC ACID (6); 3-OXO-CHOLAN-24-OIC ACID (7).

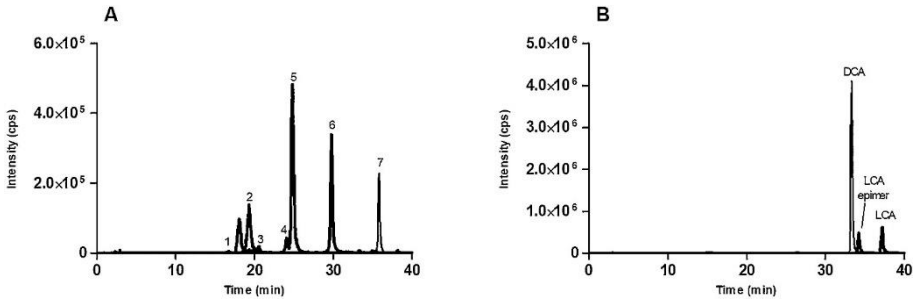

Namely, the identified oxo-BAs are: 3α,12α-dihydroxy-7-oxo-cholan-24-oic acid (peak 1), 3,12-dioxo-cholan-24-oic acid (peak 2), 7β-hydroxy-3-oxo-cholan-24-oic acid (peak 3), 12β-hydroxy-3-oxo-cholan-24-oic acid

(peak 4), 3α-hydroxy-12-oxo-cholan-24-oic acid (peak 5), 12α-hydroxy-3-oxo-cholan-24-oic acid (peak 6), and 3-oxo-cholan-24-oic acid (peak 7). The identification of these compounds was performed on the basis of retention time and qualification transition. It was supported by spiking the sample with known amounts of the relative standard. With the exception of 3α,12α-dihydroxy-7-oxo-cholan-24-oic acid (peak 1), all oxo-BAs are metabolic derivatives of secondary BAs: UDCA (peak 3), DCA (peak 2, 4, 5, 6), and LCA (peak 7). The presence of secondary BA derivatives is easily explained by considering that the oxidation reaction takes place in the colon via intestinal bacteria. The most abundant oxo-BAs derive from the secondary BAs DCA and LCA, which are the only BAs present in the colon in normal conditions. In this regard, epidemiological studies [Reddy B.S. 1977] report that individuals with high levels of secondary BAs in faeces are more likely to develop colorectal cancer [Louis P. 2014]. Therefore, this extensive metabolism to form oxo analogues might be a mechanism to limit the concentration of secondary BAs in the colon, since the toxicity and carcinogenic of these derivatives should be lower than that of their precursors. The metabolized secondary BAs, in the form of oxo-derivatives, represent about 35% of the total faecal pool (Table 8).

TABLE 8. CONCENTRATIONS OF OXO-BAS AND ENDOGENOUS FREE BAS IN FAECES. RESULTS ARE EXPRESSED AS MEAN CONCENTRATION (MG/G) ± STANDARD DEVIATION OF THE 10 SAMPLES ANALYZED.

Oxo-BA	**Mean ± SD (µg/g wet faeces)**
3α,12α-dihydroxy-7-oxo-cholan-24-oic acid	1.3 ± 0.7
3,12-dioxo-cholan-24-oic acid	64 ± 28
7β-hydroxy-3-oxo-cholan-24-oic acid	3.6 ± 1.3
12β-hydroxy-3-oxo-cholan-24-oic acid	12 ± 4
3α-hydroxy-12-oxo-cholan-24-oic acid	163 ± 78
12α-hydroxy-3-oxo-cholan-24-oic acid	53 ± 21
3-oxo-cholan-24-oic acid	59 ± 23
BA	**Mean ± SD (µg/g wet faeces)**
3α,7α,12α-trihydroxy-5β-cholan-24-oic acid (CA)	3.2 ± 1.4
3α,12α-dihydroxy-5β-cholan-24-oic acid (DCA)	467 ± 215
3α-hydroxy-5β-cholan-24-oic acid (LCA)	103 ± 38
3β-hydroxy-5β-cholan-24-oic acid (isoLCA)	88 ± 42

Of the detected compounds, one signal has not yet been identified (corresponding to the transition 389.3 > 389.2 and elution time of 18.2 min). In large intestine, α/β epimers continuously interconvert. It is

therefore plausible that the unidentified compound might be the 3β-hydroxy-12-oxo-cholan-24-oic acid, epimer of 3α-hydroxy-12-oxo-cholan-24-oic acid, the most abundant oxo-BA in faeces. Indeed, this interconversion is obtained through the formation of 3,12-dioxo-cholan-24-oic acid, also recovered at high concentrations in stool.

The most abundant oxo BA is the 3α-hydroxy-12-oxo-cholan-24-oic acid, which achieves concentrations of just one half of DCA. This suggests that, of the members of this enzyme family, the 12α-HSDH plays the major role in this metabolic pathway. This result is in agreement with Keller et al., who reported 3α-hydroxy-12-oxo-cholan-24-oic acid to be the most abundant oxo-BA in faeces of healthy individuals [Keller S. 2004]. Generally, the results obtained in this study for the oxo-BAs identification and quantitation are in accordance to those of previous investigations [Kakiyama G. 2014]. To the best of our knowledge, this is the first time that the 3,12- dioxo-choolan-24-oic acid has been quantified in faeces.

Formation of 3 oxo-derivatives, driven by 3HSDH, is still efficient, while the potential formation of 7 oxo metabolites is irrelevant. This is because elimination of the 7-hydroxyl group by the 7 deoxydrilase enzyme is faster, and only small amounts of 7 hydroxylated BAs reach the colon as a substrate for 7HSDH. In cases of BA malabsorption, where large amounts of CA reach the colon, the formation of higher amounts of 7oxo-analogues may be possible.

3.7. Plasma sample analysis

To avoid excessive faecal loss, conjugated BAs are actively absorbed by the terminal ileum, while unconjugated BAs undergo passive absorption by the colon, hepatic uptake, and excretion in bile. Normally, the first-pass hepatic uptake is never complete, and some of the unconjugated BAs spill into the systemic blood circulation [Hofmann A.F. 1984]. Given the relatively high amounts recovered from faeces, it is plausible that some of the oxo-BAs produced in the colon might be involved in a similar process. This assumption is further supported by the increased lipophilicity, since LogP values of oxo-BAs are higher than that of their precursors [Roda A. 1990, Artursson P. 2001] (Table 10).

TABLE 10. EXPERIMENTAL AND PREDICTED LOGP VALUES FOR ENDOGENOUS BAS AND SOME OF THEIR OXO-DERIVATIVES. EXPERIMENTAL LOGP VALUES WERE TAKEN FROM RODA ET AL. [RODA, A.1990], WHILE PREDICTED VALUES WERE CALCULATED USING ALOGPS SOFTWARE. VALUES REFER TO THE ACID IN THE NON-IONIZED FORM.

Compound	Experimental LogP	Predicted LogP
3α,7α,12α-trihydroxy-5b-cholan-24-oic acid (CA)	2.02	2.26
7α,12α-dihydroxy-3-oxo-cholan-24-oic acid	-	2.24
3α,12α-dihydroxy-7-oxo-cholan-24-oic acid	-	2.61

3α,7α-dihydroxy-12-oxo-cholan-24-oic acid	-	2.56
3α,7α-dihydroxy-5b-cholan-24-oic acid (CDCA)	3.28	3.01
7α-hydroxy-3-oxo-cholan-24-oic acid	-	3.11
3α,12α-dihydroxy-5b-cholan-24-oic acid (DCA)	3.50	3.30
12α-hydroxy-3-oxo-cholan-24-oic acid	-	3.39
3α-hydroxy-12-oxo-cholan-24-oic acid	-	3.78
3,12-dioxo-cholan-24-oic acid		4.03
3α,7β-dihydroxy-5b-cholan-24-oic acid (UDCA)	3.00	3.01
7β-hydroxy-3-oxo-cholan-24-oic acid	-	3.74
3α-hydroxy-5b-cholan-24-oic acid (LCA)	-	4.38

Therefore, we used the developed analytical method to analyze plasma samples from healthy subjects. Before entering the systemic circulation, BAs are taken up by the liver, where they are conjugated with glycine (and to a lesser extent with taurine). Before the analysis, we therefore treated plasma samples with CHG to ensure that eventual conjugated oxo-BAs were converted to their free form. Indeed, as standards of conjugated oxo-BAs were not available and a proper method for their direct determination in serum was not set up, their conversion into their unconjugated form was necessary for an actual identification. To define all possible forms present in the systemic circulation or in other biological compartments, future studies will require a more comprehensive analytical method that can identify and quantify oxo-BA conjugates too.

Fig. 8 reports a typical chromatogram obtained from the analysis of plasma samples in which 3 major oxo-BAs were detected, namely 3α-hydroxy-7-oxo-cholan-24-oic acid, 3α-hydroxy-12-oxo-cholan-24-oic acid, and 12α-hydroxy-3-oxo-cholan-24-oic acid. Their quantification and that of the endogenous BAs is reported in Table 11.

FIG. 8. TOTAL ION CURRENT CHROMATOGRAM OBTAINED IN MRM ACQUISITION MODE FROM THE ANALYSIS OF OXO-BAS (A) AND ENDOGENOUS FREE BAS (B) IN PLASMA SAMPLES AFTER ENZYMATIC DECONJUGATION. PEAKS RELATIVE TO OXO-BAS WERE IDENTIFIED AS FOLLOWS: 3A-HYDROXY-7-OXO-CHOLAN-24-OIC ACID (1), 3A-HYDROXY-12-OXO-CHOLAN-24-OIC ACID (2), 12A-HYDROXY-3-OXO-CHOLAN-24-OIC ACID (3).

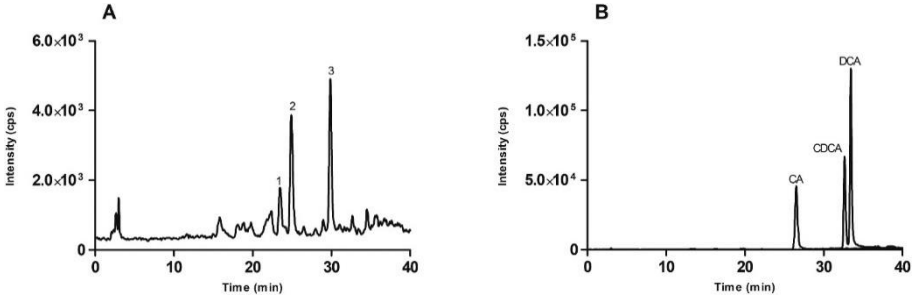

TABLE 11. CONCENTRATIONS OF OXO-BAS AND ENDOGENOUS FREE BAS IN PLASMA AFTER ENZYMATIC DECONJUGATION. RESULTS ARE EXPRESSED AS MEAN CONCENTRATION (NG/ML) ± STANDARD DEVIATION OF 10 SAMPLE ANALYSIS.

Oxo-BA	Mean ± SD (ng/mL plasma)
3α-hydroxy-7-oxo-cholan-24-oic acid	12 ± 5
3α-hydroxy-12-oxo-cholan-24-oic acid	26 ± 9
12α-hydroxy-3-oxo-cholan-24-oic acid	36 ± 15

BA	Mean ± SD (ng/mL plasma)
3α,7α,12α-trihydroxy-5β-cholan-24-oic acid (CA)	179 ± 42
3α,7β-dihydroxy-5β-cholan-24-oic acid (UDCA)	23 ± 11
3α,7α-dihydroxy-5β-cholan-24-oic acid (CDCA)	188 ± 63
3α,12α-dihydroxy-5β-cholan-24-oic acid (DCA)	291 ± 77
3α-hydroxy-5β-cholan-24-oic acid (LCA)	26 ± 10

The two main oxo-BAs recovered in plasma are the compounds obtained from the oxidation of one hydroxyl group, in position 3 or 12, of DCA. These compounds are also present in faeces at high concentrations, confirming the assumption of passive absorption by the colon. This evidence is further supported by the predicted LogP (Table 10). This value is very similar to that of DCA, which is known to be efficiently absorbed by passive diffusion in the large intestine [Hofmann A.F. 1984]. In analogy, LogP values higher than 4 are known to lead to poor absorption [Artursson P. 2001], explaining the absence of 3-oxo-cholan-24-oic acid and 3,12-dioxo-cholan-24-oic acid in serum, despite their relatively high levels in stool. Indeed, the permeability starts to decrease for very hydrophobic compounds. This is because they generally have low aqueous solubility, and partition at a slower rate from the (lipophilic) cell membranes to the extracellular fluids [Wils P. 1994].

Furthermore, unlike in faeces, oxo-BAs are just a small fraction of plasma BAs, being about 10% of their precursor. This might be due to poor passive absorption in the colon or efficient hepatic uptake by the liver

and poor spillover into the systemic compartment. Unfortunately, the hepatic uptake and intestinal absorption of oxo-BAs is still largely unknown. According to their physicochemical properties in term of lipophilicity and pKa, oxo-BAs are strongly bond to human serum albumin similarly to common BAs and therefore share a similar un-bound fraction which drives their hepatic uptake .

4. Conclusion

The BA qualitative and quantitative composition in biological fluids is mainly driven by the liver and intestinal metabolism with time-related variations during the day and by eventual hepatobiliary diseases. In particular, the gut microbiota is considered to be a virtual endocrine organ and the hundreds of species and thousands of strains of prokaryotes help to differentiate individuals [Tremaroli V. 2012], paving the way for personalized medicine. This concept is even more relevant for compounds characterized by hormone-like activity, such as BAs.

Once the primary BAs have been synthesized, they undergo a complex series of biotransformations both in liver and intestine, which are aimed to finely regulate their activity and their level through the enterohepatic circulation [Watanabe M. 2006]. The extensive BA metabolism in the intestine might be responsible for the production of additional derivatives of secondary BAs with potential receptor activity. In this sense, the role of oxo-BAs has not been studied comprehensively yet. Bacteria enzymes involved in these metabolic pathways could be under/overexpressed in relation to nutritional and pathological factors. They can therefore modulate the formation of these metabolites, which still could maintain a biological role and do not merely act as “inert” excretion molecules.

The sterolbiome encompasses all the genes of the human gut microbiome that are involved in the uptake and metabolism of host, pharmaceutical, and diet-derived steroids. The more precise term for this steroid sub-family would be “acidic sterolbiome”. That is because these steroid-like structures contain an acidic group that induces peculiar polar characteristics and pH-dependent ionization and solubility.

Here, a new HPLC–ESI-MS/MS method for the simultaneous determination of 21 oxo-BAs and seven BA precursors in human faeces was developed and fully validated according to ICH guidelines, obtaining appropriate values of recovery, accuracy and precision to the scope of this study. Non commercially available oxo-BA standards were synthesized, purified, and properly characterized in order to increase the number of analyzable compounds.

Together with secondary BAs, for the first time several oxo-BAs were simultaneously recovered in human feaces. In addition, Oxo-BAs were recovered in systemic circulation as result of non-complete hepatic uptake, supporting the assumption of a potential role as signaling molecules.

The determined content of Oxo BAs in feaces showed high inter-sample variability. These data, obtained from healthy subjects, indicate that the gut sterolbiome is highly personalized. Therefore, we expect that this new analytical tool will be important at the light of the concept of precision medicine. In addition, it could be applied to study BAs activity towards FXR, as well as the structure relationship with the gut microbiota.

The analytical method reported herein has the potential of being improved, shortening the analysis time and enhancing resolution, through transfer to a more performing new generation UHPLC platform. This format could add value to the actual findings, making this approach more applicable in clinical researches (high-throughput screening).

With this new analytical tool, it could be possible to accurately study the hormone-like activity of the oxo-BAs. Such studies could explain how and why they are formed by intestinal bacteria and elucidate their physio-pathological role as part of a more general acidic steroid metabolomic approach.

Reference

Artursson, P., Palm, K., & Luthman, K. (2001). Caco-2 monolayers in experimental and theoretical predictions of drug transport. Advanced drug delivery reviews, 46(1-3), 27-43.

Bortolini, O., Bottai, M., Chiappe, C., Conte, V., & Pieraccini, D. (2002). Trihalide-based ionic liquids. Reagent-solvents for stereoselective iodination of alkenes and alkynes. Green Chemistry, 4(6), 621-627.

Bovara, R., Carrea, G., Riva, S., & Secundo, F. (1996). A new enzymatic route to the synthesis of 12-ketoursodeoxycholic acid. Biotechnology letters, 18(3), 305-308.

Carrott, P. J. M., & Carrott, M. R. (2007). Lignin–from natural adsorbent to activated carbon: a review. Bioresource technology, 98(12), 2301-2312.

Chiang, J. Y. (2009). Bile acids: regulation of synthesis. Journal of lipid research, 50(10), 1955-1966.

Danielsson, H. (1963). Present status of research on catabolism and excretion of cholesterol. In Advances in lipid research (Vol. 1, pp. 335-385). Elsevier.

Doden, H., Sallam, L. A., Devendran, S., Ly, L., Doden, G., Daniel, S. L., ... & Ridlon, J. M. (2018). Metabolism of oxo-bile acids and characterization of recombinant 12α-hydroxysteroid dehydrogenases from bile acid 7α-dehydroxylating human gut bacteria. Appl. Environ. Microbiol., 84(10), e00235-18.

Duboc, H., Rajca, S., Rainteau, D., Benarous, D., Maubert, M. A., Quervain, E., ... & Bridonneau, C. (2013). Connecting dysbiosis, bile-acid dysmetabolism and gut inflammation in inflammatory bowel diseases. Gut, 62(4), 531-539.

Eneroth, P., Gordon, B., Ryhage, R., & Sjövall, J. (1966). Identification of mono-and dihydroxy bile acids in human feces by gas-liquid chromatography and mass spectrometry. Journal of lipid research, 7(4), 511-523.

Fantin, G., Fogagnolo, M., Medici, A., Pedrini, P., Poli, S., & Gardini, F. (1993). Microbial oxidation with Bacillus stearothermophilus: High enantioselective resolution of 1-heteroaryl and 1-aryl alcohols. Tetrahedron: Asymmetry, 4(7), 1607-1612.

García-Cañaveras, J. C., Donato, M. T., Castell, J. V., & Lahoz, A. (2012). Targeted profiling of circulating and hepatic bile acids in human, mouse, and rat using a UPLC-MRM-MS-validated method. Journal of lipid research, 53(10), 2231-2241.

Gosetti, F., Mazzucco, E., Zampieri, D., & Gennaro, M. C. (2010). Signal suppression/enhancement in high-performance liquid chromatography tandem mass spectrometry. Journal of Chromatography A, 1217(25), 3929-3937.

Goto, J., Teraya, Y., Nambara, T., & Iida, T. (1991). Studies on steroids: CCLIII. Capillary gas chromatographic behaviour of diethylhydrogensilyl—diethylsilylene derivatives of stereoisomeric bile acids. Journal of Chromatography A, 585(2), 281-288.

Guidance for industry: Q2B validation of analytical procedures: methodology; 1996

Hamilton, J. P., Xie, G., Raufman, J. P., Hogan, S., Griffin, T. L., Packard, C. A., ... & Hofmann, A. F. (2007). Human cecal bile acids: concentration and spectrum. American Journal of Physiology-Gastrointestinal and Liver Physiology, 293(1), G256-G263.

Haefelfinger, P. (1981). Limits of the internal standard technique in chromatography. Journal of Chromatography A, 218, 73-81.

Hofmann, A. F., & Borgström, B. (1964). The intraluminal phase of fat digestion in man: the lipid content of the micellar and oil phases of intestinal content obtained during fat digestion and absorption. The Journal of clinical investigation, 43(2), 247-257.

Hofmann, A. F. (1984). Chemistry and enterohepatic circulation of bile acids. Hepatology, 4(S2), 4S-14S.

Hylemon, P. B. (1985). Metabolism of bile acids in intestinal microflora. In New comprehensive biochemistry (Vol. 12, pp. 331-343). Elsevier.

Humbert, L., Maubert, M. A., Wolf, C., Duboc, H., Mahé, M., Farabos, D., ... & Rainteau, D. (2012). Bile acid profiling in human biological samples: comparison of extraction procedures and application to normal and cholestatic patients. Journal of Chromatography B, 899, 135-145.

Jones, S. A. (2012). Physiology of FGF15/19. In Endocrine FGFs and klothos (pp. 171-182). Springer, New York, NY.

Kakiyama, G., Pandak, W. M., Gillevet, P. M., Hylemon, P. B., Heuman, D. M., Daita, K., ... & White, M. B. (2013). Modulation of the fecal bile acid profile by gut microbiota in cirrhosis. Journal of hepatology, 58(5), 949-955.

Keller, S., & Jahreis, G. (2004). Determination of underivatised sterols and bile acid trimethyl silyl ether methyl esters by gas chromatography–mass spectrometry–single ion monitoring in faeces. Journal of Chromatography B, 813(1-2), 199-207.

Louis, P., Hold, G. L., & Flint, H. J. (2014). The gut microbiota, bacterial metabolites and colorectal cancer. Nature reviews microbiology, 12(10), 661.

Muto, A., Takei, H., Unno, A., Murai, T., Kurosawa, T., Ogawa, S., ... & Hoshina, T. (2012). Detection of Δ4-3-oxo-steroid 5β-reductase deficiency by LC–ESI-MS/MS measurement of urinary bile acids. Journal of Chromatography B, 900, 24-31.

Nahar, L., & Turner, A. B. (2003). Synthesis of ester-linked lithocholic acid dimers. Steroids, 68(14), 1157-1161.

Nakagaki, M., Danzinger, R. G., Hofmann, A. F., & Roda, A. (1983). Hepatic biotransformation of two hydroxy-7-oxotaurine-conjugated bile acids in the dog. American Journal of Physiology-Gastrointestinal and Liver Physiology, 245(3), G411-G417.

Parks, D. J., Blanchard, S. G., Bledsoe, R. K., Chandra, G., Consler, T. G., Kliewer, S. A., ... & Lehmann, J. M. (1999). Bile acids: natural ligands for an orphan nuclear receptor. Science, 284(5418), 1365-1368.

Perwaiz, S., Mignault, D., Tuchweber, B., & Yousef, I. M. (2002). Rapid and improved method for the determination of bile acids in human feces using MS. Lipids, 37(11), 1093-1100.

Reddy, B. S., & Wynder, E. L. (1977). Metabolic epidemiology of colon cancer: fecal bile acids and neutral sterols in colon cancer patients and patients with adenomatous polyps. Cancer, 39(6), 2533-2539.

Roda, A., Pellicciari, R., Gioiello, A., Neri, F., Camborata, C., Passeri, D., ... & Montagnani, M. (2014). Semisynthetic bile acid FXR and TGR5 agonists: physicochemical properties, pharmacokinetics, and metabolism in the rat. Journal of Pharmacology and Experimental Therapeutics, 350(1), 56-68.

Roda, A., Aldini, R., Camborata, C., Spinozzi, S., Franco, P., Cont, M., ... & Adorini, L. (2017). Metabolic Profile of obeticholic acid and endogenous bile acids in rats with decompensated liver cirrhosis. Clinical and translational science, 10(4), 292-301.

Roda, A., Minutello, A., Angellotti, M. A., & Fini, A. (1990). Bile acid structure-activity relationship: evaluation of bile acid lipophilicity using 1-octanol/water partition coefficient and reverse phase HPLC. Journal of lipid research, 31(8), 1433-1443.

Ridlon, J. M., Kang, D. J., Hylemon, P. B., & Bajaj, J. S. (2014). Bile acids and the gut microbiome. Current opinion in gastroenterology, 30(3), 332.

Riva, S., Chopineau, J., Kieboom, A. P. G., & Klibanov, A. M. (1988). Protease-catalyzed regioselective esterification of sugars and related compounds in anhydrous dimethylformamide. Journal of the American Chemical Society, 110(2), 584-589.

Roda, A., Aldini, R., Camborata, C., Spinozzi, S., Franco, P., Cont, M., ... & Adorini, L. (2017). Metabolic Profile of obeticholic acid and endogenous bile acids in rats with decompensated liver cirrhosis. Clinical and translational science, 10(4), 292-301.

Roda, A., Hofmann, A. F., & Mysels, K. J. (1983). The influence of bile salt structure on self-association in aqueous solutions. Journal of Biological Chemistry, 258(10), 6362-6370.

Roda, A., Pellicciari, R., Gioiello, A., Neri, F., Camborata, C., Passeri, D., ... & Montagnani, M. (2014). Semisynthetic bile acid FXR and TGR5 agonists: physicochemical properties, pharmacokinetics, and metabolism in the rat. Journal of Pharmacology and Experimental Therapeutics, 350(1), 56-68.

Sánchez, B., Delgado, S., Blanco-Míguez, A., Lourenço, A., Gueimonde, M., & Margolles, A. (2017). Probiotics, gut microbiota, and their influence on host health and disease. Molecular nutrition & food research, 61(1), 1600240.

Scherer, M., Gnewuch, C., Schmitz, G., & Liebisch, G. (2009). Rapid quantification of bile acids and their conjugates in serum by liquid chromatography–tandem mass spectrometry. Journal of Chromatography B, 877(30), 3920-3925.

Subbiah, M. T., Tyler, N. E., Buscaglia, M. D., & Marai, L. (1976). Estimation of bile acid excretion in man: comparison of isotopic turnover and fecal excretion methods. Journal of lipid research, 17(1), 78-84.

Tremaroli, V., & Bäckhed, F. (2012). Functional interactions between the gut microbiota and host metabolism. Nature, 489(7415), 242.

Trifunović, J., Borčić, V., & Mikov, M. (2017). Bile acids and their oxo derivatives: potential inhibitors of carbonic anhydrase I and II, androgen receptor antagonists and CYP3A4 substrates. Biomedical Chromatography, 31(5), e3870.

Tserng, K. Y. (1978). A convenient synthesis of 3-keto bile acids by selective oxidation of bile acids with silver carbonate-Celite. Journal of lipid research, 19(4), 501-504.

Wang, H., Chen, J., Hollister, K., Sowers, L. C., & Forman, B. M. (1999). Endogenous bile acids are ligands for the nuclear receptor FXR/BAR. Molecular cell, 3(5), 543-553.

Watanabe, M., Houten, S. M., Mataki, C., Christoffolete, M. A., Kim, B. W., Sato, H., ... & Schoonjans, K. (2006). Bile acids induce energy expenditure by promoting intracellular thyroid hormone activation. Nature, 439(7075), 484.

Wils, P., Warnery, A., Phung-Ba, V., Legrain, S., & Scherman, D. (1994). High lipophilicity decreases drug transport across intestinal epithelial cells. Journal of Pharmacology and Experimental Therapeutics, 269(2), 654-658.

Yin, S., Su, M., Xie, G., Li, X., Wei, R., Liu, C., ... & Jia, W. (2017). Factors affecting separation and detection of bile acids by liquid chromatography coupled with mass spectrometry in negative mode. Analytical and bioanalytical chemistry, 409(23), 5533-5545.

Zhou, S., & Cook, K. D. (2000). Protonation in electrospray mass spectrometry: wrong-way-round or right-way-round?. Journal of the American Society for Mass Spectrometry, 11(11), 961-966.

Paper 2

Serum Bile Acids Profiling in Inflammatory Bowel Disease patients treated with Anti-TNFs

Reproduced from:

Serum Bile Acids Profiling in Inflammatory Bowel Disease Patients Treated with Anti-TNFs

Roda G., Porru E., Katsanos K., Skamnelos A., Kyriakidi K., Fiorino G., Christodoulou D., Danese S., Roda, A.

Cells 2019, 8(8), 817; https://doi.org/10.3390/cells8080817

Abstract

Inflammatory bowel diseases (IBD), ulcerative colitis (UC) and Crohn's disease (CD), represent systematic chronic conditions with a deficient intestinal absorption. We first attempt to investigate the serum bile acids (sBAs) profile in a large cohort of IBD patients to evaluate changes under anti-TNF alpha treatment. Methods: Forty CD and 40 UC patients were enrolled, and BAs were quantified by high-pressure liquid chromatography-electrospray-tandem mass spectrometry (HPLC-ES-MS/MS). Up to 15 different sBA concentrations and clinical biomarkers where added to a Principal Component Analysis (PCA) to discriminate IBD from healthy conditions and treatments. Principal component analysis allowed a separation into two clusters within CD patients: those receiving anti-TNF alpha showed increase in total sBAs compared to not exposed ones. Specifically, secondary sBAs significantly increase after anti-TNF alpha treatment. Furthermore, multivariate analysis based on sBA concentrations highlighted a different qualitative sBA profile for UC and CD patients treated with conventional therapy. Conclusion: According to our results, anti-TNF alpha in CD restores the sBA profile by re-establishing the physiological levels, with secondary BAs potentially serving as indirect biomarkers of the healing process.

1. Introduction

Inflammatory bowel diseases (IBD), which include ulcerative colitis (UC) and Crohn's disease (CD), represent chronic inflammatory conditions with a deficient intestinal absorption as well as an impaired hepatic spill over. These alterations lead to non-physiological concentration of BAs in peripheral blood, bile, and intestinal content [Duboc H. 2013]. However, even parameters like circadian rhythm [Watanabe M. 2006], post-prandial peaks [Aldini R. 1982], gallbladder and intestinal motility and inflammation [Kirwan W.O. 1975] as well as hepatic uptake and secretion [Kullak-Ublick G.A. 2004] can affect the levels of sBAs.

BAs are endogenous acidic steroids synthetized in the liver from cholesterol, representing its main excretion pathway from the body [Hofmann A.F. 1964]. BAs are mainly known for their role in lipid transport through enterohepatic circulation, but the subsequent discovery of their function as agonists of Farnesoid X receptor (FXR) [Parks D.J. 1999] and TGR5 [Kawamata Y. 2003] has unlighted other physiological functions, in which they act as enteric hormones.

The enterohepatic circulation is a complex mechanism which permits to keep costant the amount of BAs in the body, hampering an excessive faecal loss, and to regulate the gut microbiota composition, strictly involved in the health and disease of the individual [Chiang J.Y. 2009]. BAs are mainly reabsorbed in the terminal ileum through an active transport mechanism selective for their conjugates with glycine and taurine and inefficient for unconjugated BAs. Passive absorption in intestine is also involved and limited to unconjugated BAs particularly for dihydroxy BAs such as chenodeoxycholic (CDCA) and deoxycholic acid

(DCA) with higher lipophilicity than trihydroxylated cholic acid (CA). This passive absorption occurs via 7-α-dehydroxylation by colon microbiota, contributing to maintain of the physiological pool size [Lynch S.V. 2006]. In CD, intestinal inflammation, often associated to a deficit of active transporters in the ileum, is responsible for a BA malabsorption (BAM) and consequent increased faecal loss and reduction of their physiological pool [Hofmann A.F. 2009]. In UC, the involvement of the large intestine might account for a deficit in the passive absorption, with consequent variation in the BA pool as well. Moreover, the altered microbiota in these patients could impact and modify the BA qualitative composition. This is particularly relevant when the implicated compounds act as enteric hormones, controlling FXR or TGR5 receptors [Monte M.J. 2009]. Although it is clear that BA enterohepatic circulation is affected in IBD, only few and disagreeing studies report the alteration in their serum or fecal concentrations and their relationship with different treatments [Tiraterra E. 2018]. Indeed, an inadequate selection of patient population, sample size and analytical methods have proven to be critical and limiting factors [Ejderhamn J. 1991, Gnewuch C. 2009]. This study represents the first attempt to screenshot serum BA profiles in a large cohort of IBD patients to evaluate the effect and efficacy of anti-TNF alpha treatment on BA metabolism. Understanding whether specific BA profiles are associated to disease phenotype, disease progression or treatment might help to introduce them as a toolkit in clinical practice to assess disease states, severity, and response to treatment like mucosal healing as a companion diagnostic.

2. Materials and Methods

2.1. Study Population

All consecutive patients seen between May 31, 2018 and July 1 2018 were prospectively enrolled in one referral centre in Greece. Mandatory criteria for inclusion in the study were: age > 18 years old, a confirmed diagnosis of IBD by conventional endoscopic and histological criteria, absence of concomitant liver diseases. Patients with a personal history of colectomy, a diagnosis of secondary sclerosing cholangitis, liver dysfunction or a history of orthotopic liver transplant (OLT) were excluded.

For all patients clinical and demographic information, including sex, age, Montreal classification, age at diagnosis, concomitant treatments (5-ASA, steroids, immunosuppressant drugs), endoscopy disease activity, and clinical disease activity, were collected. Laboratory tests excluding liver involvement (total and direct bilirubin, aspartate aminotransferase (AST), alanine transferase (ALT)) and disease activity (platelets (PLT) and C reactive protein) were collected. Clinical activity was scored according to the Mayo score for UC [Vashist N.M. 2018], and the Harvey–Bradshaw index for CD [Evertsz F.B. 2013]. Endoscopic activity was evaluated according to the Mayo endoscopic score for UC and the Simple Endoscopic Score (SES) for CD [Daperno M. 2004].

A group of 20 healthy subjects (CTRL) was included to obtain reference values for sBA levels. The subjects were under regular diet and none of them had history of alimentary disorders, intestinal diseases or hepatic dysfunction. A fasting serum sample was obtained from each patient and then stored at −20 °C before sBA analysis.

2.2. Study objectives

The primary goal of this study was to assess BA profile in patients with IBD, both UC and CD, in comparison to healthy subjects. The secondary target was the assessment of BA profile in response to different treatments (anti-TNFs, steroids, conventional therapy like 5-ASA) and in relation to disease extension, disease duration, age at diagnosis, and inflammatory state.

2.3. Chemicals and solutions

Pure standards of all the studied BAs, namely cholic acid (CA), chenodeoxycholic acid (CDCA), deoxycholic acid (DCA), ursodeoxycholic acid (UDCA), lithocholic acid (LCA), and their respective glycine and taurine conjugated, were purchased from Sigma-Aldrich (ST. Louis, MO, USA). The semi-synthetic BA obethicholic acid (OCA) and its glycine (G-OCA) and taurine (T-OCA) conjugated forms were kindly provided by prof. Roberto Pellicciari (University of Perugia, Italy) and used as internal standards.

Stock standard solutions of all the BA standards were prepared in MeOH at concentration 1 mM. These stock solutions were aliquoted and stored at -20 °C to minimize potential solvent evaporation. Mixed working solutions containing all compounds were made by appropriate dilution of the stock solutions in MeOH in the range 0.1–100 µM and stored at 4 °C.

2.4 Analytical method HPLC-ESI-MS/MS

All the studied BAs were identified and quantified in serum samples by high-pressure liquid chromatography-electrospray-tandem mass spectrometry (HPLC-ES-MS/MS) after an appropriate clean-up procedure. Liquid chromatography analysis was performed using an Alliance HPLC system model 2695 from Waters combined with a triple quadruple mass spectrometer QUATTRO-LC (Micromass) using an electrospray interface. The analytical column was a Waters XSelect CSH Phenyl-hexyl column, 5 µm, 150 × 2.1 mm, protected by a self-guard column Waters XSelect CSH Phenyl- hexyl 5 µm, 10 × 2.1 mm. BAs were separated by elution gradient mode with a mobile phase composed of a mixture ammonium acetate buffer 15 mM, pH 8.0 (Solvent A) and acetonitrile: methanol = 75:25 v/v (Solvent B). The separation was obtained with a total run time of 35

minutes, using the following gradient mode: 10 min 35%(B), 11 min at 45%(B), 4 min at 90%(B), 10 min at 35%(B), at 0.15 mL/min flow rate. Each change in the gradient mode was immediate. The column was settled at 45 °C and the injected sample volume was 5 µL.

All the chromatograms were acquired in electrospray negative ionization with the mass spectrometer operating in multiple reactions monitoring mode. Capillary voltage was set at -2.7 KV, cone at 60 V (unconjugated BAs) or 90 V (conjugated BAs), source and desolvation temperature were respectively set at 130 °C and 200 °C, while the collision gas was argon .

Calibration solutions in the range 0.01–10 µM were prepared before the analysis by 1:10 dilution of the working solution in BA-free serum (obtained following the procedure described in [Carrot P.J. 2007]) and subsequent solid phase extraction, as described in paragraph 2.5. The quality control samples (QCs) containing all the analytes were obtained at concentrations 0.2 µM, 1.0 µM and 5.0 µM. These samples were used for the method validation or injected randomly during the analysis in order to check the normal behaviour of the analytical system. Linear calibration curve parameters were obtained from the plot of the analyte/internal standard peak area ratio versus analyte concentration using a least-squares regression analysis.

Validation of the proposed RP-HPLC method was performed with respect to linearity, limit of detection (LOD), limit of quantitation (LOQ), accuracy (bias%), precision (CV%), recovery and robustness according to ICH guidelines. The recovery of the SPE procedure was calculated as percentage ratio of each analyte concentration at three concentration levels with samples spiked after and before SPE extraction. Matrix effect was evaluated for all analytes as ratio between the absolute matrix effect and the peak area of standard sample in mobile phase. Absolute matrix effect was calculated as difference between the peak area of the standard sample in matrix and the peak area of standard sample in mobile phase.

2.5 Sample preparation

An aliquots of each plasma samples (100 µl) were fortified with 10 µL of the internal standard working solution and were diluted by adding 2 mL of NaOH 0.1N and heated to 64ºC for 30 minutes. The solid phase extraction cartridge (ISOLUTE, IST) was conditioned with 5 ml of methanol and 5 ml of water. Plasma samples were loaded into the conditioned cartridge and then washed with 10 ml of water. The bile acids were then eluted with 5 ml of methanol. The eluate was dried under vacuum and reconstituted with 100 µl of the mobile phase 65:35 v/v (ammonium acetate buffer 15mM pH=8.0) : (acetonitrile:methanol = 75:25 v/v), and injected into the HPLC-ES-MS/MS system.

2.6. Ethical Considerations

This study was performed according to the directive of the Greek National Committee for Data Protection (HDPA 2472/1997) and was approved by the local ethics committee (n.12/10-5-2018). All patients signed an informed consent form.

2.7. Statistical Analysis

To visualize the clustering of the different groups of patients, PCA was performed with R-based CAT (Software developed by Italian Chemometrics Group, Italian Analytical Chemistry Division). Parameters used for the multivariate analysis were the determined concentrations of the following different classes: free SBAs, glycine-conjugate and taurine-conjugate sBAs (five BAs for each group), primary and secondary BAs, ratio between primary and secondary BAs. Further PCAs were carried out using single BA concentrations to attempt to evaluate which sBAs are altered in IBD and in patients treated with anti-TNFα therapy. In addition, patient ages, disease duration, and clinical biomarkers were used for chemometric analysis and interpretation of the results. Total bilirubin (TBIL), direct bilirubin (DBIL), ALT, (ALT, endoscopic activity, clinical disease activity, and PLT, C-reactive protein (CRP) were collected. Data were pre-processed by converting each concentration value to log (concentration) and by using the “autoscale” function of the software. Hotelling T2 and Q were used as statistic methods to detect possible outliers. The confidence interval was settled at 95%. The T2 and Q residuals do not indicate outliers for the reported PCAs.

Univariable statistical data analysis was performed using GraphPad Prism 5.0 software (La Jolla, CA, USA). The quantitative data are presented as mean ± standard deviation (SD). Discriminative marker variables were determined based on the absolute loadings and the variances explained by the PCs. A paired t-test was used to assess any significant differences in the sBA quali-quantitative concentrations among the different groups, setting the level of statistical significance at p value <0.05.

3. Results

3.1. Demographic and Clinical Characteristics

Eighty patients with IBD, 40 CD and 40 UC patients were prospectively enrolled. Fifty percent of patients in each group were in treatment with biologics drugs such as Golimumab (Simponi, Janssen Biologics), Adalimumab (Humira, Abbvie), Infliximab (Remicade, Schering-Plough). The remaining 50% of patients had never received anti-TNF alpha treatment in their disease history. The demographic and clinical characteristics

of the enrolled patients are described in Table 1. Liver function tests were within the normal range in all samples with available data. No patient had a prior history of abdominal, liver surgery and OLT.

TABLE 1. DEMOGRAPHIC AND CLINICAL CHARACTERISTICS OF PATIENTS.

	PLT's (×1000)	CRP (mg/L)	Endoscopic activity*	Disease activity*	TBIL	Montreal Classification	Date of Diagnosis	Medication
CD1	349	9	1	0	0.4	L1B1	2012	BIO
CD2	303	5	0	0	0.6	L1B3	2011	BIO
CD3	284	2	2	1	0.4	L2B3	1990	BIO
CD4	250	2	0	0	0.9	L1B1	2009	BIO
CD5	406	7	1	1	0.5	L3B1	2011	BIO
CD6	260	2	1	2	0.9	L1B1	NA	BIO
CD7	287	2	0	0	0.4	L1B1	2009	BIO
CD8	395	29	2	1	1.2	L1B1	2011	BIO
CD9	281	2	0	0	0.4	L1B2	2013	BIO
CD10	228	3	0	0	0.9	L1B1	2003	BIO
CD11	485	14	2	2	0.5	L1B2	2006	BIO
CD12	303	3	2	1	0.4	L1B1	2010	BIO
CD13	302	12	1	2	0.4	L1B1	2000	BIO
CD14	244	1	0	0	1.2	L1B1	1997	BIO
CD15	407	5	1	1	0.6	L3B1	2012	BIO
CD16	183	2	0	0	0.9	L3B1	NA	BIO
CD17	162	4	0	0	0.5	L1B1	2012	BIO
CD18	245	1	0	0	0.4	L1B1	2012	BIO
CD19	270	NA	0	0	1.2	L3B2	1997	BIO
CD20	385	7	1	3	0.6	L3B2	2014	BIO
UC1	NA	NA	NA	NA	NA	E3	2008	BIO
UC2	NA	NA	NA	NA	NA	E3	2012	BIO
UC3	157	7	0	0	0.7	E2	NA	BIO
UC4	381	21	1	1	0.3	E3	2004	BIO
UC5	196	4	0	0	1.2	E2	2016	BIO
UC6	253	3	0	0	0.4	E3	1995	BIO
UC7	267	2	1	1	0.4	E3	1996	BIO
UC8	261	5	0	0	0.4	E3	NA	BIO
UC9	343	1	0	0	0.4	E3	2006	BIO
UC10	470	6	1	0	0.4	E3	2000	BIO
UC11	209	5	1	1	0.3	E3	NA	BIO
UC12	228	2	1	1	0.5	E3	1985	BIO
UC13	176	3	0	0	2.5	E3	1984	BIO
UC14	203	6	2	3	0.6	E3	2006	BIO
UC15	242	3	1	1	0.3	E3	1997	BIO
UC16	322	5	1	2	0.9	E3	2010	BIO
UC17	275	2	1	1	0.6	E2	2013	BIO
UC18	254	5	2	1	0.5	E2	1994	BIO
UC19	253	5	1	0	1	E3	NA	BIO
UC20	232	2	0	0	0.6	E2	NA	BIO

CD1	323	1	0	0	0.6	L3B1	2011	BIO
CD2	329	6	0	3	0.3	L1B1	2016	NO BIO
CD3	222	12	0	0	0.2	L1B1	2016	steroids
CD4	257	2	0	0	0.4	L1B1	2006	NO BIO
CD5	NA	NA	0	0	NA	L3B1	2008	NO BIO
CD6	211	3	0	0	0.8	L3B1	1998	NO BIO
CD7		NA	0	0	NA	L2B1	1989	NO BIO
CD8	209	4	0	0	1.3	L1B1	2016	NO BIO
CD9	312	3	0	0	0.5	L1B1	1997	NO BIO
CD10	335	5	0	1	0.6	L1B2	2006	steroids
CD11	279	2	0	0	0.8	L1B1	2010	NO BIO
CD12	258	7	0	0	0.9	L1B1	2015	NO BIO
CD13	409	27	0	0	0.4	L4B1	2017	steroids
CD14	166	6	1	0	1	L2B1	1974	NO BIO,
CD15		NA	0	0	NA	L2B1	2013	NO BIO
CD16	455	20	2	2	0.3	L3B3	NA	NO BIO
CD17	326	26	1	0	0.3	L1B1	2002	NO BIO
CD18	NA	NA	NA	NA	NA	NA	NA	NO BIO
CD19	NA	NA	NA	NA	NA	NA	NA	NO BIO
CD20	NA	NA	NA	NA	NA	NA	NA	NO BIO
UC1	NA	NA	0	0	0.15	E3	1993	NO BIO
UC2	NA	NA	0	1	1.4	E2	2015	NO BIO
UC3	219	2	0	0	1.3	E3	2007	NO BIO
UC4	181	3	0	0	0.5	E2	2013	NO BIO
UC5	NA	NA	0	0	NA	E3	2004	NO BIO
UC6	457	2	2	1	0.5	E3	1990	NO BIO steroids
UC7	NA	NA	1	0	NA	E2	2010	NO BIO
UC8	346	5	2	1	0.4	E3	2016	NO BIO
UC9	319	13	0	1	0.5	E2	2016	NO BIO
UC10	224	3	0	0	1	E2	2017	NO BIO
UC11	255	2	1	2	0.6	E3	2011	NO BIO
UC12	NA	NA	0	0	NA	E2	2000	NO BIO
UC13	NA	NA	0	0	NA	E3	2009	NO BIO
UC14	NA	NA	0	0		E3	2017	NO BIO
UC15	242	3	0	0	0.4	E2	2017	NO BIO, steroids,
UC16	279	5	0	1	0.5	E3	1997	NO BIO
UC17	201	NA	0	1	0.4	E3	2007	NO BIO
UC18	401	7	0	0	0.6	E3	1989	NO BIO, steroids
UC19	199	37	3	3	0.4	E3	2013	NO BIO, steroids
UC20	285	4	1	0	0.5	E2	2007	NO BIO

* 0 = not active, 1 = mild, 2 = moderate, 3 = severe

PLT: platelets, CRP: C reactive protein, TBIL: total bilirubin,

BIO means therapy with anti-TNFα drugs

NO BIO means therapy with AZA: azathioprine, 5-ASA: 5-aminosalicylic acid or no medication

3.2. Set up and validation of the analytical method HPLC-ESI-MS/MS

The experimental MS conditions were properly tuned by direct infusion of each compound (1 µM of each analyte; 2 mL/h infusion rate). Normal MS and tandem MS experiments were carried out to asses the most convenient detection conditions. Figure 1 reports the mass spectra of the Internal Standard OCA and its conjugated forms. These compounds have been reported as representative of all the other analysed BAs.

FIG. 1. TANDEM MS SPECTRA OF OCA (A), T-OCA (B) AND G-OCA (C), PRECURSOR IONS: M/Z 419.4, 526.4, 476.4, RESPECTIVELY)

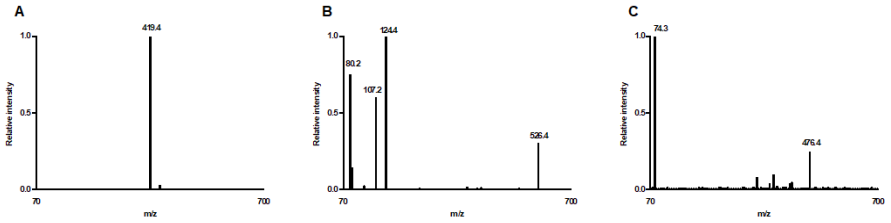

The use of tandem MS in respect to regular MS afforded higher S/N ratio for all BA classes and higher selectivity for conjugated. As showed in figure 1A, unconjugated BAs do not generate fragments under gas collision, therefore only one transition corresponding to $[M-H]^-$ > $[M-H]^-$ was used. On the other hand, as shown n figure 1B and 1C, conjugated BAs exhibit fragmentation when exposed to collision gas, therefore the transitions $[M-H]^-$ > $[M-H]^-$ and the transitions $[M-H]^-$ > [taurine fragment] (m/z 124.4) or $[M-H]^-$ > [glycine fragment] (m/z 74.3) were used both for identity confirmation and quantification. In Table 6 the retention times and the utilized MS/MS transitions have been reported.

TABLE 6. RETENTION TIMES AND MS/MS TRANSITIONS FOR ALL THE ANALYSED BAS.

BA	Retention time (min)	Transition (m_1/z_1 > m_2/z_2)
CA	8.3	407.4 > 407.4
CDCA	14.3	391.4 > 391.4
DCA	17.8	391.4 > 391.4
UDCA	6.2	391.4 > 391.4
LCA	23.3	375.4 > 375.4

GCA	7.4	464.6 > 464.6 (quantification) 464.6 > 74.6 (confirmation)
GCDCA	13.1	448.6 > 448.6 (quantification) 448.6 > 74.6 (confirmation)
GDCA	17.8	448.6 > 448.6 (quantification) 448.6 > 74.6 (confirmation)
GUDCA	5.3	448.6 > 448.6 (quantification) 448.6 > 74.6 (confirmation)
GLCA	22.1	432.6 > 432.6 (quantification) 432.6 > 74.6 (confirmation)
TCA	7.4	514.4 > 514.4 (quantification) 514.4 > 124.4 (confirmation)
TCDCA	13.1	498.4 > 498.4 (quantification) 498.4 > 124.4 (confirmation)
TDCA	17.8	498.4 > 498.4 (quantification) 498.4 > 124.4 (confirmation)
TUDCA	5.3	498.4 > 498.4 (quantification) 498.4 > 124.4 (confirmation)
TLCA	22.1	482.4 > 482.4 (quantification) 482.4 > 124.4 (confirmation)
OCA	24.7	419.4 > 419.4
T-OCA	22.8	526.4 > 526.4 (quantification) 526.4 > 124.4 (confirmation)
G-OCA	20.9	476.4 > 476.4 (quantification) 476.4 > 74.3 (confirmation)

The total ion current of both free sBAs and glycine-conjugated sBAs is reported in Figure 2.

FIG. 2. TOTAL ION CURRENT CHROMATOGRAM REPORTING THE HPLC SEPARATION ON A PHENYL-HEXYL COLUMN OF ENDOGENOUS BAS, OCA, T-OCA AND G-OCA. THE ELUTION ORDER IS: GUDCA (1), UDCA (2), GCA (3), CA (4), GCDCA (5), CDCA (6), GDCA (7), DCA (8), G-OCA (9), GLCA (10), T-OCA (11), LCA (12), OCA (13).

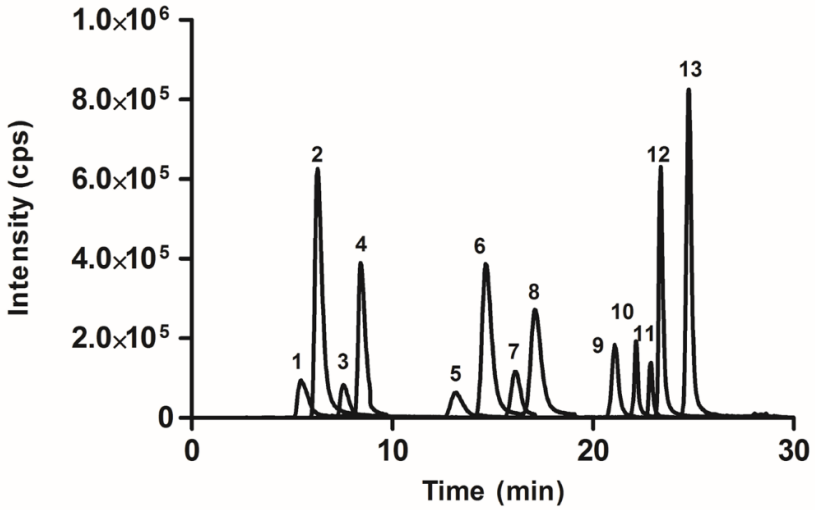

LOD values in plasma ranged from 2 ng/mL to 10 ng/mL, while LOQ values from 5 ng/mL to 25 ng/mL for all the investigated analytes. Variation coefficients and bias% determined, both intra- and inter-daily, were less than 5% for all analytes at the concentrations of the QC samples. The comparison between standard

solutions, fortified samples and blank serum samples was used to evaluate potential interfering signal. No interfering signals were found, highlighting the good method selectivity in multiple reaction monitoring (MRM) mode. The efficiency of solid phase extraction during sample clean-up was calculated by Rec%. Experimental values were close to 100% for all the investigated analytes, indicating the efficacy of this process. Matrix effect percentage was evaluated at the three concentration levels of the QCs and values above -20% were determined, highlighting the necessity to use matrix-matched calibration based on spiked blank-serum samples as described in paragraph 2.4.

3.3. CD patients in conventional therapy and Principal Component Analysis

First, multivariate analysis was carried out by considering concentrations of the different sBA classes as selected variables to discriminate CTRL subjects, UC and CD patients in conventional treatments. The outputs of the PCA are reported in Figure 3.

FIG. 3. SCORES PLOT AND LOADING PLOT OF THE PCA (PRINCIPAL COMPONENT ANALYSIS) FOR HEALTHY SUBJECTS (CTR, ULCERATIVE COLITIS (UC NB) AND CROHN'S DISEASE (CD NB) PATIENTS UC TREATED WITH CONVENTIONAL THERAPIES. THE FIRST PC EXPLAINS THE 53.9% OF THE TOTAL VARIANCE AMONG THE SAMPLES. THE SECOND PC EXPLAINS THE 22.1% OF THE TOTAL VARIANCE.

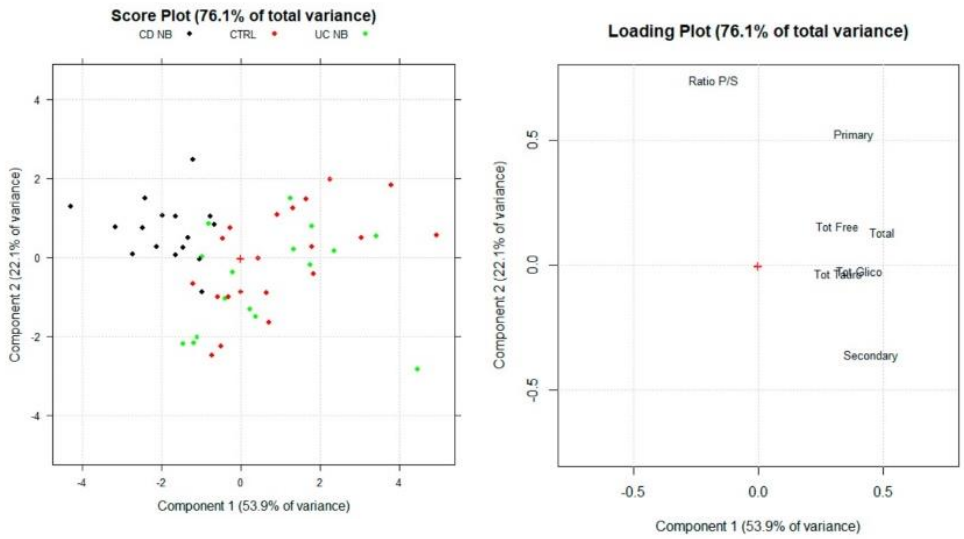

The sBA profiles are similar between UC patients and healthy subjects. The loading plots show that higher levels of sBA correlate with UC patients (sBAs 3.74 ± 1.44 uM) and CTRL subjects (sBAs 3.94 ± 2.12 µM) while lower levels are associated to CD patients (2.25 ± 1.45 µM). Nevertheless, the loading plot highlights how the concentrations of the BA classes are important for a correct discrimination between CD and UC patients. CD patients show higher levels of the ratio between primary and secondary sBAs.

3.4. Serum BA Profile in CD Patients Treated with Anti-TNF Alpha

PCA was carried out for CD patients using concentrations of the different BA classes and biomarkers as indicated in the method section. The multivariate analysis technique highlighted a different sBA qualitative profile between CTRL, patients treated with anti-TNF alpha (CD B) and patients treated with conventional therapy (CD NB) (Figure 4). Three of the CD NB patients (patients receiving steroid treatment) were clustered in the CD B along the positive side of PC1. Steroid therapy has been reported to restore BA plasma concentration [Kwon R.S 2004]. Consequently, these patients have been considered as a separate group (CD S).

The new orthogonal space obtained by PCA demonstrates a quite clear separation on the first principal component (PC1). According to the PCA, higher levels of sBAs are associated with CTRL (sBAs 3.94 ± 2.12 μM) and CD B patients (sBAs 4.11 ± 1.23 μM), while lower levels have been associated with CD NB patients (sBAs 1.98 ± 0.42 μM). Of note, secondary BA concentration is the most discriminating parameter contributing to the clustering. Secondary sBAs significantly increase ($p < 0.05$) after anti-TNF alpha (1.54 ± 0.83 μM) compared to CD NB (0.44 ± 0.17 μM) as graphed in figure 5. CD B patients reach secondary BA levels similar to the CTRL group (1.39 ± 0.86 μM). Indeed, the loading plot of the multivariate analysis describes the relative weight of each variable in the clustering of the samples on each PC. Secondary sBAs and total sBAs have the highest loading values for the PC1, highlighting the correlation between these variables and the clusters of CD B patients and the CTRL group. On the other hand, the lowest loading value for the PC1 of the mean ratio between primary and secondary sBAs is associated with the cluster of the CD NB patients. The mean ratio between primary and secondary sBAs decreases ($p < 0.05$) in CD B patients (2.25 ± 1.45) compared to CD NB (4.00 ± 1.87), reaching values similar to those of CTRL group (1.93 ± 0.95).

FIG. 4. PRINCIPAL COMPONENT ANALYSIS (PCA) SCORES PLOT AND LOADING PLOT FOR HEALTHY SUBJECTS (CTRL), CROHN'S DISEASE PATIENTS TREATED WITH ANTI-TNF ALPHA (CD B) AND CROHN'S DISEASE PATIENTS TREATED WITH CONVENTIONAL THERAPY (CD NB). THE FIRST PC EXPLAINS 34.9% OF THE TOTAL VARIANCE AMONG THE SAMPLES. CD B AND CRTL CLUSTERS ARE ON THE POSITIVE SIDE OF THE PC1, WHILE CD NB CLUSTER IS ON THE NEGATIVE SIDE OF THE PC1. THE SECOND PC EXPLAIN 19.5% OF THE TOTAL VARIANCE, EVEN THOUGH CLUSTERING WAS NOT ASSESSED FOR GROUPS. CROHN'S DISEASE PATIENTS WITH STEROID TREATMENT (CD S) ARE PLOTTED.

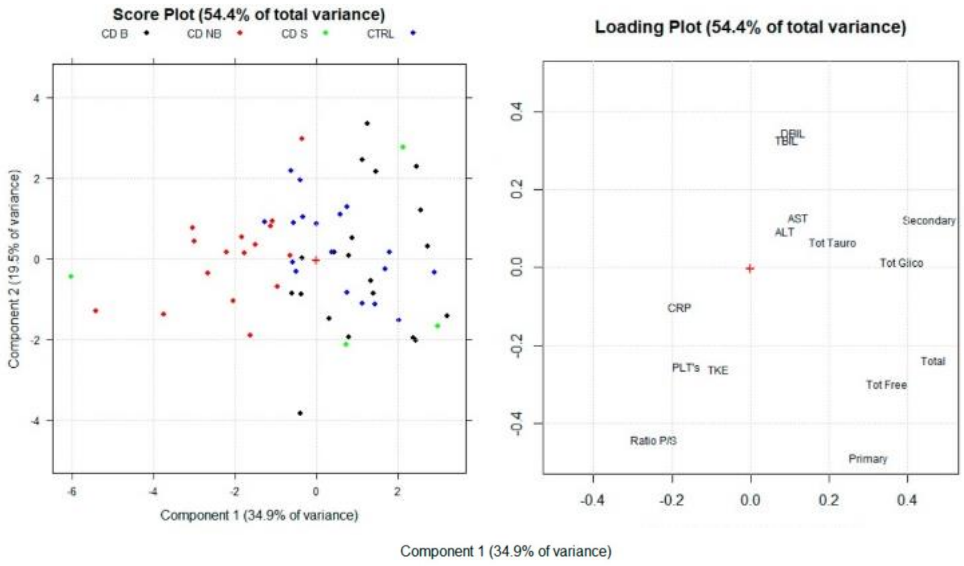

FIG. 5. MEAN CONCENTRATIONS OF TOTAL (TSBAS), PRIMARY (PBAS) AND SECONDARY BILE ACIDS (SBAS) IN CROHN'S DISEASE PATIENTS TREATED WITH ANTI-TNF ALPHA (CD B), CROHN'S DISEASE PATIENTS TREATED WITH CONVENTIONAL TREATMENT (CD NB) AND HEALTHY SUBJECTS (CTRL).

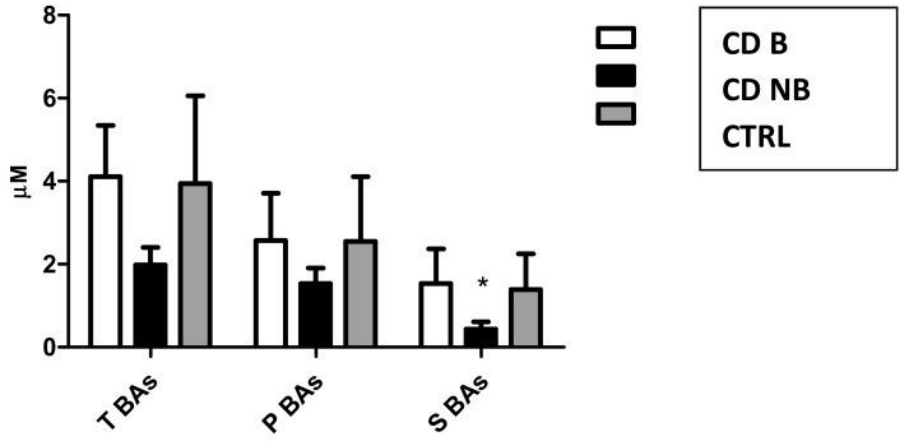

A second multivariate analysis was carried out using only single sBA concentrations to investigate which ones mostly characterize the studied groups. The results of the second PCA is reported in Figure 6.

FIG. 6. SCORE PLOT AND LOADING PLOT OF THE PRINCIPAL COMPONENT ANALYSIS (PCA) OBTAINED BY CONSIDERING SINGLE BA CONCENTRATIONS AS SELECTED VARIABLES. PC1 AND PC2 EXPLAIN THE 41.2% OF THE TOTAL VARIANCE.

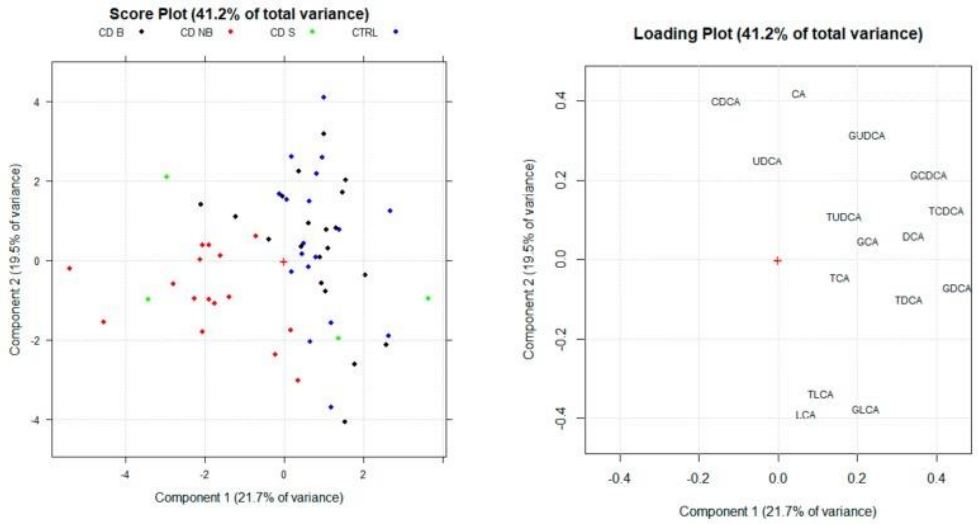

As expected, high serum concentrations of the main secondary sBAs (deoxycholic acid and its conjugated forms) are associated with CD B and CTRL clusters. Therefore, high plasma levels of other BAs, such as chenodeoxycholic acid and its conjugated forms are also correlated with CD B and CTRL subjects. Specifically, according to the loading value on the first PC, the concentration of the taurine and glycine conjugates seems to be the main discriminating variable.

3.5. Serum BA Profile in UC Patients Treated with Anti-TNF Alpha Therapy

Mean sBAs concentrations in patients treated with anti-TNF alpha (UC B), conventional therapy (UC NB), and CTRL subjects were respectively 3.26 ± 2.32, 3.74 ± 1.44, and 3.94 ± 2.12 µM (p value n.s.) (Figure 7).

FIG. 7. MEAN CONCENTRATIONS OF TOTAL (T BAS), PRIMARY (P BAS), AND SECONDARY (S BAS) BAS IN ULCERATIVE COLITIS PATIENTS TREATED WITH ANTI-TNF ALPHA (UD B), ULCERATIVE COLITIS PATIENTS TREATED WITH CONVENTIONAL THERAPY (UC NB), AND HEALTHY SUBJECTS (CTRL).

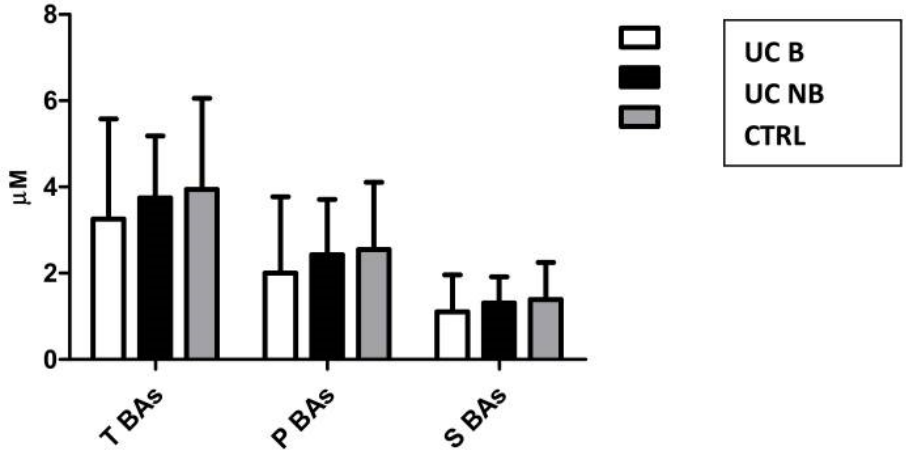

PCA was carried out using concentrations of the different BA classes and biomarkers as indicated in the method section. No difference was assessed between groups (p value ns) (Figure 8). Different profiles between groups were not assessed even when single sBAs were used for further PCAs. Indeed, no specific BA showed significant concentration variations over the treatment.

FIG. 8. SCORES PLOT AND LOADING PLOT OF THE PRINCIPAL COMPONENT ANALYSIS (PCA) FOR HEALTHY SUBJECTS (CTRL), ULCERATIVE COLITIS PATIENTS TREATED WITH ANTI-TNF ALPHA (UC B) AND ULCERATIVE COLITIS PATIENTS TREATED WITH CONVENTIONAL THERAPY (UC NB) GROUPS. THE FIRST PC EXPLAIN 25% OF THE TOTAL VARIANCE AMONG THE SAMPLES. THE SECOND PC EXPLAIN 19.5% OF THE TOTAL VARIANCE.

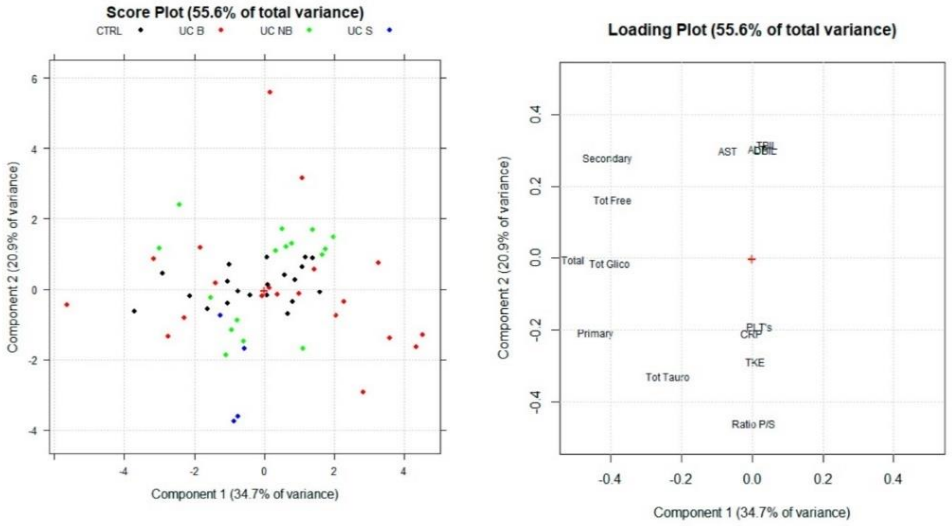

3.6. Secondary Outcomes

3.6.1. Disease Duration

Median disease duration for CD patients was 12 years (IQR 5.75-15.5), while for UC patients 13 years (IQR 5-21). Serum BAs were analyzed by dichotomizing and comparing patients within the CD B and CD NB groups with time to diagnosis lower and above 12 years. A similar approach has been adopted for UC patients.

The values of sBAs in CD B and CD NB patients with less than 12 years disease duration were respectively 4.11 ± 1.41 and 2.07 ± 0.36 µM, while in patients with longer disease they were respectively 4.19 ± 1.04 and 1.86 ± 0.41 µM. The sBA levels were not significantly different (p value < 0.05) between groups with the same treatment and disease duration. Similar results were obtained in UC where significant differences between groups were not recorded. Indeed, concentrations of sBAs in UC B and UC NB patients with longer disease were respectively 3.49 ± 2.23 and 3.58 ± 0.89 µM, while in patients with shorter disease were respectively 2.88 ± 2.26 and 3.95 ± 1.58 µM.

3.6.2. Age at Diagnosis

Median age at diagnosis was 30 (IQR 24–51) in the CD group and 37 (IQR 40–72) in the UC group. The sBAs were analyzed by dichotomizing based on median age. The values of sBAs in CD B and CD NB patients with earlier diagnosis were respectively 4.07 ± 1.31 and 1.99 ± 0.41 μM, while in older patients at diagnosis they were respectively 4.34 ± 0.92 and 1.90 ± 0.50 μM. Levels of sBAs were not significantly different (p value < 0.05) between the groups subjected to the same pharmacological treatment and no specific BA was associated with the age at diagnosis or biological treatment. No significant difference was determined in UC patients, where the sBAs levels in UC B and UC NB patients with earlier diagnosis were respectively 3.23 ± 2.59 and 3.95 ± 1.58 μM, while in older patients at diagnosis they were 3.18 ± 1.99 and 3.53 ±1.24 μM.

3.6.3. Disease Extension

With respect to disease location and according to the Montreal classification, the majority of the UC B and UC NB were classified as E3 (75% E3 and 25% E2). Among CD B patients, 11 out of 20 were L1B1, 1 was L1B2 and two were L1B3. Only one out of 20 CD B patients was L2B3, while two were L3B2 and three were L3B1. Eight out of 20 CD NB were L1B1, one L1B2, three were L2B1, one was L3B3, three were L3B1 and one L4B1. Location was not available for three patients. The sBAs qualitative composition was assessed by dichotomizing and basing on the disease extension between patients with inflammation limited to ileum (L1) and patients with more extensive illness (L2 and, L3). The values of sBAs in CD B and CD NB patients with L1 classifications were respectively 4.25 ± 1.38 and 1.94 ± 0.30 μM. The levels of sBAs in CD B and CD NB patients with L2 classification were respectively 2.93 and 1.95 ± 0.14 μM. This trend is respected also in patients with L3 classification, where the levels of sBAs in CD B and CD NB patients were respectively 3.77 ± 0.77 μM and 2.06 ± 0.53 μM. L1 patients showed the greatest concentration in relation to ileal inflammation which, according to the literature [Uchiyama K. 2018], affects the active transport of BAs. Despite these results, the increase in sBAs levels after biological treatment is met even in L2 and L3 patients without a specific localization of the illness in the ileum. As reported above, the increase in sBAs levels is strictly correlated with secondary BAs. Specifically, DCA reaches concentrations after biological treatment in L1, L2, and L3 patients respectively of 0.61 ± 0.41 μM, 0.33 μM and 0.83 ± 0.68 μM without significant differences if compared to DCA levels in CTRL subjects (0.56 ± 0.40 μM). On the other hand, patients under conventional therapy reach DCA concentrations of 0.07 ± 0.07 μM, 0.04 ± 0.04 μM and 0.05 ± 0.04 μM respectively in L1, L2, and L3 patients, with significant differences if compared to other groups ($p < 0.05$).

3.6.4. Inflammatory State

Serum BAs were analyzed by dichotomizing patients both treated and untreated with anti-TNF alpha therapy based on CRP levels using a cut-off of 7. Serum BAs were respectively 4.25 ± 1.42 μM and 2.03 ± 0.26 μM in CD B and CD NB patients with CRP lower than 7. The levels of sBAs in CD B and CD NB patients with CRP

higher than 7 mg/L were respectively 3.79 ± 0.91 μM and 1.95 ± 0.50 μM. This data is consistent with those comparing biological and conventional therapy reported above.

Serum BAs concentrations were assessed within CD B patients with higher or lower CRP values (3.66 ± 0.77 μM and 4.30 ± 1.38 μM respectively). Significant differences (p value < 0.05) were determined if secondary sBAs levels (1.03 ±0.54 μM and 1.75 ± 0.85 μM respectively) were considered. According to these results, production and absorption of secondary BAs seem to be affected by the inflammatory state. Biological therapy is more effective in restoring BAs pool when inflammatory response has been quietened by anti-TNF alpha (CRP < 7 mg/L). No significant difference was determined in UC patients with different CRP levels.

3.6.5. Steroid Treatment

The subgroup of 5 CD patients treated with steroid therapy showed higher sBAs pool (3.99 ± 0.80 μM) compared to CD NB (1.98 ± 0.42 μM), reaching concentrations similar to healthy individuals (3.94 ± 2.12 μM). Specifically, steroid treatment improves secondary sBAs concentration as well as biological treatment.

4. Conclusions

This study represents the first attempt to identify sBA profiles in IBD patients to evaluate the effect of anti-TNF alpha treatment on their serum profiles.

Qualitative and quantitative variation of sBAs levels might be related to many causes, such as impaired biosynthesis from cholesterol, faulty transport of hepatocytes or enterocytes through the cellular membrane, defective transport among the physiological compartments involved in the enterohepatic circulation, inflammatory state or abnormal bacterial overgrowth in the large intestine. Only few studies have analyzed sBA profiles in IBD patients in specific circumstances [Tiratterra E. 2018].

In this study, in order to exclude all the possible misleading variables, we performed an highly accurate selection of the patient population, basing on several criteria (exclusion of liver involvement by anamnesis and blood tests, exclusion of combination therapy, inclusion of ileum involvement in CD group, extensive colitis in UC group).

According to our results, the total concentration of secondary BAs in serum of CD patients represents the most discriminating parameter. Unlike CD patients treated with conventional therapies, CD patients receiving biologic treatment seem to restore secondary sBA levels similar to those of healthy subjects. This result indirectly suggests the positive effect of the treatment on the intestine wall and biofilm microbiota, responsible for primary BA biotransformation to secondary BAs via 7-dehydroxylation and, in addition for BAs efficient absorption.

Basing on our results, disease extension did not affect significantly secondary or primary sBA concentrations in CD B patients. However, a greater tendency was assessed toward a decrease of secondary BAs in patients with ileal disease where the active transport of BAs is affected [Uchiyama K. 2018].

Significant differences in secondary BA levels were found in CD B patients with different CRP values suggesting that TNFs treatment might restore BA pool depending on the inflammatory state.

Our study for the first time suggests that biological treatment in CD patients restores BA physiological levels. Particularly, the increase of DCA and other secondary BA concentrations seems closely associated with the anti-TNFα therapy. These results suggest that the passive absorption in the colon tract of the most lipophilic BAs has been restored. Moreover, we showed that production and absorption of secondary BAs seem to be affected by the inflammatory state. As expected, biological therapy seems to be more effective in restoring sBA concentrations when the inflammatory response has been stopped by anti-TNF alpha (CRP < 7).

Indirectly, this study further highlights the underestimated role of secondary BAs often considered excretory molecules eliminated in stools without any peculiar properties. Secondary BAs and particularly DCA still play a physiological role in controlling the FXR activity in the intestine and further studies are required to better define this role. An excessive production and accumulation of secondary BAs in subjects with bacteria overgrowth was neglected and can be the cause of hepatobiliary diseases. This is related to the potential toxicity of DCA like detergent and lipophilic compound, inducing also an increase in biliary cholesterol secretion leading to cholesterol gallstones formation. An ideal cocktail of primary and secondary BAs is the requisite to maintain the physiological equilibrium of BAs. The BA pool is controlled not only by its hepatic synthesis but mainly by the intestinal wall and bacteria metabolism that is impaired in IBD patients.

One limitation to our study is the sample size, especially when a specific treatment was considered such as steroids. A large cohort of selected patients will be therefore necessary to fully define the BAs role in IBD. However, generally these data show that each subject presents a peculiar sBA composition and response to treatment that should be more carefully evaluated in terms of time and dose by evaluating the complete sBA profile and if possible the serum level of the administered drug to relate the bioavailability of the drug (pharmacokinetic) with the sBA levels.

Classification models (PLS-DA, SIMCA) in multivariate analysis could be created if more patients were to be enrolled for this kind of study. According to our results, these models could be powerful tools also in clinical practice to obtain important information for preliminary diagnosis, disease activity, and the healing process of IBD patients.

In conclusion, this study suggests the restoring the effect of the TNF-alpha therapy on the enterohepatic circulation in CD. In particular, our preliminary results open new perspectives on the role of sBAs as non-invasive biomarkers for clinical remission in Crohn's disease and potentially for mucosal healing in ulcerative

colitis and colonic Crohn's disease in relationship to microbiota and BA. Therefore, a complete and systematic characterization of the BA profile, including secondary metabolites, can be of great help at the light of the concept of precision medicine in IBD patients.

Reference

Aldini, R., Roda, A., Festi, D., Sama, C., Mazzella, G., Bazzoli, F., ... & Barbara, L. (1982). Bile acid malabsorption and bile acid diarrhea in intestinal resection. Digestive diseases and sciences, 27(6), 495-502.

Carrott, P. J. M., & Carrott, M. R. (2007). Lignin–from natural adsorbent to activated carbon: a review. Bioresource technology, 98(12), 2301-2312.

Chiang, J. Y. (2009). Bile acids: regulation of synthesis. Journal of lipid research, 50(10), 1955-1966.

Daperno, M., D'Haens, G., Van Assche, G., Baert, F., Bulois, P., Maunoury, V., ... & Mary, J. Y. (2004). Development and validation of a new, simplified endoscopic activity score for Crohn's disease: the SES-CD. Gastrointestinal endoscopy, 60(4), 505-512.

Duboc, H., Rajca, S., Rainteau, D., Benarous, D., Maubert, M. A., Quervain, E., ... & Bridonneau, C. (2013). Connecting dysbiosis, bile-acid dysmetabolism and gut inflammation in inflammatory bowel diseases. Gut, 62(4), 531-539.

Ejderhamn, J., Rafter, J. J., & Strandvik, B. (1991). Faecal bile acid excretion in children with inflammatory bowel disease. Gut, 32(11), 1346-1351.

Evertsz, F. B., Hoeks, C. C., Nieuwkerk, P. T., Stokkers, P. C., Ponsioen, C. Y., Bockting, C. L., ... & Sprangers, M. A. (2013). Development of the patient Harvey Bradshaw index and a comparison with a clinician-based Harvey Bradshaw index assessment of Crohn's disease activity. Journal of clinical gastroenterology, 47(10), 850-856.

Gnewuch, C., Liebisch, G., Langmann, T., Dieplinger, B., Mueller, T., Haltmayer, M., ... & Schmitz, G. (2009). Serum bile acid profiling reflects enterohepatic detoxification state and intestinal barrier function in inflammatory bowel disease. World journal of gastroenterology: WJG, 15(25), 3134.

Hofmann, A. F., & Borgström, B. (1964). The intraluminal phase of fat digestion in man: the lipid content of the micellar and oil phases of intestinal content obtained during fat digestion and absorption. The Journal of clinical investigation, 43(2), 247-257.

Hofmann, A. F. (2009). Chronic diarrhea caused by idiopathic bile acid malabsorption: an explanation at last. Expert review of gastroenterology & hepatology, 3(5), 461-464.

Kawamata, Y., Fujii, R., Hosoya, M., Harada, M., Yoshida, H., Miwa, M., ... & Hinuma, S. (2003). AG protein-coupled receptor responsive to bile acids. Journal of Biological Chemistry, 278(11), 9435-9440.

Kirwan, W. O., Smith, A. N., Mitchell, W. D., Falconer, J. D., & Eastwood, M. A. (1975). Bile acids and colonic motility in the rabbit and the human. Gut, 16(11), 894-902.

Kullak-Ublick, G. A., Stieger, B., & Meier, P. J. (2004). Enterohepatic bile salt transporters in normal physiology and liver disease. Gastroenterology, 126(1), 322-342.

Kwon, R. S., & Carey, M. C. (2004). Do steroids ameliorate bile acid malabsorption in Crohn's disease?. Gut, 53(1), 10-11.

Lynch, S. V., & Pedersen, O. (2016). The human intestinal microbiome in health and disease. New England Journal of Medicine, 375(24), 2369-2379.

Monte, M. J., Marin, J. J., Antelo, A., & Vazquez-Tato, J. (2009). Bile acids: chemistry, physiology, and pathophysiology. World journal of gastroenterology: WJG, 15(7), 804.

Parks, D. J., Blanchard, S. G., Bledsoe, R. K., Chandra, G., Consler, T. G., Kliewer, S. A., ... & Lehmann, J. M. (1999). Bile acids: natural ligands for an orphan nuclear receptor. Science, 284(5418), 1365-1368.

Ridlon, J. M., Kang, D. J., & Hylemon, P. B. (2006). Bile salt biotransformations by human intestinal bacteria. Journal of lipid research, 47(2), 241-259.

Tiratterra, E., Franco, P., Porru, E., Katsanos, K. H., Christodoulou, D. K., & Roda, G. (2018). Role of bile acids in inflammatory bowel disease. Annals of gastroenterology, 31(3), 266.

Uchiyama, K., Kishi, H., Komatsu, W., Nagao, M., Ohhira, S., & Kobashi, G. (2018). Lipid and Bile Acid Dysmetabolism in Crohn's Disease. Journal of immunology research, 2018.

Vashist, N. M., Samaan, M., Mosli, M. H., Parker, C. E., MacDonald, J. K., Nelson, S. A., ... & Jairath, V. (2018). Endoscopic scoring indices for evaluation of disease activity in ulcerative colitis. Cochrane Database of Systematic Reviews, (1).

Vessey, D. A. (1978). The biochemical basis for the conjugation of bile acids with either glycine or taurine. Biochemical Journal, 174(2), 621-626.

Paper 3

Trapping of plasma-derived bile acids in subdural hematomas

Reproduced from:

Trapping of plasma-derived bile acids in subdural hematomas

Emanuele Porru, Erik Edström, Ahmed A. Saeed, Gösta Eggertsen, Anita Lövgren-Sandblom, Aldo Roda, Ingemar Björkhem

Journal of Steroid Biochemistry and Molecular Biology (under revision)

Abstract

Bile acids are known to pass the blood-brain barrier and are present at low concentrations in the brain. In a previous work it was shown that subdural hematomas are enriched with bile acids and that the levels in such hematomas are higher than in the peripheral circulation. The mechanism behind this enrichment was never elucidated. Bile acids have a high affinity to albumin, and subdural hematomas contain almost as high albumin levels as the peripheral circulation. A subdural hematoma is encapsulated by fibrin which may allow passage of small molecules like bile acids but may prevent passage of proteins like albumin. We speculated that bile acids originating from the circulation may be "trapped" in the albumin in subdural hematomas. In the present work we measured the conjugated and unconjugated primary bile acids cholic acid and chenodeoxycholic acid in subdural hematomas and in peripheral circulation of 24 patients. In most patients the levels of both conjugated and free bile acids were higher in the hematomas than in the circulation but the enrichment of unconjugated bile acids was markedly higher than that of conjugated bile acids. In 6 patients with a known time interval between the primary bleeding and the operation there was a linear relation between this time period and the accumulation of bile acids. The linear relation was most obvious for unconjugated bile acids. The results are consistent with a continuous flux of bile acids, in particular unconjugated bile acids, across the blood-brain barrier. If a subdural hematoma is present, there will be a trapping of these bile acids in the albumin. We discuss the possible physiological importance of albumin binding of bile acids in the brain.

1. Introduction

Unconjugated bile acids are known to pass the blood-brain barrier and are present at low concentrations in the brain [Mano N. 2004, Higashi T. 2017, Ismail M.A.M. 2017]. There is a high correlation between circulating and brain levels of the unconjugated bile acids, and it has been suggested that the major mechanism for the transport of unconjugated bile acids into the brain across the blood-brain barrier is by passive diffusion [Higashi T. 2017]. This could be related to their lipophilicity with octanol/water partition coefficient (LogP) higher than 2, particularly for unconjugated dihydroxy bile acids [Roda A. 1990]. In the circulation the major fraction of bile acids is conjugated with taurine or glycine. There is a high affinity between albumin and bile acids [Roda A. 1982] and most of the bile acids in the circulation is bound to albumin (70-80%). Under normal conditions very little albumin is present in the brain. In connection with a subdural bleeding, however, there is an injection of albumin into the central nervous system. The albumin in the hematoma will be encapsulated by fibrin membranes that can be passed by low-molecular weight compounds. The encapsulated albumin is likely to contain both free and conjugated bile acids. Provided there is a constant flux of unconjugated bile acids into the brain as suggested, the amount of unconjugated bile acids is likely to increase due to a

"trapping" in the albumin. In a previous work we showed that there are significantly higher concentrations of total bile acids in subdural hematomas than in the circulation [Nagata K. 1993]. In that study only total levels of bile acids were measured, however, and the relation between free and conjugated bile acids was never defined. The levels of albumin in the circulation and in the hematomas were also never measured. In similarity with bile acids the bile acid precursor 7 alpha hydroxy-3-oxo-4-cholestenoic acid (7Hoca) has a high affinity to albumin. In contrast to bile acids this steroid is formed in the brain. We could demonstrate an efficient "trapping" of this steroid in albumin-containing subdural hematomas, a trapping that increased with the time from the bleeding to the time of the surgical removal of the hematoma [Saeed A.A. 2017]. In the present work we have measured conjugated and free bile acids in subdural hematomas and in the circulation of patients. The levels have been related to the levels of albumin and the time between the bleeding and the collection of the hematoma. The results suggest that there is an efficient trapping of bile acids, in particular unconjugated bile acids, in the albumin-containing hematoma and that this trapping is similar to the trapping of 7Hoca.

2. Material and methods

2.1 Specimens from patients with cerebral hematoma.

Hematoma and blood samples were collected from patients operated on due to subdural bleeding. Eighteen of the 24 patients were the same as those in a previous publication [Saeed A.A. 2017]. Two patients in the original population were excluded because of extremely high levels of bile acids in the circulation (>3SD). All the patients were involved in the study after providing informed consent. All the investigations were approved by the ethical committee. The hematomas were frozen at -70C immediately after the collection and stored for a maximum of 3 years before analysis.

2.2 Standards

Material of the purest form was used for standardization (Sigma-Aldrich, Dorset, UK; cholic acid and chenodeoxycholic acid 98% pure). All stocks were prepared in methanol (HPLC grade, Thermo-Fisher Scientific UK Ltd, Loughborough, UK). These stocks were then diluted with methanol to provide mixed working stocks containing each of cholic acid, deoxycholic acid and chenodeoxycholic acid at a concentration of 100 µg/ml. Standards were diluted with the same solvent to produce a 7 points standard curve from 0,01 µg/ml to 5 ug/ml for total bile acids. A mixed deuterated internal standard solution, composed by d4-deoxycholic acid (2,2,4,4-d4 (3α, 5β, 12α) – 3, 12-dihydroxy-5-cholan-24-oic acid), d4-chenodeoxycholic acid (2,2,4,4-d4–3α, 7α-dihydroxy-5β-cholanic acid) and d4-cholic acid (2,2,4,4-d4 (3α, 5β, 7α, 12α) – 3, 7, 12-

trihydroxycholan-24-oic acid), was added to each standard (0.5 µg) and evaporated to dryness under a stream of nitrogen prior to chemical derivatization. Calibration curve for free bile acid quantification was obtained in the same way in a linearity range from 0,001 µg/ml to 1 µg/ml.

2.3 Gas chromatography and mass spectrometry set up for bile acids

The bile acids chenodeoxycholic acid and cholic acid were assayed by isotope dilution mass spectrometry (ID-GCMS) with deuterium labeled internal standards by using a method adapted from Björkhem I. and Falk O. [Björkhem I. 1983]. 250 ml of each samples was hydrolysed by sodium hydroxide solution and heated at 130°C for 12h. Following extraction and delipidation, bile acids were chemically derivatized by methylation [Presser A. 2004] and trimethylsylilation [Langer S.H. 1958] prior to analysis by ID-GCMS. In the assay of unconjugated bile acids, the saponification step was deleted.

3 µL of each sample were injected into a GC-MS system (Agilent GC4890, MS 5973) based on electron ionization (EI) system and a single quadrupole mass analyzer. The column used was an Agilent J&W Ultra 1 column (0.2 mm x 25m, 0.33 µm, 100% dimethylpolysiloxane). The analytical condition was the following: injector temperature 270°C, splitless mode, oven temperature from 180°C ramped to 300°C, total run time 42 min and helium gas flow rate 1 mL/min. In Table 1 the retention times and the utilized MS ions have been reported. In figure 1 the mass spectra in full scan mode of the CDCA.

TABLE 1. RETENTION TIMES AND THE MS IONS FOR ALL THE ANALYSED BAS.

BA	**Retention time (min)**	**Ions (m_1/z_1)**
CA	24.64	623
d4-CA	24.60	627
CDCA	24.38	370
d4-CDCA	24.35	374

FIG. 1. MASS SPECTRA OF CDCA IN FULL SCAN ACQUISITION MODE.

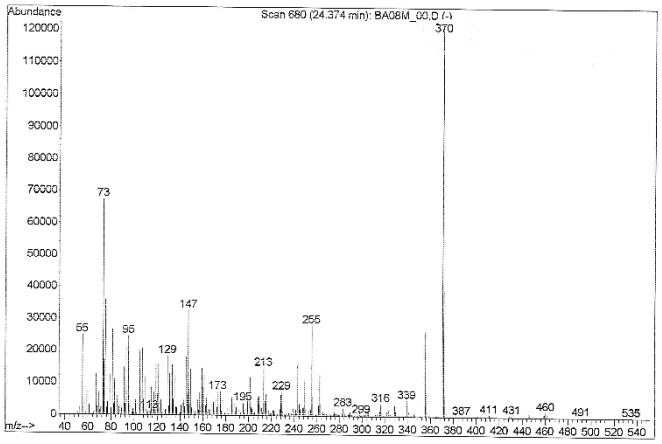

In figure 2 the chromatogram of CA and CDCA at 1 µg/ml.

FIG. 2. CHROMATOGRAM OF THE ANALYSED BAS.

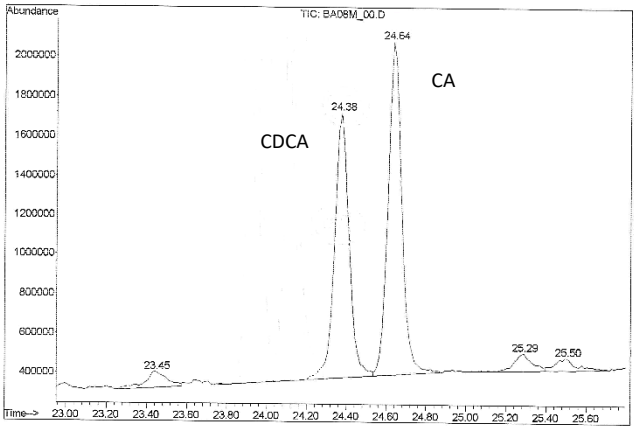

2.4 Albumin determination

Albumin was determined in hematoma material and blood using Tina-quant Albumin Gen. 2 kit (Roche). It is an immunoturbidimetric assay where Anti-albumin antibodies react with the antigen in the sample to form antigen/antibody complexes which, following agglutination, are measured turbidimetrically.

2.5 Electrophoresis

To confirm the binding ability of albumin to bile acids in hematomas, the protein extracted from a hematoma was subjected to agarose gel electrophoresis. The different protein bands were hydrolyzed as above followed by extraction, derivatization and analysis by ID-GCMS.

2.6 Statistical analysis

Univariable statistical data analysis was performed using GraphPad Prism 5.0 software (La Jolla, CA, USA). T-test was used after checking the normal distribution of the data. The 95% confidence level was used.

3. Results

Bile acids are known to be efficiently bound to albumin in the circulation and this could be expected to be the situation also in hematomas. To confirm this, we analyzed a hematoma by agarose gel electrophoresis followed by extraction of the different protein bands and analysis for bile acids. We found that 73-90% of the different bile acids were located in the albumin band.

The levels of cholic acid and chenodeoxycholic acid were measured in the 24 hematoma samples and in the 24 blood samples. The difference between the levels of conjugated cholic acid in hematomas and peripheral circulation (83 +/- 13 ng/ml and 97 +/- 28 ng/ml respectively) was not statistically significant ($p>0.05$). In 11 hematoma samples the level of conjugated cholic acid was lower in the hematoma than in the circulation.

The levels of conjugated chenodeoxycholic acid in the hematomas and peripheral circulation were found to be 373 +/- 45 ng/ml and 281 +/- 60 ng/ml, respectively. As for conjugated cholic acid, these concentrations were not statistically different ($p = 0.15$). In 5 patients the level of conjugated chenodeoxycholic acid was lower in the hematoma than in the circulation.

On the contrary, the difference between the concentrations of unconjugated cholic acid in hematomas and peripheral circulation (53 +/- 12 ng/ml and 24 +/- 9 ng/ml respectively) was statistically significant ($p=0.0017$). In all but 6 of the 24 patients the levels of free cholic acid were lower in the hematoma than in the peripheral circulation. The levels of unconjugated chenodeoxycholic acid were found to be 196 +/- 65 ng/ml and 85 +/- 57 ng/ml in the hematomas and in the circulation, respectively. As for unconjugated cholic acid, this difference was statistically significant ($p = 0.03$). In 4 of the patients the level of free chenodeoxycholic acid was lower in the hematoma than in the circulation.

FIG. 3. RATIOS BETWEEN CONCENTRETIONS OF BILE ACIDS IN HEMATONA (H) AND PERIFERIAL BLOOD (B) SAMPLES, FOR BOTH FREE AND CONJUGATED FORMS OF CHOLIC ACID (CA) AND CHENODEOXYCHOLIC ACID (CDCA).

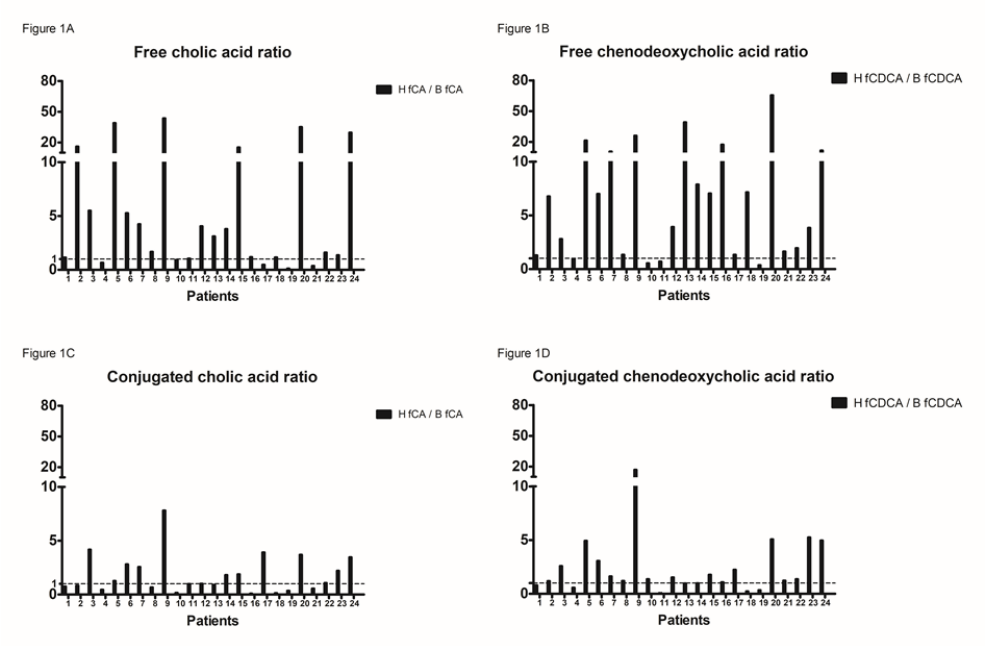

In Fig. 3A is shown the ratio between the level of free cholic acid in the hematoma and in the peripheral circulation (H fCA/B fCA) for each patient. In 6 of the patients the level of unconjugated cholic acid was more than 10-fold higher in the hematoma than in the circulation

In Fig. 3B the relation between the level of free chenodeoxycholic acid in the hematoma and in the peripheral circulation (H fCDCA/B fCDCA) for each patient is shown. In 7 of the patients the level of unconjugated chenodeoxycholic acid was more than 10-fold higher in the hematoma than in the circulation.

In Fig. 3C the ratio between the level of conjugated cholic acid in the hematoma and in the peripheral circulation (H cCA/B cCA) for each patient is shown. In 13 of the patients the ratio was above 1. In general, the ratio was considerably lower than the corresponding ratio between unconjugated cholic acid in hematoma and circulation.

In Fig. 3D is shown the ratio between the level of conjugated chenodeoxycholic acid in hematoma and circulation (H cCDCA/B cCDCA) for each patient. In 5 of the patients the ratio was less than 1. In general, the ratio was considerably lower than the corresponding ratio between unconjugated chenodeoxycholic acid in hematoma and circulation.

In addition to the absolute levels of the two different bile acids, we also calculated the ratio between the bile acid and the albumin concentration. Because the albumin concentration of the hematoma was similar to the albumin concentration in the peripheral circulation (23 +/- 2 mg/ml and 19 +/- 2 mg/ml), albumin corrections did not change the general patterns shown in Fig. 3.

In 6 of the patients with accumulation of unconjugated bile acids we had information about the approximate time between the first symptoms of the bleeding and the surgical removal of the hematoma. As seen in Fig 4, there was an accumulation of unconjugated bile acids in hematoma samples during the bleeding time.

FIG. 4. ACCUMULATION OF BILE ACIDS IN HEMATOMA SAMPLES EXPRESED AS BLEEDING TIME VERSUS THE RATIOS BETWEEN CONCENTRATIONS OF BILE ACIDS IN HEMATONA (H) AND PERIFERIAL BLOOD (B) SAMPLES, FOR BOTH FREE AND CONJUGATED FORMS OF CHOLIC ACID (CA) AND CHENODEOXYCHOLIC ACID (CDCA).

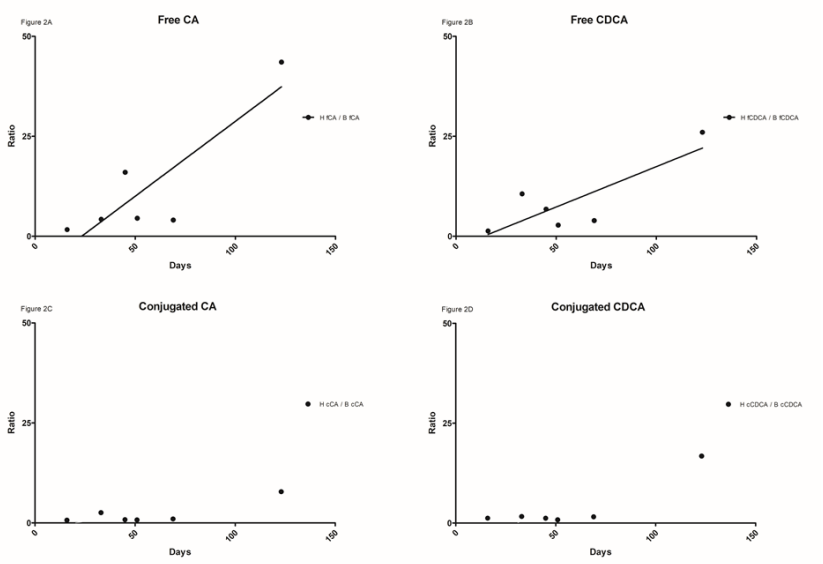

In contrast there was a little or no increased concentration of conjugated bile acid with time between bleeding and surgery in 5 patients. In one patient however, there was a significantly increased level of conjugated bile acid 123 days after the primary bleeding.

4. Discussion

The results from the investigation of most of our patients are in agreement with our hypothesis that there is a continuous flux of unconjugated bile acids from the circulation into the brain and that these specific bile acids are trapped in albumin-containing subdural hematomas. The preferential flux of unconjugated bile acids in relation to conjugated bile acid may in part be due to their higher lipophicity (1-2 fold higher LogP) [Roda A. 1990]. This may account for their efficient transfer across lipid membrane domains even when fully ionized at physiological pH. This is also likely to be the mechanism behind the enrichment of bile acids in subdural hematomas reported more than 25 years ago [Nagata K. 1993].

However, not only the unconjugated bile acids but also the conjugated forms accumulated to some extent in the hematomas of some patients. The conjugated bile acid must originate from the circulation and it seems likely that, at least part of this accumulation, is due to re-bleeding. If this is the case, the conjugated bile acids are likely to reach the brain bound to albumin. We cannot however exclude the possibility that there is some

direct flux of conjugated bile acid across the blood-brain barrier. In any case, the accumulation of conjugated bile acids was in general considerably lower than the corresponding accumulation of the free bile acids. Therefore, the phenomenon is characterized by two steps: diffusion across lipid membrane domains which is related to the bile acids lipophilicity [Fong C.W. 2015] and second the strong interaction with human albumin which is similar for unconjugated and conjugated bile acids.

In 6 of our patients the concentration of unconjugated bile acids was higher in the circulation than in the hematoma for at least one of the two bile acids. The reason for this is unclear but at least two different explanations are possible. The bile acids in the circulation are subject to significant variations due to diurnal rhytms, dietary factors, or gastrointestinal disturbances. It should be pointed out that the blood sample was taken at just one point in time whereas the accumulation of bile acids in hematoma is likely to reflect bile acids in the circulation during a longer time period. The possibility must also be considered that a partial degradation of albumin may occur after some time with a release of the bound bile acid. In fact, 3 of the 6 hematoma samples with lower bile acid levels than in the circulation had a different colour than the other samples, possibly reflecting some type of degradation. The total albumin concentration as measured with the above method was however similar to that of the other hematoma samples. Thus if a degradation had occurred it did not affect the total amount of albumin.

It is interesting to compare the degree of accumulation of unconjugated bile acids in subdural hematomas with the corresponding accumulation of 7Hoca. The mean accumulation of 7Hoca was about 6 fold and the accumulation of unconjugated bile acid was 3-6 fold. In the case of unconjugated bile acids some patients had an accumulation more than 20-fold whereas the maximum accumulation of 7Hoca was about 10-fold [Saeed A.A. 2017].

The possible biological importance of the binding of bile acids to albumin in hematomas can only be speculated on. Bile acids have been reported to interact with receptors involved in neurotransmission (for a review- see ref. M. McMillin 2016). Such interaction may cause negative effects. Binding to albumin can be expected to prevent such negative effects by reducing the concentration of free unconjugated bile acids.

Reference

Björkhem, I., & Falk, O. (1983). Assay of the major bile acids in serum by isotope dilution-mass spectrometry. Scandinavian journal of clinical and laboratory investigation, 43(2), 163-170.

Fong, C. W. (2015). Permeability of the blood–brain barrier: molecular mechanism of transport of drugs and physiologically important compounds. The Journal of membrane biology, 248(4), 651-669.

Higashi, T., Watanabe, S., Tomaru, K., Yamazaki, W., Yoshizawa, K., Ogawa, S., ... & Mano, N. (2017). Unconjugated bile acids in rat brain: Analytical method based on LC/ESI-MS/MS with chemical derivatization and estimation of their origin by comparison to serum levels. Steroids, 125, 107-113.

Ismail M.A.M., Mateos L., Maioli S., Merino-Serrais P., Ali Z., Lodeiro M., Westman E., Leitersdorf E., Gulyás B., Olof-Wahlund L., Winblad B., Savitcheva I., Björkhem I., Cedazo-Mínguez A. (2017). 27-Hydroxycholesterol impairs neuronal glucose uptake through an IRAP/GLUT4 system dysregulation. The Journal of Experimental Medicine, 214 699-717.

Langer, S. H., Connell, S., & Wender, I. (1958). Preparation and properties of trimethylsilyl ethers and related compounds. The Journal of Organic Chemistry, 23(1), 50-58.

Mano, N., Goto, T., Uchida, M., Nishimura, K., Ando, M., Kobayashi, N., & Goto, J. (2004). Presence of protein-bound unconjugated bile acids in the cytoplasmic fraction of rat brain. Journal of lipid research, 45(2), 295-300.

McMillin, M., & DeMorrow, S. (2016). Effects of bile acids on neurological function and disease. The FASEB Journal, 30(11), 3658-3668.

Nagata, K., Axelson, M., Bjoerkhem, I., Matsutani, M., & Takakura, K. (1993). Significance of cholesterol metabolites in chronic subdural hematoma. In Recent Advances in Neurotraumatology (pp. 49-52). Springer, Tokyo.

Presser, A., & Hüfner, A. (2004). Trimethylsilyldiazomethane–a mild and efficient reagent for the methylation of carboxylic acids and alcohols in natural products. Monatshefte für Chemie/Chemical Monthly, 135(8), 1015-1022.

Roda, A., Minutello, A., Angellotti, M. A., & Fini, A. (1990). Bile acid structure-activity relationship: evaluation of bile acid lipophilicity using 1-octanol/water partition coefficient and reverse phase HPLC. Journal of lipid research, 31(8), 1433-1443.

Roda, A., Minutello, A., Angellotti, M. A., & Fini, A. (1990). Bile acid structure-activity relationship: evaluation of bile acid lipophilicity using 1-octanol/water partition coefficient and reverse phase HPLC. Journal of lipid research, 31(8), 1433-1443.

Roda, A., Cappelleri, G., Aldini, R., Roda, E., & Barbara, L. (1982). Quantitative aspects of the interaction of bile acids with human serum albumin. Journal of lipid research, 23(3), 490-495.

Saeed, A. A., Edström, E., Pikuleva, I., Eggertsen, G., & Björkhem, I. (2017). On the importance of albumin binding for the flux of 7α-hydroxy-3-oxo-4-cholestenoic acid in the brain. Journal of lipid research, 58(2), 455-459.

Chapter 2. Nutraceutical

Nowadays, there is a growing interest in the nutraceutical field. But what does “nutraceutical” mean?

In the United States of America, they are classified as dietary supplements and food additives by the FDA. Dietary supplement is a component introduced in diet to provide benefits. Depending on the jurisdiction, nutraceuticals may claim to improve health, prevent illnesses and increase life expectancy. This huge family of compounds includes vitamins, minerals, herbs or other botanicals, amino acids, enzymes; and they can also be extracts to obtain tablets, capsules, topic formulations, or powders.

In our world where trends suggest foods always more functionalized, enriched and healthy, these products are taking part of a booming market. The European dietary supplement market in 2015 was ca. h14 billion. On the other hand, the main problem is that nutraceuticals are largely unregulated and not subjected to any clinical trial because not defined drugs. In the last decade many scientists have been talking about the potential risks to evaluate nutraceutical as safe compounds exclusively based solely on their “natural” genesis.

Several studies on nutraceuticals have been carried out supporting their physiological activities and their safety. Nevertheless, many nutraceutical products have not been studied properly and there is a lack of information about their activity, biodistribution, metabolism and potential side effects. In a recent survey based on 3667 cases, it has been extrapolated that ca. 25,000 emergency department admissions per year can be attributed to dietary supplements in the United States [Geller A. 2015]. For example, risks may arise due to the impurities, as reported in a recent publication [Brodziak-Dopierala B. 2018] about contamination of heavy metals in case of herbal dietary supplements.

There is another aspect which is worth mentioning: the products from the nutraceutical catabolic pathway are often not evaluated, as well as their effects and biodistribution on the human body. In such scenario, this chapter specifically deals with the natural molecules Berberine (BBR). It is a naturally occurring compound in plants such as goldenseal and oregon grape. This quaternary ammonium salt has been recognized for multiple physiological activities and its ability to regulate cholesterol levels. Several studies in literature report pharmacological effects and metabolism of BBR. However, some recent manuscripts highlight that a better evaluation of berberine metabolism, biodistribution and activities is necessary for safety purposes.

Reference

Brodziak-Dopierała, B., Fischer, A., Szczelina, W., & Stojko, J. (2018). The Content of Mercury in Herbal Dietary Supplements. Biological trace element research, 185(1), 236-243.

Geller, A. I., Shehab, N., Weidle, N. J., Lovegrove, M. C., Wolpert, B. J., Timbo, B. B., ... & Budnitz, D. S. (2015). Emergency department visits for adverse events related to dietary supplements. New England Journal of Medicine, 373(16), 1531-1540.

Paper 4

Combined analytical approaches to define biodistribution and biological activity of semi-synthetic berberrubine, the active metabolite of natural berberine

Reproduced from:

Combined analytical approaches to define biodistribution and biological activity of semi-synthetic berberrubine, the active metabolite of natural berberine.

Emanuele Porru, Placido Franco, Donato Calabria, Silvia Spinozzi, Marinella Roberti, Cristiana Caliceti, Aldo Roda

Analytical and Bioanalytical Chemistry (2018) 410:3533–3545. https://doi.org/10.1007/s00216-018-0884-2

License Number: 4698311251100

Abstract

Berberine (BBR) is a natural alkaloid obtained from Berberis species plants, known for its protective effects against several diseases. Among the primary BBR metabolites, berberrubine (M1) showed the highest plasma concentration but few and conflicting data are available regarding its concentration in biological fluids related to its new potential activity on vascular cells.

A combined analytical approach was applied to study biodistribution of M1 in comparison with BBR. The optimization of sample clean-up combined with a fully validated HPLC-ESI-MS/MS tailored for M1 allows sufficient detectability and accuracy to be reached in the different studied organs even when administered at low dose, comparable to that assumed by human. A predictive human vascular endothelial cell-based assay to measure intracellular xanthine oxidase has been developed and applied to study unexplored activities of M1 alongside other common activities. Results showed that oral M1 treatment in rats exhibits higher plasma levels than BBR, reaching maximum concentration 400-fold higher than BBR (204 vs 0.5 ng/mL); moreover, M1 exhibits higher concentrations than BBR also in all the biological compartments analysed. Noteworthy, the two compounds follow two different excretion routes: M1 through urine, while BBR through feces. In vitro studies demonstrated that M1 inhibited intracellular xanthine oxidase activity, one of the major sources of reactive oxygen species in vasculature, with an IC50 = 9.90 ± 0.01 μg/mL and reduced the expression of the inflammatory marker ICAM-1. These peculiar characteristics allow new perspectives to be opened up for the direct use of M1 instead of BBR in endothelial dysfunction treatment.

1. Introduction

It is well recognized that the major determinants of several chronic diseases (e.g., cardiovascular diseases, diabetes and metabolic syndrome) in Western countries are not genetic factors but epigenetic alterations, principally due to diet and lifestyle. Therefore, many efforts are put towards the study of nutraceuticals and functional foods as crucial for their potential impact on both human health and community social costs [Franco P. 2016]. The current European regulations consider nutraceuticals as food supplements and therefore they do not require conventional drug approval based on preclinical and toxicological studies. By this way, their biodistribution in the human body, their dose-related metabolism, target organ activity, and potential toxicity have been poorly studied [Marazzi G. 2011]. This may hamper the definition and discovery of active molecules or toxic impurities in a given extract.

Berberine (BBR: Benzo(g)-1,3-benzodioxolo(5,6-a)quinolizinium, 5,6-dihydro-9,10-dimethoxy-), a quaternary ammonium salt from the protoberberine group of isoquinoline alkaloids, naturally occurring in plants of the Berberis species, has been recognized for multiple pharmacological activities including antimicrobial activity, lipid-lowering capacity, inhibition of ventricular tachyarrhythmia, and reduction of endothelial inflammation

[Amin A.H. 1969, Sabir M. 1971]. Pharmacokinetic studies on BBR carried out in rat and human showed a poor oral bioavailability, which requires relatively high dosages for effective activity [Qiu F. 2008]. These studies showed that BBR undergoes phase I metabolism in the liver by the action of CYP450, where oxidative demethylation occurs at positions 2, 3, 9, and 10 [Li Y. 2011]. Phase I metabolites are then conjugated with glucuronic and sulfuric acids to form phase II metabolites, which are readily excreted. In human and rat, the main BBR metabolites (figure 1) are berberrubine (M1: benzo(g)-1,3-benzodioxolo(5,6-a) quinolizinium, 5,6-dihydro-9-hydroxy-10-methoxy-), thalifendine (M2: Benzo(g)-1,3-benzodioxolo(5,6-alpha)quinolizinium, 5,6-dihydro-10-hydroxy-9-methoxy-), demethyleneberberine (M3: Dibenzo[a,g]quinolizinium,5,6-dihydro-2,3-dihydroxy-9,10-dimethoxy-), and jatrorrhizine (M4: Dibenzo[a,g]quinolizinium, 5,6-dihydro-3-hydroxy-2,9,10-trimethoxy-).

FIG. 1. PRIMARY HEPATIC METABOLISM OF BBR

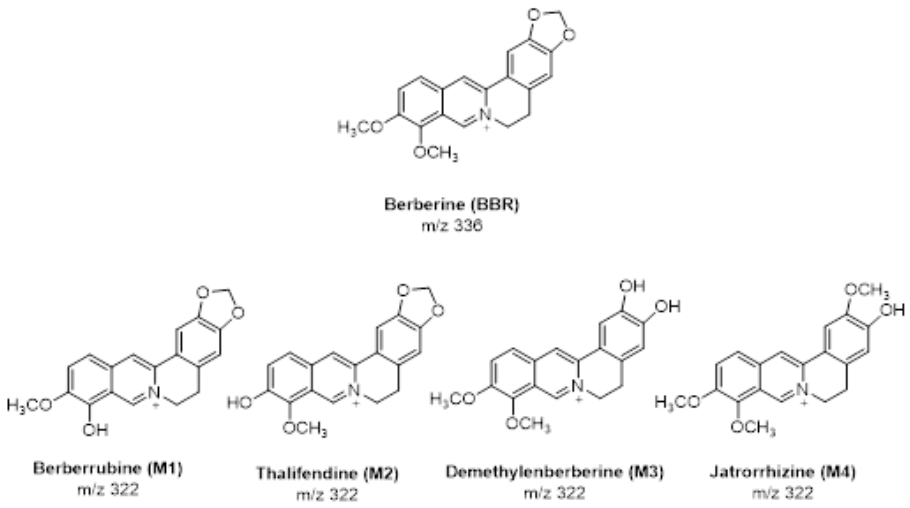

In a previous study, we demonstrated that among phase I metabolites, M1, more than BBR itself, shows the highest plasma concentrations, suggesting that this molecule may be potentially more pharmacologically active than its precursor. Despite its potential use in clinical practice, just few authors reported data regarding the biodistribution and the in vivo behaviour after its direct administration [Wang X. 2015]. Additionally, few papers [Yang N. 2016] reported protocols not fully validated for M1 analysis, especially as regards the pre-analytical sample treatment from biological matrices. This is mainly due to the lack of commercially available standard, with consequent problems in the evaluation of the matrix effect and recoveries after clean-up procedures.

In this work, we developed a suitable and fully validated HPLC-ESI-MS/MS method for the analysis of M1 in different biological fluids and organs to define the biodistribution and mass balance of this compound in comparison to BBR, after their direct oral administration in normal rats. M1 has been synthetized as

previously reported by us [Spinozzi S. 2014] and efficient clean-up procedures have been developed in order to minimize the matrix effect related to the different biological samples investigated, including the plasma, urine, liver, kidneys, intestinal contents, and stools. Considering the low solubility of this class of compounds, we administrated a dose (2 mg/kg) that is completely soluble in aqueous medium chosen for the gavage, in order to improve the reproducibility of the experiments, avoiding the administration of non-dissolved molecules. Indeed, it has been reported that the absorption of orally administrated compounds in their crystalline state is dissolution-rate limited [Li F. 2015]. Additionally, the use of metastable supersaturated solutions of drugs, which are typically formed after dispersion of the formulation, is still debated [C.W. Pouton 2006]. Therefore, the use of a dose entirely dissolved in the administration medium was preferred to overcome these issues. Furtherly, considering that M1 is expected to be better absorbed than BBR and that high doses of the latter are associated to some side effects (gastrointestinal disorders) [Kulkarni S.K. 2010], assessing the bioavailability at low dosages might be a way to overcome such kind of drawbacks. It has been recently reported that M1 possesses hepatoprotective activity by inhibiting the lipid peroxidation [El-Salam M.A. 2015, Wang K. 2017], lipid lowering effects by upregulating the low-density lipoprotein receptor (LDLR) reducing the cellular lipid accumulation in human hepatic cells [Zhou Y. 2014], anti-diabetic effects by glucose lowering activity and induction of glucose consumption, glycogenesis, and modulation of glucose-6-phosphatase hexokinase expression in human liver cells [Chen H.Y. 2012, N. Yang 2017]. Recent reports demonstrated the effectiveness of BBR supplementation in endothelial dysfunction [Caliceti C. 2017], but the role of M1 in this context remains unexplored. Therefore, we developed and validated a rapid and ultrasensitive cell based chemiluminescent bioassay to determine intracellular xanthine oxidase activity, a biomarker of oxidative stress linked to endothelial dysfunction [Caliceti C. 2016]; moreover, conventional activity bioassays have been also performed including qRT-PCR to quantify the expression of several genes involved in oxidative and inflammatory signalling pathways. To the best of our knowledge, this is the first attempt that correlates a highly predictive in vitro biological activity evaluation of M1 and BBR in human living non-engineered vascular endothelial cells with the in vivo biodistribution after their direct administration.

Several papers reported whole cell bioassays based on bioluminescence detection methods [Gui Q. 2017, C.M. Rathbun 2017]. However, in these studies, the probe enzyme responsible for the detection was overexpressed inside the cell, being not representative of human physiological conditions. Moreover, as far as we know, a study that evaluates xanthine oxidase activity as biomarker has not been reported by any authors. In our work, this combination of an *in vitro* model with *in vivo* evaluation of biodistribution is used to simulate the physiological human situation, making this assay greatly reliable in the assessment of the beneficial properties of these molecules. This innovative and validated combined analytical approach, based on assessment of metabolism and biodistribution, their relationship with the more relevant physicochemical properties and in vivo/in vitro activity characterization, represents a smart and powerful tool to evaluate the

safety and the biological activities useful for a complete nutraceutical profiling. Our final aim was to propose a correct approach to better evaluate nutraceuticals with the goal to open new perspectives on the use of M1 instead of BBR in view of its possible future application in cosmetic, nutraceutical, and pharmaceutical fields.

2. Materials and methods

2.1 Chemicals and reagents

Berberine chloride, (R, S)-noscapine, Tris-HCl salt, oxypurinol, xanthine oxidase from bovine milk, luminol sodium salt, Na-EDTA salt, gelatin from bovine skin, penicillin/streptomycin, and Trypsin-EDTA were purchased from Sigma-Aldrich (St. Louis, MO, USA). M200 medium, low serum growth supplements, SuperScript III reverse transcriptase, random hexamers, dNTPs, RNase OUT, and LDH assay kits were from Thermo Fisher Scientific (Carlsbad, CA, USA). Fetal bovine serum (FBS) was from Lonza (Basel, Switzerland). RNeasy Mini Kit was from Qiagen (Hilden, Germany). PerfeCta SYBR Green SuperMix with ROX kit was from Quanta Biosciences (Gaithersburg, MD, US). Primers for RT-PCR were purchased from IDT (Coralville, IA, USA). Jatrorrhizine (M3) chloride was purchased from AlloraChem srl (Rimini, Italy). Berberrubine (M1) and demethyleneberberine (M4) were synthesized according to [Spinozzi S. 2014]. All other reagents were of HPLC-grade: sodium perborate, boric acid, NaOH, FeCl2, methanol, and acetonitrile were purchased from Carlo Erba Reagents (Milan, Italy) and LiChrosolv. Oasis HLB (hydrophilic–lipophilic balance 200 mg, 6 mL) SPE columns were purchased from Waters (Milford, MA, USA). Unless otherwise stated, all other reagents were obtained from Sigma-Aldrich and used without further purification.

2.2 HPLC-ESI-MS/MS

Liquid chromatography was performed using a 2690 Alliance system (Waters, Milford, MA, USA). Analytical separation was performed using a C18 (5 µm, 150 mm× 2.0 mm i.d.) column (Luna, Phenomenex). The mobile phases were 10mM formic acid in water adjusted to pH 4.0 with ammonia (solvent A) and a solution of acetonitrile-methanol (95:5 v/v) (solvent B). Separation was achieved at 0.15-mL/min flow rate under gradient elution conditions: 95% A for 5 min, 95– 40% A from 5 to 15 min, 40–20% from 15 to 20 min, 20% A from 20 to 25 min, 20–95% A from 25 to 27 min, and 95% A from 27 to 35 min. All the changes in the mobile phase composition were linear. The injected sample volume was 5 µL. The analytical column was maintained at 30 °C. The column effluent was introduced into the ESI source, operating in positive ionization mode, connected to a triple quadruple mass spectrometer (Quattro-LC, Micromass) operating in multiple reaction monitoring (MRM) acquisition mode.

The most abundant signals for each compound in full scan acquisition mode were monitored for the quantification [m/z 336→320 (BBR), m/z 322→307 (M1), m/z 324→280 (M3), m/z 338→323 (M4), and m/z 414→220 (R, S)-noscapine]. In addition, a series of potential metabolites of M1 by CYP450 were investigated in single ion monitoring (SIM), monitoring the following ions: m/z 308 (10-hydroxy M1), m/z 324 (2-hydroxy M1, 3-hidroxy M1), m/z 310 (dihydroxy M1), m/z 296 (trihydroxy M1). Nitrogen was used as nebulizer gas at 75 L/h flow rate and as desolvation gas at 850 L/h. Ion source block and desolvation temperatures were set at 130 and 250 °C, respectively. Capillary voltage was 3.0 kV. The cone voltage was 45 V. MassLynx software version 4.0 was used for data acquisition and processing.

2.3 Sample preparation

Plasma and urine

Analytes were extracted from plasma and urine using an Oasis HLB (hydrophilic–lipophilic balance 200 mg, 6 mL) SPE columns. The optimized extraction procedure consisted on conditioning with 2 mL of MeOH and 2 mL of water, loading with 600 µL of plasma/urine (+ 20 µL of noscapine as internal standard, 25 ng/mL) diluted with 2 mL of ammonium formate (10 mM pH 7.0), washing with 1 mL of formic acid (2%, v/v) and then 2 mL of ammonium formate (10 mM pH 7.0), elution with 2 mL of MeOH, followed by 1 mL of MeOH containing 1% (v/v) CH_3COOH and 1 mL of MeOH containing 2% (v/v) NH_4OH. The eluate was vacuum dried, reconstituted with 200 µL of mobile phase, filtered, and injected into the HPLC-ES-MS/MS system.

Liver and kidney

Aliquots weighing approximately 1 g each were homogenized in 2 mL of phosphate buffer (0.05 M, pH 7.2) and then washed with 3 mL of methanol. The extract was subjected to sonication bath for 5 min, incubated at 37 °C for 20 min and centrifuged at 2100 rpm for 15 min. Four hundred microliters of the supernatant were spiked with 20 µL of the internal standard working solution and dried under vacuum. The residue was then re-suspended with 2 mL of ammonium formate (10 mM pH 7.0) and SPE was carried out as described above). The eluate was dried under vacuum, reconstituted with 200 µL of the mobile phase, filtered, and injected into the HPLCES- MS/MS system.

Stool and intestinal content

Approximately 0.1 g of intestinal content/stool were homogenized in 1 mL of isopropyl alcohol. The mixture was incubated at 37 °C under stirring for 24 h and then centrifuged at 2100 rpm for 10 min. The supernatant was collected and 100 µL were spiked with 100 µL of the internal standard solution, diluted with 800 µL of mobile phase, filtered, and injected into the HPLC-ES-MS/MS system.

2.4 Method validation

The method validation for the determination of M1, BBR, and related metabolites in all the studied biological matrices (plasma, urine, liver, kidneys, intestinal contents, and feces) was performed according to the international guidelines [Guidance for industry]. Selectivity was determined by analysing blank matrices in MRM mode to check for potentially interfering signals.

Accuracy and precision, expressed respectively as bias% and variation coefficient (CV%), were determined intra and inter-daily, through the triplicate analysis of quality control (QC) samples at low (1 ng/mL), medium (5 ng/mL), and high (25 ng/mL) concentrations. Bias was calculated as the ratio percentage between the difference of experimental standard concentration ($[std]_{exp}$) and theoretical standard concentration ($[std]_{theor}$) over theoretical standard concentration. General equation used for the calculation of bias% is reported below (equation 1):

Equation 1. $$bias\% = \frac{[std]_{exp} - [std]_{theor}}{[std]_{theor}} \times 100$$

The precision was determined by coefficient of variation percentage (CV%) as the ratio between the standard deviation (SD) and the experimental standard concentration ($[std]_{exp}$). General equation used for the calculation of CV% is reported below (equation 2):

Equation 2. $$CV\% = \frac{SD}{[std]_{theor}} \times 100$$

Limit of detection (LOD) and limit of quantification (LOQ) of the method were experimentally determined as the concentrations affording a signal-to-noise (S/N) ratio respectively of 3 and 10. The matrix effect (ME%) for all analytes was evaluated as ratio between the absolute matrix effect and the peak area of standard solutions in mobile phase (A_{mp}). The absolute matrix effect was calculated as difference between the peak area of the spiked standard sample (A_{matrix}) and the peak area of the standard solution. General equation used for the calculation of M.E.% is reported below:

Equation 3. $$ME\% = \frac{A_{matrix} - A_{mf}}{A_{mf}} \times 100$$

The recovery after clean-up procedures was calculated as percentage ratio of each analyte at three concentration levels with blank samples spiked after and before extraction. General equation used to determine recovery percentage is reported below:

$$Rec\% = \frac{[Std]_{before}}{[Std]_{after}} \times 100$$

2.5 Standard solutions and quantification

Stock solutions for each analyte were prepared in MeOH at 1mg/mL and stored at − 20 °C. Stock solutions were furtherly diluted to obtain working solutions containing BBR, M1, M3, and M4. A seven-point calibration curve (0.5, 1, 2.5, 5, 10, 25, and 50 ng/mL), obtained by appropriate dilution in mobile phase of the working solutions and addition of a fixed amount of internal standard (2.5 ng/mL), was used for the quantification of the different analytes within all the different biological matrices, except for plasma. For quantification in plasma, calibration curves in blank serum were used, by subjecting the single concentration points to the SPE clean-up described above. Due to the lack of the corresponding analytical standard, the metabolite M2 was quantified using the isomer M1 calibration curve. Linear calibration curve parameters were obtained from the plot of the analyte/internal standard peak area ratio versus analyte concentration using a least-squares regression analysis.

2.6 Biodistribution and mass balance

The biodistribution and mass balance studies were carried out by single oral dose administration of 2 mg/kg of BBR and M1, dissolved in PBS buffer (pH 7.4), to healthy Wistar-Han rats (male, 180–220 g, 6–7 weeks). Globally, 61 rats were assigned to distinct groups as follows: 30 rats were treated with M1, 30 with BBR, and one was used as blank control. The rats were housed individually at a temperature of 25 °C and fasted for 12 h before drug administration. The animals were sacrificed after intraperitoneal anesthesia (Zoletil100® 100 mg/kg) by exsanguination via vena cava puncture and samples were collected at different time points (5 rats each): 0.25, 0.5, 1, 2, 6, and 24 h post dose. The choice of these time points is based on the awareness that these molecules undergo rapid absorption and diffusion within the first hours after the administration. For mass balance, urine and feces were collected only from rats sacrificed 24 h after administration, as they were the only ones housed in metabolic cages. Blood samples were collected and immediately transferred into tubes containing sodium heparin anticoagulant and placed on wet ice until centrifugation to obtain plasma. All samples were stored at − 80 °C. All experiments were carried out according to the guidelines set forth by EEC Directive 86/609 on care and use of experimental animals. The protocol was approved by the Institutional Ethics Committee of the University of Bologna (Protocol 398/2016). All studies involving animals are reported in accordance with the ARRIVE guidelines [Kilkenny C. 2010].

2.7 Cell based assays

Cell culture protocol

Different batches (pooled from 22 donors) of human umbilical vein endothelial cells (HUVECs) purchased from Thermo Fischer Scientific (Waltham, MA USA) were utilized for all cell-based assays. HUVECs were cultivated as reported in [Caliceti C. 2013].

Cytotoxicity (lactate dehydrogenase release)

Lactate dehydrogenase (LDH) release from HUVECs was monitored by collecting aliquots of medium, using a standard spectrophotometric method [Rizzo B. 2013]. The method is based on the quantification of LDH in the media by a coupled enzymatic reaction in which LDH catalyzes the conversion of lactate to pyruvate via NAD+ reduction to NADH. Diaphorase reduces tetrazolium salt, oxidizing NADH, to a red formazan product, that can be measured at 490 nm. The increase in absorbance between the treatment after 24 h (representing t1) and the control (representing t0) was monitored at 37 °C using a Varioskan™ Flash Multimode Reader.

RNA extraction and quantitative real-time PCR

HUVECs, starved overnight with phenol red-free M200 medium containing growth factors and 2% FBS, were pretreated with M1 and BBR, both at 300 ng/mL for 8 h before 24 h exposure to TNFα (10 ng/mL). Total RNA was extracted using a commercial RNA extraction kit (Qiagen). Two hundred fifty nanograms of total RNA were reverse transcribed in a volume of 25 µL using 250 units of SuperScript III reverse transcriptase and 50 ng of random hexamers. Reaction conditions were as suggested by manufacturer. Mixture of cDNA (2 µL) was used for real-time PCR experiments to measure the amount of ICAMtranscript. Realtime PCR reactions were conducted on an Applied Biosystems 7500 Fast Real-Time PCR System using PerfeCta SYBR Green SuperMix with ROX kit (Quanta Biosciences) according to the manufacturer's protocol in a final volume of 25 µL. Primers concentration was 500 nM. The following primers were used: ICAM: forward 5'- AGCTTCGTGTCCTGTATGGC-3', reverse 5'- TTTTCTGG CCACGTCCAGTT-3'; RPL13A: forward 5'- CACCCTGG AGGAGAAGAGGA-3', reverse 5'- CCGTAGCCTCATGA GCTGTT-3'. Changes in gene expression were calculated by the $2^{-\Delta\Delta Ct}$ formula using RPL13A as reference gene [Caliceti C. 2013].

Determination of oxygen radical scavenging capacity (ORAC)

The antioxidant activity of M1 and BBR was estimated by oxygen radical absorbance capacity (ORAC) assay [Cao G. 1993], using fluorescein as fluorescent probe. Briefly, 50 µL of blank, Trolox standard solutions (2-12 µg/mL), BBR (360-0.4 µg/mL) and M1 (360-0.4 µg/mL) solutions were transferred to triplicate wells in a black 96-well plate. After incubation at 37 °C for 10 min, 50 µL of fluorescein (25 ng/mL) was added to each well

and incubated at 37 °C for another 20 min. Fluorescein consumption was immediately measured after adding 25 µL of AAPH (60 mg/mL) to each well by recording the fluorescence signal (excitation at 485 nm and emission at 535 nm) at 5 minute-intervals for 1 h on a microtiter plate reader (Varioskan Flash Multimode Reader, Thermo Fisher Scientific, USA). Final values were calculated using the linear relationship (Y = a + bX) between Trolox concentration (X) (µg/mL) and the area under the fluorescence versus time curve for samples minus the area under the curve for the blank (Y). ORAC values were expressed as µg Trolox equivalent/mg of sample. Data were presented as mean ± SD of five experiments.

Estimation of antioxidant capacity through chemiluminescent (CL) method

The chemiluminescence method to determine the antioxidant effect is based on the competition between the reaction of peroxyl radicals with luminol, giving rise to light emission, and the scavenging of peroxyl radicals by antioxidants. Indeed, the addition of a solution of known antioxidants to a glowing steady-state chemiluminescent reaction temporarily quenches light output. The extent of light emission quenching is related to the amount and the strength of antioxidant added [Chapple I.L.C.]. Assays were performed in black 96-well plates. The chemiluminescent cocktail was prepared by adding small amounts of a 1/100.000 (v/v) dilution of a stock horseradish peroxidase solution (1 mg/mL in 0.1 mol/L TriseHCl buffer, pH 7.4) to 10 mL of ECL reagent substrate (Life Technoligies) to obtain a CL system with a light emission of about 5-10 RLU (Relative Light Units), measured by a microtiter plate luminometer (Luminoskan Ascent, Thermo Fisher Scientific, USA). 100 µL of the chemiluminescent mixture was dispensed in quadruplicate into the wells containing 10 µL of Trolox (2-12 µg/mL) and several dilutions of the samples. Distilled water was used as a negative control and Trolox as the standard reference. The kinetics of light emission was immediately monitored for 60 min each 20 s.

To each well (except for the control), the time of emission inhibition, defined as the time where the CL signal intensity reaches a value equal to half of the maximum signal obtained in that well, was determined by analyzing CL kinetic curves. Using the data obtained from the wells containing the Trolox standard solutions, a calibration curve that correlates the time of inhibition with the concentration of Trolox was constructed. Using this curve, the antioxidant activities of various dilutions of each sample were then calculated by interpolation of the inhibition times on the calibration curve generated in the same assay. The values obtained for the various dilutions of each sample were corrected for the respective dilution factor and averaged to obtain the antioxidant activity of the starting solutions and the results were expressed as µg Trolox equivalent/mg of sample. Data were presented as mean ± SD of five experiments.

Chemiluminescent intracellular xanthine oxidase assay

Xanthine oxidase activity was quantified in presence or absence of M1 and BBR; 5 × 103 cells/well were plated in a 96-black wells microtiter plate; the day after, cells were incubated at 37 °C with CL reaction cocktail solution and the CL emission was monitored for 20 min; CL reaction cocktail in absence of cells was used as control to normalize the CL signals. M1 and BBR were solubilized in DMSO, used as vehicle (V). The reaction mixture was constituted of 100 µM EDTA, 10 µM FeCl2, 40 µM sodiumperborate, and 0.1 mM luminol sodium salt in borate buffer, 0.1 M, pH 10.3. Briefly, the experimental procedure was adapted from the one previously described by Roda et al. [Roda A. 1998] and Caliceti et al. [Caliceti C. 2016] by adding 0.5 mL of a Fe2+-EDTA solution (116 mg Na-EDTA and 2.5 mg FeCl2 in 50 mL of distilled water), 0.05 mL of a luminol solution (20 mg luminol in 1 mL of borate buffer, 0.1 M, pH 10.3), 0.1 mL Na-perborate solution (30 mg sodium perborate in 20 mL borate buffer, 0.1 M, pH 10.3) in 50 mL of borate buffer (0.1 M pH 10.3). The solution stored in the dark at 25 °C is stable for months. Stock solutions of M1 and BBR were prepared in DMSO to obtain a final concentration of 300 µg/mL. Subsequent dilutions in reaction mixture (containing 350 µg/mL xanthine) were performed to prepare the inhibition curve, range 15– 0.015 µg/mL. The chemiluminescent cocktail was stored in the dark for 20 min, then cells were incubated with the reaction mixture at 37 °C and the light output from all wells was measured and monitored for 20 min using the LuminoskanTM Ascent luminometer automatic plate reader (Thermo Fisher Scientific, Roskilde, Denmark). Reaction mixture without xanthine oxidase was used as the negative control and reaction mixture with xanthine oxidase was used as the positive control [Caliceti C. 2016].

2.8 Statistical analysis

GraphPad Prism v. 5.04 (GraphPad Software, Inc., La Jolla, CA) was used to perform statistical analysis, to plot the CL signal as a function of xanthine oxidase activity or oxypurinol concentrations and for least-squares fitting of calibration curves. Results of qRT-PCR and LDH assay are expressed as mean ± SEM of at least five independent experiments. Differences between the means were determined by one-way ANOVA followed by Bonferroni multiple comparison test, considering a $P < 0.05$ as significant. CL kinetic profiles were shown as the mean of three replicates of each concentration of samples. The CL values used for graph data were shown as the mean value of three replicates together with standard deviation of each sample (at 95% confidence interval). The IC50 obtained from cell-based assays was calculated as the mean ± SD (n = 3, at 95%confidence interval), normalized for 5 × 103 cells (mean cell population for each well). Data on biodistribution and mass balance studies are expressed as the mean ± SD of five independent experiments. The comparisons between rats treated with M1 and BBR in a specific organ/fluid were performed considering a level of statistical significance of $P< 0.05$.

3. Results and discussion

3.1 HPLC-ESI-MS/MS method set up and validation

The experimental MS conditions were properly tuned by direct infusion of each compound (1 µM of each analyte; 2 mL/h infusion rate). In figure 2 the mass spectra of BBR is reported.

FIG. 2. TANDEM MS SPECTRA OF BBR

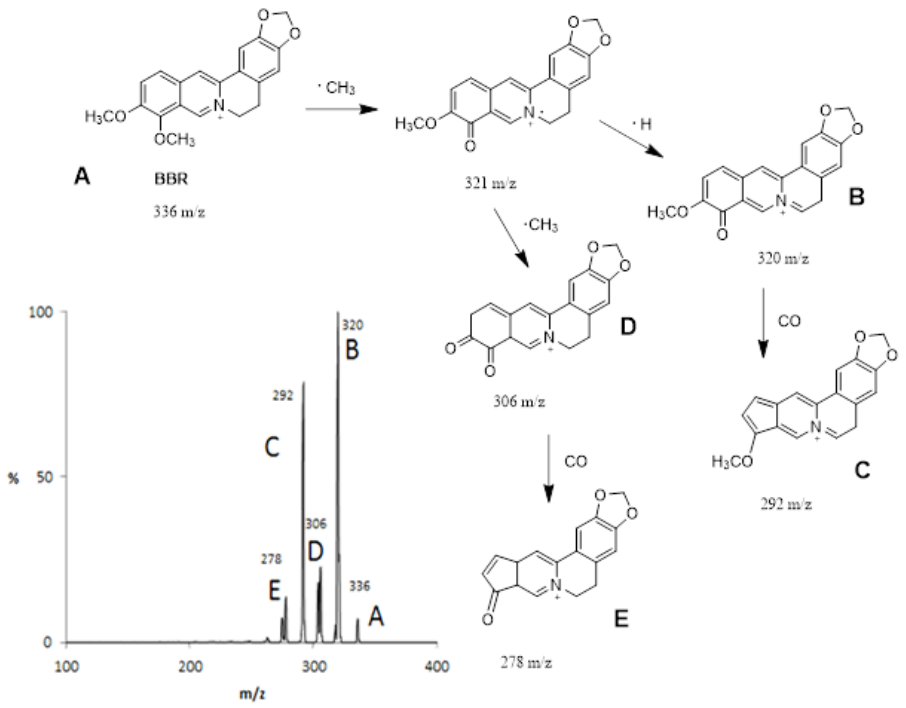

The detailed LC-MS/MS experimental conditions are reported in table 1, which were tuned by direct infusion of the single analytes.

TABLE 1. HPLC-MS/MS EXPERIMENTAL PARAMETERS

Column			LUNA C18 (5 µm, 150 × 2.0 mm i.d.) Phenomenex		
Mobile phase			Ammonium formate 10mM pH=4.00 MeOH:ACN (95:5 v/v)		
Colum temperature (°C)			30		
Elution program			Gradient elution		
Flow (mL/min)			0.15		
Autosampler temperature (°C)			7		
Injection volume (uL)			10		
MS/MS parameters	**BBR**	**M1**	**M3**	**M4**	**Noscapine (IS)**
Ionization (ESI)	positive	positive	positive	positive	positive
Capillary voltage (kV)	3.3	3.3	3.3	3.3	3.3
Cone voltage(V)	44	47	44	43	42

Source temperature(°C)	130	130	130	130	130
Desolvation temperature (°C)	250	250	250	250	250
Spraying gas flow (L/h)	65	65	65	65	65
Collision energy (%Argon)	30	30	30	30	30
Monitored reaction (MRM)	336>320	322>307	324>309	338>322	440>220

Calibration curve parameters for M1 and other compound quantification, in the range 0.5–50 ng/mL, were obtained from the plot of the analyte/internal standard peak area ratio versus analyte concentration using a linear least-square regression analysis. The obtained calibration curve equations Y = (a ± δa)X + (b ± δb) are reported in table 2. Determination coefficients (r2) of the calibration curves were ≥ 0.990 for all analytes, both in mobile phase and plasma, meaning a good linearity over two orders of concentrations.

TABLE 2. LOD, LOQ AND CALIBRATION CURVE COEFFICIENTS FOR THE STUDIED ANALYTES.

Calibration curve in mobile phase (range 0.5 – 50 ng/ml)				
	BBR	**M1**	**M3**	**M4**
LOD (ng/ml)	0.05	0,05	0,05	0,05
LOQ (ng/ml)	0.1	0,1	0,15	0,15
r^2	0.993	0.998	0.990	0.994
a±DS	-0.027 ± 0,001	0.080 ± 0.009	0,012 ± 0.005	-0.001 ± 0.007
b ±DS	0.450 ± 0.004	0.822 ± 0.007	0.478 ± 0.007	0.124 ± 0.002
Calibration curve in plasma (range 0.5 – 50 ng/ml)				
	BBR	**M1**	**M3**	**M4**
LOD (ng/ml)	0.05	0,05	0,1	0,01
LOQ (ng/ml)	0.1	0,1	0,2	0,2
r^2	0.993	0.998	0.990	0.994
a±DS	-0.025 ± 0.002	-0.045 ± 0.010	0,024 ± 0.003	-0.012 ± 0.009
b±DS	0.459 ± 0.004	0.809 ± 0.004	0.437 ± 0.012	0.149 ± 0.005

Limit of detection values in mobile phase and plasma matrix ranged from 0.05 to 0.15 ng/mL, while limit of quantification values in mobile phase and plasma matrix from 0.1 to 0.5 ng/mL for all analytes. Variation coefficients and bias% calculated, both intra- and inter-daily, were less than 8% for all analytes at the different concentration levels, indicating that the method possesses satisfying precision and accuracy, and then suitable for the purpose of the study (table 3).

TABLE 3. PRECISION AND ACCURACY VALUES INTRA-DAY (N=3) AND INTER-DAY (N=9) AT THREE CONCENTRATION LEVELS

Precision and Accuracy in mobile phase									
		BBR		M1		M3		M4	
	Theoric concetration (ng/ml)	CV %	Bias %	CV %	Bias %	CV %	Bias %	CV %	Bias %
	1	3	1	3	3	4	-1	2	1

Intra-day	5	2	4	1	1	3	-1	2	2
	25	4	-2	4	2	5	2	3	3
Inter-day	1	2	4	2	4	1	2	2	2
	5	1	-2	3	-2	2	1	4	1
	25	5	-4	1	-3	4	3	2	2
Precision and Accuracy in plasma									
		BBR		M1		M3		M4	
	Theoretical concetration (ng/ml)	CV %	Bias %	CV %	Bias %	CV %	Bias %	CV %	Bias %
Intra-day	1	1	3	2	1	1	3	2	-2
	5	2	3	1	1	4	1	4	-2
	25	5	-1	3	2	2	-2	3	4
Inter-day	1	2	-2	4	-1	4	4	3	3
	5	5	1	2	-1	2	1	3	-1
	25	2	3	1	3	3	2	1	3

The comparison between standard solutions and fortified samples with known amounts of analyte and blank samples showed good selectivity in multiple reaction monitoring (MRM) mode, as no interfering signals, potentially able to affect the identification of the target analytes, were observed.

Matrix effect percentage was evaluated at three concentration levels in all the studied matrices (table 4). Matrix effect values higher and lower than 0% indicated, respectively, ionic increase (positive matrix effect) or ionic suppression (negative matrix effect). In all the studied matrices, with the exception of plasma, matrix effect values were negligible, being always below 10% for all the studied analytes. In plasma, matrix effect higher than 20% were observed, leading to the necessity of calibration curves built in plasma.

TABLE 4. MATRIX EFFECT VALUE AT THREE CONCENTRATION LEVEL FOR ALL STUDIED BIOLOGICAL MATRIX AND FLUID

Matrix effect serum (ME% ± SD)					
	Theoretical concetration (ng/ml)	BBR	M1	M3	M4
QC 1	1	-24 ± 7	-19 ± 6	-12 ± 5	-14 ± 5
QC 2	5	-18 ± 6	-18 ± 4	-9 ± 6	-8 ± 4
QC 3	25	-24 ± 5	-26 ± 9	-15 ± 3	-12 ± 6
Matrix effect liver (ME% ± SD)					
	Theoretical concetration (ng/ml)	BBR	M1	M3	M4
QC 1	1	-8 ± 2	-5 ± 1	-8 ± 3	-3 ± 3
QC 2	5	-5 ± 2	-7 ± 3	-7 ± 2	-4 ± 1
QC 3	25	-7 ± 2	-2 ± 3	-7 ± 2	0 ± 2
Matrix effect kidney (ME% ± SD)					
	Theoretical concetration (ng/ml)	BBR	M1	M3	M4
QC 1	1	-6 ± 5	-3 ± 3	-5 ± 3	-3 ± 3
QC 2	5	-2 ± 2	2 ± 2	1 ± 4	-5 ± 2
QC 3	25	0 ± 2	3 ± 2	-2 ± 4	7 ± 3
Matrix effect small intestine content (ME% ± SD)					
	Theoretical concetration (ng/ml)	BBR	M1	M3	M4
QC 1	1	-3 ± 1	-1 ± 1	1 ± 3	0 ± 1
QC 2	5	1 ± 2	-5 ± 3	6 ± 2	3 ± 2

QC 3	25	2 ± 2	4 ± 6	5 ± 2	2 ± 1
Matrix effect large intestine content (ME% ± SD)					
	Theoretical concetration (ng/ml)	BBR	M1	M3	M4
QC 1	1	0 ± 2	1 ± 4	6 ± 1	0 ± 5
QC 2	5	-2 ± 5	3 ± 2	8 ± 3	1 ± 3
QC 3	25	3 ± 3	0 ± 2	9 ± 4	2 ± 1
Matrix effect feces (ME% ± SD)					
	Theoretical concetration (ng/ml)	BBR	M1	M3	M4
QC 1	1	4 ± 4	-5 ± 1	-8 ± 3	-3 ± 4
QC 2	5	3 ± 3	-7 ± 3	-7 ± 2	-4 ± 3
QC 3	25	6 ± 4	-2 ± 3	3 ± 2	-4 ± 4
Matrix effect urine (ME% ± SD)					
	Theoretical concetration (ng/ml)	BBR	M1	M3	M4
QC 1	1	0 ± 2	6 ± 1	2 ± 3	0 ± 3
QC 2	5	3 ± 1	8 ± 3	0 ± 3	1 ± 3
QC 3	25	5 ± 5	8 ± 4	4 ± 4	4 ± 2

The efficiency of the extraction methods during sample clean-up was calculated by Rec% (table 5).

TABLE 5. RECOVERY VALUES AT THREE CONCENTRATION LEVELS FOR PLASMA, KIDNEY AND LIVER

Recovery in plasma (Rec% ± DS)					
	Theoretical concetration (ng/ml)	BBR	M1	M3	M4
QC 1	1	92 ± 4	98 ±2	88 ±3	96 ±3
QC 2	5	94 ± 6	97 ±4	92 ±1	97 ±2
QC 3	25	92 ± 5	96 ±6	96 ±5	96 ±4
Recovery in liver (Rec% ± DS)					
	Theoretical concetration (ng/ml)	BBR	M1	M3	M4
QC 1	1	91 ± 4	95 ±2	93 ±4	91 ±4
QC 2	5	90 ± 2	98 ±4	92 ±6	97 ±3
QC 3	25	95 ± 4	97 ±2	91 ±4	92 ±4
Recovery in kidney (Rec% ± DS)					
	Theoretical concetration (ng/ml)	BBR	M1	M3	M4
QC 1	1	94 ± 6	96 ±1	92 ±3	92 ±1
QC 2	5	92 ± 8	92 ±3	95 ±1	95 ±2
QC 3	25	92 ± 4	98 ±3	97 ±2	91 ±5

Experimental values were close to 100% for all the investigated analytes for all the matrixes investigated, indicating the efficacy of these process. The pre analytical treatment of the different matrices was tailored in order to obtain a sensitive and selective quantification of M1, BBR, and phase 1 metabolites. For this reason, different SPE procedures have been tested throughout the screening of different eluents and stationary phases, in order to obtain improved performances in respect to other reported procedures [Ma J.Y. 2013 Liu, Y.T. 2010]. The main advantages of the pre-analytical protocols that we have developed consist

on the low matrix effects and the high recoveries at different concentration levels, and the possibility to concentrate the sample with consequent increase in the sensitivity of the detection. These optimized performances allowed us to detect very low amounts of M1 and BBR, considering our choice to administer a dose (2 mg/kg) of M1 and BBR in relation with their low solubility in physiological buffer. Several authors utilized up to 20-fold higher doses to overcome the sensitivity issue, without any concern on reproducibility of the studies.

3.2 Comparative biodistribution of M1 and BBR after oral administration

Plasma

The mean plasma concentration-time curves in rats receiving oral doses of 2 mg/kg are illustrated in Fig. 3. After its administration, BBR was already metabolized after 15 min in M1, M2, and M3. BBR, M2, M3, and M4 maximum plasma levels (0.5 ± 0.2, 0.8 ± 0.3, 2.9 ± 1.1, and 0.2 ng/mL) were reached after 2, 0.5, 24, and 1 h, respectively, while the mean maximum plasma concentration of the main metabolite M1 (9.3 ±2.4 ng/mL) was reached 24 h after gavage (Fig. 3a).

FIG. 3 CONCENTRATION-TIME CURVES (0.25, 0.5, 1, 2, 6, AND 24 H) OF BBR (A) ANDM1 (B) IN THE PLASMA AFTER DIRECT ORAL ADMINISTRATION (2MG/KG) IN RATS. THE RESULTS ARE EXPRESSED AS MEAN ± SD OF FIVE INDEPENDENT EXPERIMENTS

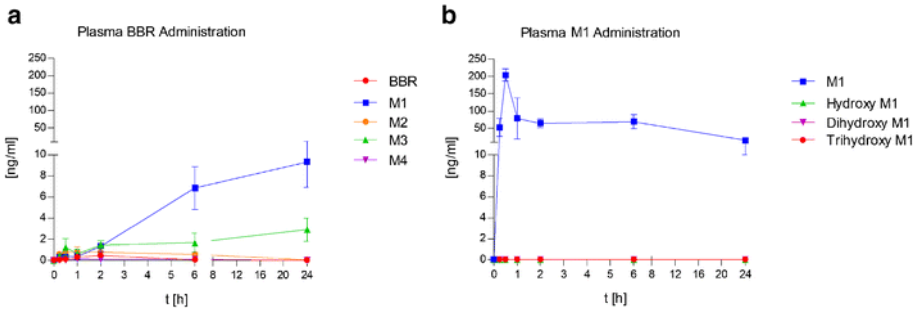

These data are in line with previous papers; Zuo et al. [Zuo F. 2006] reported that, after BBR oral administration (40 mg/kg) in rats, its maximum plasma concentration was reached 2 h post dose (around 5 ng/mL), while M1 highest concentration was reached after 24 h (around 40 ng/mL). We can explain our lower values, compared to the mentioned ones, considering the much lower dose we have administrated. After M1 administration its maximum plasma concentration (204 ± 18 ng/mL) was reached 0.5 h after administration. Subsequently, it dropped rapidly (79 ± 59 ng/mL) after 1 h and then it slowly decreased to 16.6 ± 6.1 ng/mL after 24 h (Fig. 3b). None of the supposed M1 metabolites was observed, being this molecule always detected as such. Accordingly, Wang et al. [Wang K. 2017] found that after M1 administration (15 mg/kg), its maximum plasma concentration was reached between 0.5 and 1 h post dose (around 1250 ng/mL). Direct M1 administration resulted in a largest bioavailability as its maximum plasma concentration was around 20 times higher than maximum total BBR plasma level, intended as the sum of BBR and all the quantified metabolites

(P < 0.01).These findings can be explained considering the physicochemical properties of M1 and BBR (Table 6). Indeed, as reported by Caliceti et al. [Caliceti C. 2016.2], M1 structure leads to multiple species in solution at different pH values, influencing the lipophilicity and the capability to cross biological membranes. As reported by Spinozzi et al. [S. Spinozzi 2014], M1 exists as enolic form at acidic pH (log P of − 0.02 at pH 4.5), while the neutral (quinoid) form is predominant at basic pH (log P of 1.6 at pH 8.5). Therefore, M1 at basic intestinal pH is better absorbed, resulting in higher plasma concentrations compared to BBR (figure 4).

FIG. 4. PH-MEDIATED PASSIVE DIFFUSION OF M1 THROUGH THE CELL MEMBRANE

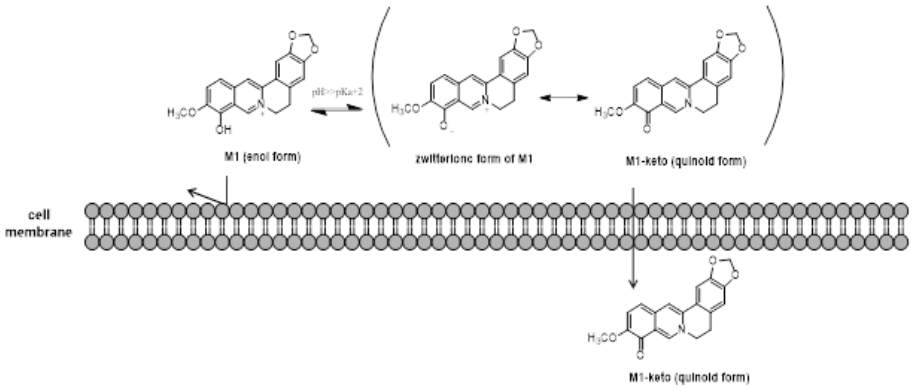

Considering that M1 biological activity on LDL mRNA enhancer has been reported [Y. Li 2011], and considering the higher bioavailability, it might be assumed that the major role in BBR treatments is played by M1 itself rather than its metabolic precursor.

TAB. 6. SOLUBILITY AND LOGP VALUES OF BBR AND M1 AT DIFFERENT PH IN PHOSPHATE BUFFER

pH	Solubility (mM)		Log *P*	
	BBR	**M1**	**BBR**	**M1**
4.5	8.2	4.2	− 1.2	− 0.02
6.0	7.6	2	− 1.2	0.9
7.0	9.0	1	− 1.2	1.1
8.6	9.6	0.5	− 1.2	1.6

Liver

The time-concentration curve in the liver following BBR administration shows that it was metabolized to M1, M2, and M3 after 15 min (Fig. 5a). The maximum hepatic concentrations of M1, M2, and M3 (6.1 ± 1.5, 3.5 ± 2.3, and 2.9 ± 1.1 ng/g) were reached after 24, 6, and 2 h, respectively. BBR maximum hepatic concentration (21.4 ± 7.9 ng/g) was reached after 2 h and was significantly higher than its metabolite hepatic levels (P < 0.01). BBR hepatic concentration did not change significantly after 6 h (20.3 ± 8.3 ng/g), decreasing to 3.4 ±

0.6 ng/g only after 24 h. Higher BBR hepatic levels compared to the metabolite M1 might be explained considering the efficient secretion into the bile and back diffusion in plasma of the latter in its enolic form. Higher BBR lipophilicity, indeed, may be correlated to a delayed biliary excretion and a prolonged stay in the liver. After M1 administration, its maximum hepatic concentration (193 ± 25 ng/g) was reached 1 h post dose. Subsequently, it decreased rapidly (25.4 ± 8.2 ng/g) after 2 h, remained constant until 8 h and then it decreased (5.4 ± 1.6 ng/g) after 24 h (Fig. 5b). Comparing maximum hepatic levels, direct M1 administration resulted in higher concentrations than total BBR ($P < 0.01$). Again, this behaviour may be explained considering an efficient absorption of M1 in its quinoid form at basic intestinal pH.

Kidney

In the kidneys, after BBR administration, M2, M3, and M4 reached maximum levels (1.2 ± 0.7, 2.6 ± 0.9, and 2.7 ± 1.3 ng/g) after 1, 0.5, and 1 h, respectively (Fig. 5c). The concentration of the main metabolite M1 increased over time, reaching a plateau (53.1 ± 16.8 ng/g) after 6 h without significant differences ($P > 0.05$) with BBR maximum levels (40.5 ± 19.9 ng/g) reached 2 h post dose. After M1 administration, its maximum kidney level (2070 ± 340 ng/g) was reached after 0.5 h (Fig. 5d). Subsequently, it decreased rapidly (362 ± 90 ng/g) after 1 h and maintaining constant its concentration still after 24 h (121 ± 31 ng/g). Direct M1 administration resulted in M1 kidney levels up to about 50 times higher than total BBR kidney levels ($P < 0.01$). It is interesting to point out that M1 tends to accumulate in the kidneys, as reflected by plasma levels, in which this compound is still present at relatively high concentrations after 24 h. This represents a very important aspect that needs to be carefully considered, especially at the light of the recent findings from Yang et al. [Yang N. 2016]. The authors reported that, despite the clear anti-obesity and lipid-lowering effect of M1, this compound showed a noticeable nephrotoxicity in mice fed with high fat diet, without affecting hepatic functions. According to the authors, the enhanced urinary elimination due to high fat diet might be responsible for the accumulation in the kidneys, aggravating the nephrotoxicity effects respect to normal mice. These findings suggest that, although M1 is not considered a proper drug, its potential use in clinical practice, especially in lipidemic disorder treatment, should be carefully considered in relation to the administrated doses.

Intestinal content

After BBR administration, its concentration in the small intestine content increased over time reaching maximum level (149 ± 52 μg/g) 6 h post dose and then decreased rapidly (12.6 ± 2.6 ng/g) after 24 h. M1, M2, M3, and M4 maximum concentrations (0.66 ± 0.17, 1.42 ± 0.54, 1.72 ± 0.52, and 6.61 ± 2.34 μg/g)were reached at 24, 6, 24, and 6 h post dose, respectively (Fig. 5e). In the small intestine of M1-treated rats, berberrubine concentration increased rapidly at 2 h post dose (123 ± 15 μg/g) and progressively decreased (6.64 μg/g ± 2.64) after 24 h (Fig. 5f). No significant differences ($P > 0.05$) between maximum levels of the two administrated molecules were observed. In the large intestine of BBR-treated rats, its concentration

increased over time reaching the maximum (56.2 ± 10.4 µg/g) 24 h post dose. M1, M2, M3, and M4 maximum concentration (2.31 ± 0.55, 1.99 ± 0.53, 3.45 ± 0.82, and 1.77 ± 0.45 µg/g) were reached after 24 h (Fig. 5g). In the large intestine of M1-treated rats, the concentration increased over time, reaching the maximum level (16.0 ± 4.5)24 h post dose (Fig. 5h), with significant differences ($P < 0.01$) compared to total BBR maximum concentration.

FIG. 5 CONCENTRATION-TIME CURVES (0.25, 0.5, 1, 2, 6, AND 24 H) OF BBR (AND METABOLITES) AND M1 IN THE LIVER (A, B), KIDNEY (C, D), SMALL INTESTINE CONTENT (E, F), AND LARGE INTESTINE CONTENT (G, H) IN RATS AFTER SINGLE ORAL ADMINISTRATION (2 MG/KG). THE RESULTS ARE EXPRESSED AS MEAN ± SD OF FIVE INDEPENDENT EXPERIMENTS

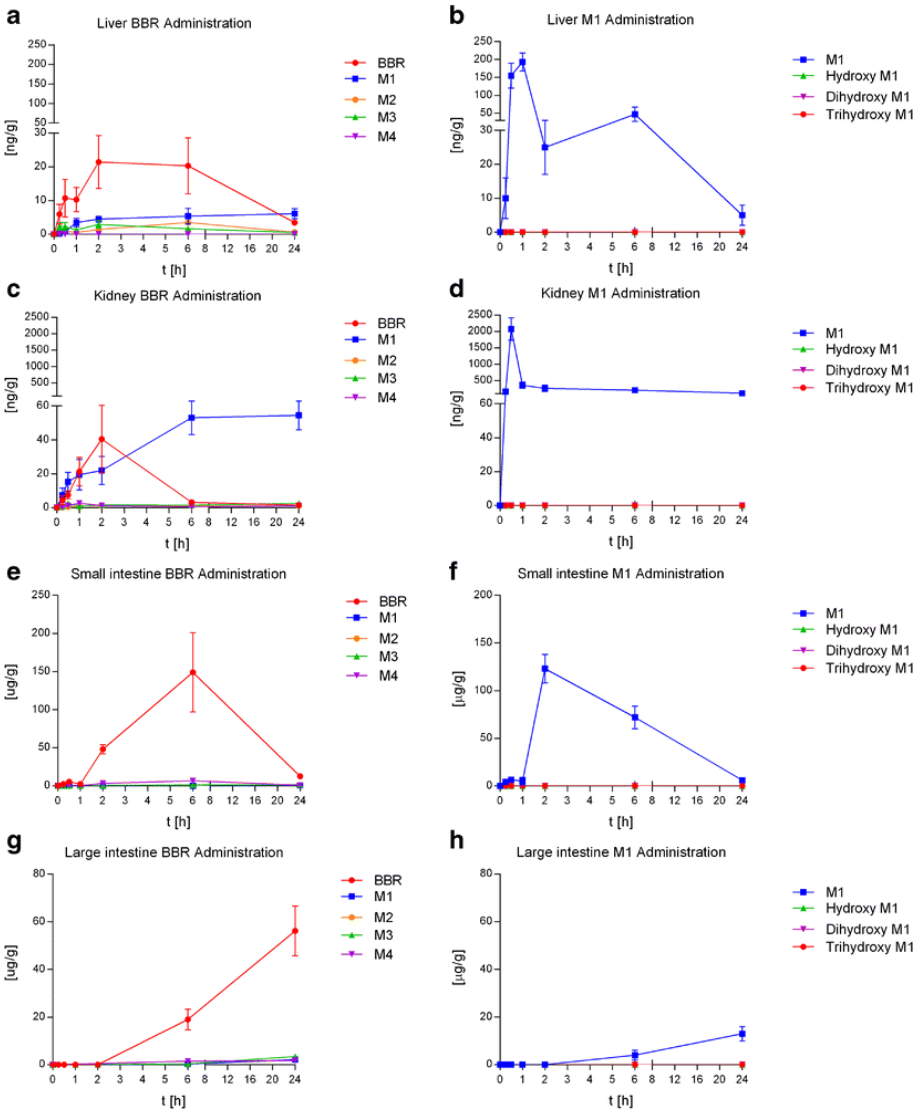

Concentration of BBR and metabolites at different time-points after BBR administration are reported in table 7.

Table 7. Plasma, liver, kidney, small and large intestine concentrations at different time-points after BBR oral administration at doses of 2 mg/kg. Data reported are expressed as mean ± SD of five independent experiments

Plasma concentration after BBR administration (ng/mL ± SD)					
t[h]	BBR	M1	M3	M2	M4
0	N.D	N.D	N.D	N.D	N.D
0.25	0.1 ± 0.1	0.3 ± 0.2	0.4 ± 0.1	0.6 ± 0.1	N.D
0.5	0.1 ± 0.1	0.4 ± 0.2	1.3 ± 0.8	0.8 ± 0.3	N.D
1.0	0.3 ± 0.2	0.5 ± 0.3	0.6 ± 0.4	0.8 ± 0.5	0.2 ± 0.1
2.0	0.5 ± 0.2	1.4 ± 0.5	1.5 ± 0.4	0.7 ± 0.2	0.1 ± 0.1
6.0	0.2 ± 0.1	6.9 ± 2.0	1.7 ± 0.9	0.6 ± 0.2	0.1 ±0.1
24.0	0.1 ± 0.1	9.3 ± 2.4	2.9 ± 1.1	0.1 ± 0.1	N.D.

Liver concentration after BBR administration (ng/g ± SD)					
t[h]	BBR	M1	M3	M2	M4
0	N.D	N.D	N.D	N.D	N.D
0.25	6.0 ± 2.9	0.2 ± 0.1	2.4 ± 1.1	0.8 ± 0.2	N.D.
0.5	10.7 ± 5.6	0.8 ± 0.3	2.3 ± 1.2	0.9 ± 0.4	N.D.
1.0	10.2 ± 3.6	1.4 ± 0.4	1.3 ± 0.5	0.5 ± 0.2	N.D.
2.0	21.4 ± 7.9	2.5 ± 0.6	2.9 ± 1.1	1.4 ± 0.7	N.D.
6.0	20.3 ± 8.3	1.4 ± 0.9	1.6 ± 0.4	3.5 ± 2.3	N.D.
24.0	3.4 ± 0.6	6.1 ± 1.5	0.5 ± 0.1	0.6 ± 0.1	N.D.

Kidney concentration after BBR administration (ng/g ± SD)					
t[h]	BBR	M1	M3	M2	M4
0	N.D	N.D	N.D	N.D	N.D
0.25	4.5 ± 2.6	7.4 ± 4.2	0.8 ± 0.2	0.2 ± 0.1	0.2 ± 0.1
0.5	7.6 ± 2.4	15.2 ± 5.6	2.5 ± 0.9	0.5 ± 0.1	1.2 ± 0.2
1.0	21.3 ± 8.9	19.4 ± 9.0	1.1 ± 0.8	1.2 ± 0.7	2.7 ± 1.3
2.0	40.5 ± 19.9	21.9 ± 8.3	1.7 ± 0.8	1.0 ± 0.4	1.2 ± 0.4
6.0	3.2 ± 1.5	53.1 ± 16.8	1.5 ± 0.3	1.0 ± 0.4	0.5 ± 0.3
24.0	1.5 ± 0.5	54.5 ± 20.5	2.6 ± 0.9	1.1 ± 0.3	1.1 ± 0.3

Small intestine concentration after BBR administration (µg/g ± SD)					
t[h]	BBR	M1	M3	M2	M4
0	N.D	N.D	N.D	N.D	N.D
0.25	2.33 ± 0.6	N.D	0.12 ± 0.03	N.D	0.25 ± 0.09
0.5	5.27 ± 3.1	N.D	0.19 ± 0.05	0.12 ± 0.05	0.54 ± 0.25
1.0	2.24 ± 0.6	N.D	0.18 ± 0.09	0.09 ± 0.03	0.25 ± 0.08
2.0	48.1 ± 6.2	N.D	0.54 ± 0.13	0.45 ± 0.12	3.21 ± 1.81
6.0	149 ± 52	0.24 ± 0.06	1.12 ± 0.19	1.42 ± 0.54	6.61 ± 2.34
24.0	12.6 ± 2.6	0.66 ± 0.17	1.72 ± 0.52	0.84 ± 0.22	0.85 ± 0.29

Large intestine concentration after BBR administration (µg/g ± SD)					
t[h]	BBR	M1	M3	M2	M4
0	N.D	N.D	N.D	N.D	N.D
0.25	N.D	N.D.	N.D.	N.D.	N.D.
0.5	N.D	N.D.	N.D.	N.D.	N.D.
1.0	N.D	N.D.	N.D.	N.D.	N.D
2.0	N.D	N.D.	N.D.	N.D.	N.D
6.0	19.0 ± 4.3	0.34 ± 0.18	0.35 ± 0.09	0.36 ± 0.12	1.52 ± 0.54

24.0	56.2 ± 10.4	2.31 ± 0.55	3.45 ± 0.82	1.99 ± 0.53	1.77 ± 0.45

Concentration of M1 and metabolites at different time-points after BBR administration are reported in table 7.

TABLE 7. PLASMA, LIVER, KIDNEY, SMALL AND LARGE INTESTINE CONCENTRATIONS AT DIFFERENT TIME-POINTS AFTER M1 ORAL ADMINISTRATION AT DOSES OF 2 MG/KG. DATA REPORTED ARE EXPRESSED AS MEAN ± SD OF FIVE INDEPENDENT EXPERIMENTS

Plasma concentration after M1 administration (ng/mL ± SD)				
t[h]	M1	Hidroxy M1	Dihidroxy M1	Trihidroxy M1
N.D	N.D	N.D.	N.D.	N.D.
0.25	53.3 ± 25.6	N.D.	N.D.	N.D.
0.5	204 ± 18	N.D.	N.D.	N.D.
1.0	79.9 ± 59.6	N.D.	N.D.	N.D.
2.0	65.6 ± 12.4	N.D.	N.D.	N.D.
6.0	69.8 ± 20.2	N.D.	N.D.	N.D.
24.0	16.6 ± 6.1	N.D.	N.D.	N.D.

Liver concentration after M1 administration (ng/g ± SD)				
t[h]	M1	Hidroxy M1	Dihidroxy M1	Trihidroxy M1
N.D	N.D	N.D.	N.D.	N.D.
0.25	10.4 ± 6.2	N.D.	N.D.	N.D.
0.5	155 ± 35	N.D.	N.D.	N.D.
1.0	193 ± 25	N.D.	N.D.	N.D.
2.0	25.4 ± 8.2	N.D.	N.D.	N.D.
6.0	47.3 ± 20.2	N.D.	N.D.	N.D.
24.0	5.4 ± 1.6	N.D.	N.D.	N.D.

Kidney concentration after M1 administration (ng/g ± SD)				
t[h]	M1	Hidroxy M1	Dihidroxy M1	Trihidroxy M1
N.D	N.D	N.D.	N.D.	N.D.
0.25	167 ± 50	N.D.	N.D.	N.D.
0.5	2070 ± 340	N.D.	N.D.	N.D.
1.0	362 ± 90	N.D.	N.D.	N.D.
2.0	265 ± 95	N.D.	N.D.	N.D.
6.0	668 ± 84	N.D.	N.D.	N.D.
24.0	121 ± 31	N.D.	N.D.	N.D.

Small intestine concentration after M1 administration (µg/g ± SD)				
t[h]	M1	Hidroxy M1	Dihidroxy M1	Trihidroxy M1
0	N.D	N.D.	N.D.	N.D.
0.25	4.29 ± 0.98	N.D.	N.D.	N.D.
0.5	6.58 ± 0.89	N.D.	N.D.	N.D.
1.0	5.68 ± 4.72	N.D.	N.D.	N.D.
2.0	123 ± 15	N.D.	N.D.	N.D.
6.0	72.6 ± 12.6	N.D.	N.D.	N.D.
24.0	6.64 ± 2.64	N.D.	N.D.	N.D.

Large intestine concentration after M1 administration (µg/g ± SD)				
t[h]	M1	Hidroxy M1	Dihidroxy M1	Trihidroxy M1
0	N.D	N.D.	N.D.	N.D.

0.25	N.D	N.D.	N.D.	N.D.
0.5	0.12 ± 0.08	N.D.	N.D.	N.D.
1.0	0.10 ± 0.05	N.D.	N.D.	N.D.
2.0	0.16 ± 0.06	N.D.	N.D.	N.D.
6.0	4.12 ± 2.23	N.D.	N.D.	N.D.
24.0	16.0 ± 4.5	N.D.	N.D.	N.D.

3.3 Comparative mass balance of M1 and BBR 24 h post dose

We evaluated the biodistribution and mass balance in the different studied organs 24 h after administration in rat groups treated with BBR or M1 (Fig. 6). The total recovery of BBR, M1 and metabolites was evaluated 24 h after their administration because this time point can be reasonably considered the most relevant for a steady-state organ biodistribution. After M1 and BBR direct administration, their total recovery (intended as the sumof the administrated molecule and related metabolites) were 75.70 ± 19.33 and 82.02 ± 14.27%, respectively. In Tables 2 and 3, the percentage biodistributions of total dose recovered for BBR and M1 in the different organs are reported; the unrecovered dose, both for M1 and BBR, might be related to the non-quantified phase I/phase II metabolites or non-analyzed organs/tissues.

FIG. 6. MASS BALANCE OF M1, BBR AND METABOLITES 24 H AFTER SINGLE ORAL ADMINISTRATION (2 MG/KG). RESULTS ARE EXPRESSED AS MEAN (%) ± SD OF FIVE INDEPENDENT EXPERIMENTS. DATA REFER TO THE RECOVERY IN THE PLASMA, URINE, LIVER, KIDNEYS, INTESTINAL CONTENTS (SMALL INTESTINE AND COLON), AND FECES; UNRECOVERED/UNDETERMINED DOSE HAS ALSO BEEN REPORTED

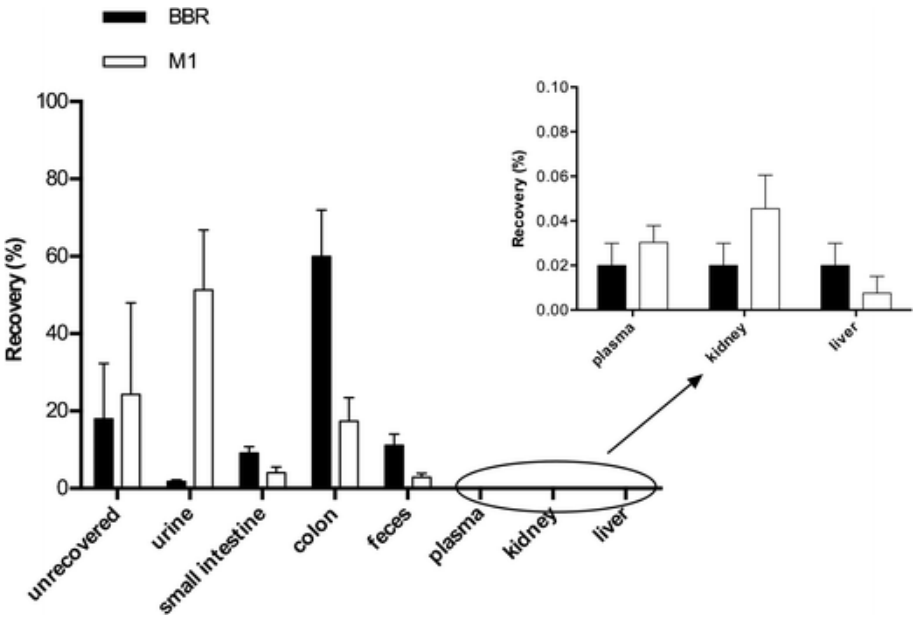

TAB. 2. RECOVERY (NG ± SD AND % ± SD) OF M1 IN VARIOUS ORGANS AND FLUIDS 24 H AFTER DIRECT ORAL ADMINISTRATION IN RATS AT A DOSE OF 2 MG/KG (MEAN VALUES ± SD, N = 5)

M1 administration recovery 24 h (ng ± SD and % recovery ± SD)									
		Plasma	Liver	Urine	Kidney	Small intestine	Colon	Feces	Total recovered
M1	Mean	117 ± 42	32.0 ± 8.6	(205 ± 62) × 10^3	188 ± 57	(16.3 ± 6.0) × 10^3	(69.4 ± 24.4) × 10^3	(11.4 ± 3.9) × 10^3	(302 ± 84) ×10^3
	%	0.03 ± 0.01	0.01 ± 0.00	51.33 ± 15.44	0.05 ± 0.01	4.08 ± 1.49	17.35 ± 6.09	2.86 ± 0.97	75.70 ± 21.18

TAB. 3. RECOVERY (NG ±SD AND %±SD) OF BBR AND METABOLITES IN THE VARIOUS ORGANS AND FLUIDS 24 H AFTER DIRECT ORAL ADMINISTRATION IN RATS AT A DOSE OF 2 MG/KG (MEAN VALUES ± SD, N = 5)

BBR administration recovery 24 h (ng ± SD and % recovery ± SD)									
		Plasma	Liver	Urine	Kidney	Small intestine	Colon	Feces	Total
BBR	Mean	0.3 ± 0.1	20.9 ± 3.3	78.3 ± 15.1	2.3 ± 0.9	(27.6 ± 4.4) × 10^3	(205 ± 40) × 10^3	(38,9 ± 10.4) × 10^3	(271 ± 49) × 10^3
	%	< 0.01	0.01 ± 0.00	0.02 ± 0.00	< 0.01	6.90 ± 1.10	51.24 ± 10.06	9.72 ± 2.61	67.88 ± 12.14
M1	Mean	64.3 ± 16.8	37.5 ± 9.2	(4.99 ± 1.10) × 10^3	84.2 ± 31.1.	(1.47 ± 0.40) × 10^3	(8.48 ± 2.23) × 10^3	1.82 ± 0.44	(17.0 ± 2.8) × 10^3
	%	0.02 ± 0.01	0.01 ± 0.00	1.25 ± 0.27	0.02 ± 0.01	0.37 ± 0.10	2.12 ± 0.56	0.46 ± 0.11	4.24 ± 0.69
M2	Mean	0.3 ± 0.2	3.4 ± 0.8	(1.07 ± 0.29) × 10^3	1.6 ± 0.5	(1.82 ± 0.44) × 10^3	(7.32 ± 2.27) × 10^3	(1.57 ± 0.51) × 10^3	(11.8 ± 2.9) × 10^3
	%	< 0.01	< 0.01	0.27 ± 0.07	< 0.01	0.45 ± 0.11	1.83 ± 0.57	0.39 ± 0.13	2.94 ± 0.73
M3	Mean	20.2 ± 8.2	3.0 ± 0.6	(0.75 ± 0.29) × 10^3	4.1 ±1.5	(3.77 ± 1.08) × 10^3	(12.4 ± 2.9) × 10^3	(0.92 ± 0.37) × 10^3	(17.9 ± 2.9) × 10^3
	%	0.01 ± 0.01	< 0.01	0.19 ± 0.07	< 0.01	0.94 ± 0.27	3.11 ± 0.72	0.23 ± 0.09	4.48 ± 0.72
M4	Mean	< 0.01	< 0.01	217 ± 98	1.6 ± 0.5	(1.97 ± 0.62) × 10^3	(6.56 ± 1.95) × 10^3	(1.17 ± 0.38) × 10^3	(9.92 ± 1.91) × 10^3
	%	< 0.01	< 0.01	0.05 ± 0.02	< 0.01	0.49 ± 0.15	1.64 ± 0.49	0.29 ± 0.09	2.48 ± 0.48

M1 was mainly recovered in the urine (51.33 ± 15.44%), followed by the colon (17.35 ± 6.09%), the small intestine (4.08 ± 1.49%), and the feces (2.86 ± 0.97%). M1 recovered dose in the plasma, liver, and kidneys after 24 h was relatively low (0.03 ± 0.01, 0.01 ± 0.00, and 0.05 ± 0.01%, respectively). Otherwise, after BBR

administration, its total recovery, intended as the sum of BBR and metabolites, is 82.02 ± 14.27%. Considering the recovered dose, BBR and its metabolites were mainly found in the colon (59.93 ± 12.05%), followed by the feces (11.09 ± 2.94%), the small intestine (9.16 ± 1.63%), and the urine (1.78 ± 0.42%). Similarly, to M1 administration, total BBR recovered dose in the plasma, liver, and kidneys after 24 h was relatively low (0.02 ± 0.00, 0.02 ± 0.00, and 0.02 ± 0.01%, respectively). These data are in line with results reported by Ma et al. [Ma J.Y. 2013], who showed that, after BBR oral administration (200 mg/kg) in rats, total BBR recovery in stool after 24 h was around 19%. These results highlight different behaviors of the two molecules administrated: the main route of excretion for M1 is by urine with approximately 1/2 of the administrated dose, while the main route of excretion for BBR and its metabolites is through the intestine, with approximately 2/3 of the administrated dose recovered in the colon content and feces. It is important to point out that the targeted metabolites of BBR and M1 in this manuscript are not the only species occurring in vivo. Since several papers reporting a full metabolomics characterization of BBR and M1 are present in literature [Wang K. 2018, Wang K. 2017(2)], we focused mainly on the assessment of the biodistribution and mass balance of the main species, for which the analytical standards requested for a full method validation were available, and on the correlation of the in vivo results with the in vitro activities determined only for these molecules. Consequently, we tested in vitro with cell-based assays only the compounds for which the HPLC-ESIMS/MS method has been fully validated. The unrecovered dose in the mass balance, around 24% for M1 and 18% for BBR, might be related to the missed quantification of the phase I and II metabolites, which have not been targeted because of the lack of the corresponding analytical standards and for which the method has not been validated.

3.4 In vitro study: effect of M1 and BBR in xanthine oxidase activity and inflammation in human vascular endothelial cells

In both cultured endothelial cells and blood vessels isolated from the aorta, it has been reported that BBR administration prevents the induction of oxidative and inflammatory signalling pathways, key events that lead to endothelial dysfunction [Wang Y. 2009, Liu S.J. 2015]. However, the role of M1 in this context is completely unexplored. We developed an ultrasensitive cell-based biosensor to study intracellular xanthine oxidase activity, one of the major intracellular source of ROS in endothelium and we reported that the xanthine oxidase activity in living endothelial cells (HUVECs) was (6 ± 1) × 10−7 mU/mL/cell and the IC50 of oxypurinol, the active metabolite of allopurinol, was 152 ± 76 ng/mL [Caliceti C. 2016]. As reported above, the M1 maximum plasma concentrations (Cmax) was determined after M1 and BBR administration, i.e., 204 ± 18 and 9.3 ± 2.4 ng/mL, respectively. Consequently, we choose similar concentrations to treat human endothelial cells, using oxypurinol, as reference. After 20 min of incubation, the intracellular IC50 of M1 (9.90 ± 0.01 µg/ mL) and BBR (39.9 ± 0.7 µg/mL) was calculated by a dose-response curve (Fig. 7a, b), observing

that M1 has an IC50 4-fold lower than BBR. This cell-based assay utilizing whole cells takes into consideration also the bioavailability of the compound, especially the ability to cross cell plasma membranes, so it is more representative and predictive to human situation. Considering that physicochemical properties of these compounds affect the ability to enter the cells, the coupled-intracellular enzymatic reaction and the effect-based CL kinetic detection as well as the rapidity of the bioassay (20 min), we assumed that the IC50 values are in line with the Cmax determined in humans. Since in rats, unlike in humans, the enzyme urate oxidase, that catalyzes the oxidation of uric acid to allantoin, is highly expressed [Caliceti C. 2017], it is difficult to precisely quantify uric acid levels in blood of rats treated with BBR and M1.

FIG. 7 CONCENTRATION-RESPONSE PLOT OF INTRACELLULAR XO INHIBITIONOBTAINED BY ANALYZING CL SIGNALS AFTER 20 MIN OF INCUBATION WITH FE2+-EDTA-LUMINOL REACTION COCKTAIL IN THE PRESENCE OF M1 AND BBR (A, B), RANGE 15–0.015 MG/ML. HUVECS WERE PRETREATED WITH M1 AND BBR (300 NG/ML) FOR 8 H BEFORE 24 H OF EXPOSURE TO TNFA (10 NG/ML). LDH ACTIVITY WAS SPECTROPHOTOMETRICALLY QUANTIFIED IN CELLULAR MEDIUM AS INDEX OF CYTOTOXICITY (C). TOTAL RNA WAS EXTRACTED AND QRT-PCR ANALYSIS OF ICAM GENE EXPRESSION WAS PERFORMED (D). RELATIVE CHANGES IN MRNA EXPRESSION LEVELS WERE CALCULATED ACCORDING TO THE $2^{-\Delta\Delta C_T}$ METHOD USING RPL13A AS REFERENCE GENE. RESULTS ARE EXPRESSED AS MEAN ± SEM OF FIVE INDEPENDENT EXPERIMENTS. **P < 0.01, ***P < 0.001 SIGNIFICANTLY DIFFERENT FROM THE CONTROL; °P < 0.05, °°°P < 0.001 SIGNIFICANTLY DIFFERENT FROM THE VEHICLE (DMSO).

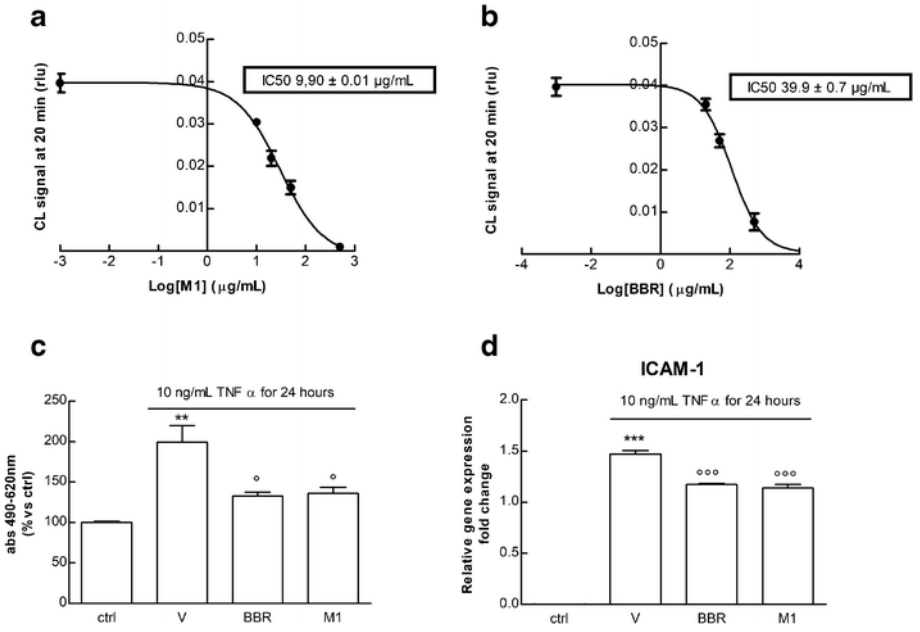

To evaluate the assay response accuracy, the inhibition effect of M1 and BBR on xanthine oxidase activity utilizing this cell-based biosensor was compared to a previously validated cell-free CL enzymatic method performed in a standard 96-well microtiter plate format [Roda A. 1998], obtaining an IC50 = 0.56 ± 0.02 and 8.24 ± 0.02 µg/mL for M1 and BBR, respectively. The results confirm the greater inhibition effect of M1 than BBR on XO activity; the slight discrepancy of the values obtained in the cell-free system with respect to the cell-based assay can be attributed, at least in part, to the capability of the compounds to cross plasma membranes. Moreover, we excluded the possible interferences of M1 and BBR in the CL reaction on free

radical production, exploiting two complementary assays based on chemiluminescent (ECL) and a fluorescent (ORAC) detection methods previously described (section 2.7 Cell based assays), able to reveal different species of ROS [Caliceti C. 2017]. Both methods showed that M1 and BBR cannot be considered ROS scavenger. Moreover, we determined several biological effects using standard procedures (LDH assay and qReal-time PCR), treating cells with M1 concentrations comparable to those quantified after BBR and M1 in vivo administration. As shown in Fig. 7c, at M1 concentration corresponding to its direct administration, the cytotoxicity induced by the pro-inflammatory cytokine tumor necrosis factor α (TNFα) was partially counteracted ($P < 0.05$), while lower doses had slight effect (data not shown). Additionally, we investigated the expression of several pro and anti-inflammatory biomarkers involved in endothelial dysfunction (NADPH oxidases 2 and 4, lectin-type oxidized LDL receptor 1, vascular cell adhesion molecule 1, inducible cell adhesion molecule 1, heme oxygenase 1, superoxide dismutase, and endothelial nitric oxide synthetase). As before, the M1 treatment at higher concentration decreased TNFα-induced ICAM-1 expression (Fig. 7d) ($P < 0.001$), the well-known NF-kB target gene involved in inflammatory responses in endothelial cells [Dunn S. 2008]. Lower concentrations of M1 poorly affect gene expression, confirming that M1 exerts its protective role in the vasculature when it is directly administrated. Based on our results, we could reasonably assume that using M1 instead of BBR as metabolic precursor of M1 is more effective in endothelial dysfunction.

4. Conclusions

In the EU, food supplements are regulated as foods although, in some cases, an excessive intake may be harmful or cause unwanted side effects; therefore, an analytical safety and biological activity profile assessment should be required [Commission Regulation (EU) 2017/1203]. In this work, we reported for the first time, the in vivo biodistribution and the in vitro anti-inflammatory activity in the vasculature of M1. The optimization of the sample cleanup combined with a fully validated HPLC-ESI MS/MS tailored for M1 allowed us to reach sufficient sensitivity and great accuracy even after the administration of very low dosages resembling the common assumption in humans. The in vitro characterization using highly predictive in vitro intracellular studies showed that M1 significantly inhibits xanthine oxidase activity and counteracted the expression of inflammatory genes at a concentration comparable with those determined after its direct administration. As far as we know, this is the first attempt that evaluates the preventive effect of M1 and BBR on the xanthine oxidase activity, which is considered one the most important biomarkers correlated with endothelial dysfunction and cardiovascular disorders. The parallel investigation of the qualitative and quantitative biodistribution after direct M1 and BBR administration by HPLC-ES/MS/MS in the different biological compartments, combined with smart, highly predictive, and effect-based intracellular studies should be mandatory for the assessment of the safety, the ADME profile, including determination of metabolites, and the biological activities for a complete nutraceutical profile characterization.

The obtained results have been correlated to the physical chemical properties of the target analytes, recently determined in our research group, allowing us to understand in depth their physiological behavior and biological profile. Although more investigations are required to evaluate the bioavailability and biological effects in humans after M1 administration, the present results seem promising and lead us to hypothesize a possible use of M1 instead of BBR as nutraceutical compound for supplements or functional foods. The main advantage of our combined analytical approach could be furtherly extended to the in vitro/in vivo characterization of natural bioactive molecules with potential use in nutraceutical field. The final goal is building a database for the multidata mining and management, which is able to correlate physicochemical properties with biological behaviour.

Reference

Amin, A. H., Subbaiah, T. V., & Abbasi, K. M. (1969). Berberine sulfate: antimicrobial activity, bioassay, and mode of action. Canadian journal of microbiology, 15(9), 1067-1076.

Cao, G., Alessio, H. M., & Cutler, R. G. (1993). Oxygen-radical absorbance capacity assay for antioxidants. Free radical biology and medicine, 14(3), 303-311.

Caliceti, C., Rizzo, P., Ferrari, R., Fortini, F., Aquila, G., Leoncini, E., ... & Mirasoli, M. (2017). Novel role of the nutraceutical bioactive compound berberine in lectin-like OxLDL receptor 1-mediated endothelial dysfunction in comparison to lovastatin. Nutrition, Metabolism and Cardiovascular Diseases, 27(6), 552-563.

Caliceti, C., Calabria, D., & Roda, A. (2016). A new sensitive and quantitative chemiluminescent assay to monitor intracellular xanthine oxidase activity for rapid screening of inhibitors in living endothelial cells. Analytical and bioanalytical chemistry, 408(30), 8755-8760.

Caliceti, C., Aquila, G., Pannella, M., Morelli, M. B., Fortini, C., Pinton, P., ... & Rizzo, P. (2013). 17β-estradiol enhances signalling mediated by VEGF-A-delta-like ligand 4-notch1 axis in human endothelial cells. PloS one, 8(8), e71440.

Caliceti, C., Franco, P., Spinozzi, S., Roda, A., & FG Cicero, A. (2016). Berberine: new insights from pharmacological aspects to clinical evidences in the management of metabolic disorders. Current Medicinal Chemistry, 23(14), 1460-1476.

Chen, H. Y., Ye, X. L., Cui, X. L., He, K., Jin, Y. N., Chen, Z., & Li, X. G. (2012). Cytotoxicity and antihyperglycemic effect of minor constituents from Rhizoma Coptis in HepG2 cells. Fitoterapia, 83(1), 67-73.

Chapple, I. L. C., Mason, G. I., Garner, I., Matthews, J. B., Thorpe, G. H., Maxwell, S. R. J., & Whitehead, T. P. (1997). Enhanced chemiluminescent assay for measuring the total antioxidant capacity of serum, saliva and crevicular fluid. Annals of Clinical Biochemistry, 34(4), 412-421.

Commission Regulation (EU) 2017/1203 of 5th July 2017.

Dunn, S., Vohra, R. S., Murphy, J. E., Homer-Vanniasinkam, S., Walker, J. H., & Ponnambalam, S. (2008). The lectin-like oxidized low-density-lipoprotein receptor: a pro-inflammatory factor in vascular disease. Biochemical Journal, 409(2), 349-355.

Franco, P., Spinozzi, S., Pagnotta, E., Lazzeri, L., Ugolini, L., Camborata, C., & Roda, A. (2016). Development of a liquid chromatography–electrospray ionization–tandem mass spectrometry method for the simultaneous analysis of intact glucosinolates and isothiocyanates in Brassicaceae seeds and functional foods. Journal of Chromatography a, 1428, 154-161.

Gui, Q., Lawson, T., Shan, S., Yan, L., & Liu, Y. (2017). The application of whole cell-based biosensors for use in environmental analysis and in medical diagnostics. Sensors, 17(7), 1623.

Guidance for industry: Q2B validation of analytical procedures: methodology; 1996

Kilkenny, C., Browne, W., Cuthill, I. C., Emerson, M., & Altman, D. G. (2010). Animal research: reporting in vivo experiments: the ARRIVE guidelines. British journal of pharmacology, 160(7), 1577-1579.

Kulkarni, S. K., & Dhir, A. (2010). Berberine: a plant alkaloid with therapeutic potential for central nervous system disorders. Phytotherapy Research: An International Journal Devoted to Pharmacological and Toxicological Evaluation of Natural Product Derivatives, 24(3), 317-324.

Li, F., Song, S., Guo, Y., Zhao, Q., Zhang, X., Pan, W., & Yang, X. (2015). Preparation and pharmacokinetics evaluation of oral self-emulsifying system for poorly water-soluble drug Lornoxicam. Drug delivery, 22(4), 487-498.

Li, Y., Ren, G., Wang, Y. X., Kong, W. J., Yang, P., Wang, Y. M., ... & Jiang, J. D. (2011). Bioactivities of berberine metabolites after transformation through CYP450 isoenzymes. Journal of translational medicine, 9(1), 62.

Liu, Y. T., Hao, H. P., Xie, H. G., Lai, L., Wang, Q., Liu, C. X., & Wang, G. J. (2010). Extensive intestinal first-pass elimination and predominant hepatic distribution of berberine explain its low plasma levels in rats. Drug Metabolism and Disposition, 38(10), 1779-1784.

Liu, S. J., Yin, C. X., Ding, M. C., Wang, Y. Z., & Wang, H. (2015). Berberine inhibits tumor necrosis factor-α-induced expression of inflammatory molecules and activation of nuclear factor-κB via the activation of AMPK in vascular endothelial cells. Molecular medicine reports, 12(4), 5580-5586.

Ma, J. Y., Feng, R., Tan, X. S., Ma, C., Shou, J. W., Fu, J., ... & He, W. Y. (2013). Excretion of berberine and its metabolites in oral administration in rats. Journal of pharmaceutical sciences, 102(11), 4181-4192.

Marazzi, G., Cacciotti, L., Pelliccia, F., Iaia, L., Volterrani, M., Caminiti, G., ... & Rosano, G. (2011). Long-term effects of nutraceuticals (berberine, red yeast rice, policosanol) in elderly hypercholesterolemic patients. Advances in therapy, 28(12), 1105-1113.

Pouton, C. W. (2006). Formulation of poorly water-soluble drugs for oral administration: physicochemical and physiological issues and the lipid formulation classification system. European journal of pharmaceutical sciences, 29(3-4), 278-287.

Qiu, F., Zhu, Z., Kang, N., Piao, S., Qin, G., & Yao, X. (2008). Isolation and identification of urinary metabolites of berberine in rats and humans. Drug Metabolism and Disposition, 36(11), 2159-2165.

Rizzo, B., Zambonin, L., Angeloni, C., Leoncini, E., Vieceli Dalla Sega, F., Prata, C., ... & Hrelia, S. (2013). Steviol glycosides modulate glucose transport in different cell types. Oxidative medicine and cellular longevity, 2013.

Roda, A., Russo, C., Pasini, P., Piazza, F., Feroci, G., Kricka, L. J., & Baraldini, M. (1998). Antioxidant properties of bile salt micelles evaluated with different chemiluminescent assays: a possible physiological role. Journal of bioluminescence and chemiluminescence, 13(6), 327-337.

Sabir, M., & Bhide, N. K. (1971). Study of some pharmacological actions of berberine. Indian journal of physiology and pharmacology, 15(3), 111.

Spinozzi, S., Colliva, C., Camborata, C., Roberti, M., Ianni, C., Neri, F., ... & Roda, A. (2014). Berberine and its metabolites: relationship between physicochemical properties and plasma levels after administration to human subjects. Journal of Natural Products, 77(4), 766-772.

Wang, K., Feng, X., Chai, L., Cao, S., & Qiu, F. (2017). The metabolism of berberine and its contribution to the pharmacological effects. Drug metabolism reviews, 49(2), 139-157.

Wang, K., Chai, L., Feng, X., Liu, Z., Liu, H., Ding, L., & Qiu, F. (2017). Metabolites identification of berberine in rats using ultra-high performance liquid chromatography/quadrupole time-of-flight mass spectrometry. Journal of pharmaceutical and biomedical analysis, 139, 73-86.

Wang, K., Qiao, M., Chai, L., Cao, S., Feng, X., Ding, L., & Qiu, F. (2018). Identification of berberrubine metabolites in rats by using ultra-high performance liquid chromatography coupled with quadrupole time-of-flight mass spectrometry. Fitoterapia, 124, 23-33.

Wang, X., Wang, S., Ma, J., Ye, T., Lu, M., Fan, M., ... & Gao, Z. (2015). Pharmacokinetics in rats and tissue distribution in mouse of berberrubine by UPLC-MS/MS. Journal of pharmaceutical and biomedical analysis, 115, 368-374.

Wang, Y., Huang, Y., Lam, K. S., Li, Y., Wong, W. T., Ye, H., ... & Xu, A. (2009). Berberine prevents hyperglycemia-induced endothelial injury and enhances vasodilatation via adenosine monophosphate-activated protein kinase and endothelial nitric oxide synthase. Cardiovascular Research, 82(3), 484-492.

Yang, N., Sun, R., Zhao, Y., He, J., Zhen, L., Guo, J., ... & Fei, F. (2016). High fat diet aggravates the nephrotoxicity of berberrubine by influencing on its pharmacokinetic profile. Environmental toxicology and pharmacology, 46, 319-327.

Zhou, Y., Cao, S., Wang, Y., Xu, P., Yan, J., Bin, W., ... & Kang, N. (2014). Berberine metabolites could induce low density lipoprotein receptor up-regulation to exert lipid-lowering effects in human hepatoma cells. Fitoterapia, 92, 230-237.

Zuo, F., Nakamura, N., Akao, T., & Hattori, M. (2006). Pharmacokinetics of berberine and its main metabolites in conventional and pseudo germ-free rats determined by liquid chromatography/ion trap mass spectrometry. Drug Metabolism and Disposition, 34(12), 2064-2072.

Conclusion

Paper 1

The extensive BA metabolism in intestine by gut microbiota is responsible for the production of derivatives of BAs with potential receptor activity. A new HPLC–ESI-MS/MS method for the simultaneous determination of 21 oxo-BAs and seven BA precursors in human faeces was developed and fully validated. Together with secondary BAs, for the first time several oxo-BAs were simultaneously recovered in human feaces. In addition, Oxo-BAs were recovered in systemic circulation as result of non-complete hepatic uptake, supporting the assumption of a potential role as signalling molecules. This new analytical tool can assist in studying the hormone-like activity of the oxo-BAs. Such studies could explain how and why they are formed by intestinal bacteria and elucidate their physio-pathological role as part of a more general acidic steroid metabolomic approach.

Paper 2

This study represents the first attempt to evaluate the effect of anti-TNF alpha treatment (biological therapy) on serum bile acid profiles of inflammatory bowel dieses patients. Our study, using multivariate statistical analysis, for the first time suggests that biological treatment in Crohn patients restores BA physiological levels. Particularly, the improvement of DCA and other secondary BA concentrations seems closely associated with the anti-TNFα therapy. This result indirectly indicates the positive effect of the treatment on the intestine wall and biofilm microbiota, responsible for primary BAs biotransformation to secondary BAs via 7-dehydroxylation, and in addition for BA efficient absorption. As expected, biological therapy seems to be more effective in restoring serum bile acid concentrations when the inflammatory response has been stopped by anti-TNF alpha (CRP < 7). Consequently, a complete and systematic characterization of the BA profile, including secondary metabolites, can be of great help in the light of the concept of precision medicine in IBD patients.

Paper 3

This project concerned with quantification of bile acids in subdural hematomas. We demonstrated a selective trapping of unconjugated bile acids in albumin-containing subdural hematomas, using isotope dilution-mass spectrometry. An increased bioaccumulation of bile acid in hematoma samples during the bleeding time was verified. The preferential flux of unconjugated bile acids in relation to conjugated bile acid may in part be due to their higher lipophicity. This may account for their efficient transfer across lipid membrane domains even when fully ionized at a physiological pH.

Paper 4

Paper 4 reports the in vivo biodistribution and the in vitro anti-inflammatory activity in the vasculature of M1. The fully validated HPLC-ESI MS/MS tailored for M1 allowed us to reach enough sensitivity and great accuracy even after the administration of very low dosages resembling the common assumption in humans. We have also demonstrated that M1 significantly inhibits xanthine oxidase activity and counteracted the expression of inflammatory genes at a concentration comparable with those determined after its direct administration.